# INSTRUMENTATION AND MONITORING OF A FULL-SCALE SHAFT SEAL INSTALLED AT ATOMIC ENERGY OF CANADA LIMITED'S UNDERGROUND RESEARCH LABORATORY

by

Blake Erwin Holowick

A Thesis submitted to the Faculty of Graduate Studies of the

University of Manitoba

In partial fulfillment of the requirements of the degree of

**MASTER OF SCIENCE**

Department of Civil Engineering

University of Manitoba

Winnipeg

**ABSTRACT**

Atomic Energy of Canada Limited's Underground Research Laboratory was built to allow study of concepts for the long-term disposal of Canada's used nuclear fuel in a deep geologic repository. In 2003, a decision was made to discontinue operation, decommission and permanently close the underground portion of this facility.

Decommissioning includes the installation of a composite seal at the intersection of the access shaft with a hydraulically active fracture zone located at 275 m depth. The seal is 5 m in diameter and consists of two 3-m-thick concrete segments that confine a 6-m-thick *in situ* compacted core of blended bentonite and sand. The objective of the shaft seal installation is to limit groundwater mixing above and below the fracture zone.

This project provided a unique opportunity to study the hydro-mechanical evolution of a full-scale shaft seal under conditions similar to those in a deep geologic repository. The Enhanced Sealing Project arose from the recognition of this opportunity, and consists of the installation and monitoring of a suite of sixty eight (68) sensors installed in the shaft seal that measure strain, temperature, total pressure, hydraulic pressure, moisture content and displacement.

This thesis provides an overview of the instrumentation and data logging techniques that have been successfully used to monitor the initial behaviour of the shaft seal in this unique underground environment.

**ACKNOWLEDGEMENTS**

I would like to thank my advisor Dr. James Blatz for taking me on as a graduate student. Even though I spent most of my days at the URL, I always knew I had him to rely on back at the University. I look forward to working with him again in the future.

Thanks to all the staff at the URL, specifically Dr. David Dixon, Jason Martino, Kim Chang-Seok, Dr. Deni Priyanto, Frank Johnston, Glen Snider, Dennis Soloway and Marilyn Ruta. Thanks to Dr. Peter Sargent and Paul Thompson for bringing me onboard to work on the Enhanced Sealing Project. A special thanks to Dr. Alex Man for contacting me out of the blue and getting me involved with this great project.

Thanks to my two summer students, James Bartz and David Flynn, for their work preparing the instruments for installation.

Thanks to my beautiful wife Janna for her constant encouragement and support throughout the last two years. Thanks to my Dad for introducing me to engineering and always being there to pass on his "wisdom".

Financial support from Atomic Energy of Canada Limited, the Natural Sciences and Engineering Research Council, the University of Manitoba Faculty of Graduate Studies and the Department of Civil Engineering is gratefully acknowledged.

**TABLE OF CONTENTS**

## LIST OF SYMBOLS

| | |
|---|---|
| $\pi$ | matric suction |
| $\Psi$ | total suction |
| $\omega_v$ | molecular mass of water vapour |
| I | psychrometer cooling current |
| $m$ | molality |
| $R$ | universal gas constant |
| RH | relative humidity |
| $R_s$ | total electrical resistance |
| $T$ | absolute temperature |
| T | psychrometer reference junction temperature |
| $u_a$ | pore-air pressure |
| $u_w$ | pore-water pressure |
| $\bar{u}_v$ | partial pressure of pore water vapour |
| $\bar{u}_{v0}$ | saturation pressure of water vapour |
| V | psychrometer cooling voltage |
| $v_{w0}$ | specific volume of water |

## LIST OF ABBREVIATIONS

| | |
|---|---|
| AECL | Atomic Energy of Canada Limited |
| ANDRA | Agence Nationale pour la gestion des Déchets Radioactifs (France) |
| AWG | American Wire Gauge |
| BPT | Backfill and Plug Test |
| BSB | Bentonite-Sand Buffer |
| COMM | Communications |
| CSE | Composite Seal Experiment |
| Ct | Thermocouple |
| DDL | Diffuse Double Layer |
| DGR | Deep Geologic Repository |
| DL | Datalogger |
| DSE | Drift Sealing Experiment |
| EDZ | Excavation Disturbed Zone |
| ESP | Enhanced Sealing Project |
| FODT | Fibre Optic Displacement Transducer |
| FOPZ | Fibre Optic Piezometer |
| FOSC | Fibre Optic Deformation Sensor |
| FOTPC | Fibre Optic Total Pressure Cell |
| FZ2 | Fracture Zone 2 |
| GSEB Lab | Geotechnical Science and Engineering Branch Laboratory |
| HCB | Highly Compacted Bentonite |
| LHHPC | Low Heat High Performance Concrete |
| LMU | Liability Management Unit |
| NAGRA | Nationale Genossenschaft für die Lagerung radioaktiver Abfälle (Switzerland) |
| NLLP | Nuclear Legacy Liabilities Program |
| NRCan | Natural Resources Canada |
| NWMO | Nuclear Waste Management Organization (Canada) |
| PR | Prototype Repository |
| PSU | Power Supply Unit |
| PVC | Polyvinyl Chloride |
| Psy | Thermocouple Psychrometer |
| SKB | Svensk Kärnbränslehantering AB (Sweden) |
| SOFO | Monitoring of Structures by Optical Fibre (French acronym) |
| TDR | Time Domain Reflectometry |
| TDS | Total Dissolved Solids |
| TPC | Total Pressure Cell |
| TSX | Tunnel Sealing Experiment |
| URL | Underground Research Laboratory |
| VWPZ | Vibrating Wire Piezometer |
| VWPZR | Vibrating Wire Piezometer in Rock |
| VWTPC | Vibrating Wire Total Pressure Cell |

## LIST OF TABLES

## LIST OF FIGURES

## LIST OF COPYRIGHTED MATERIAL FOR WHICH PERMISSION WAS OBTAINED

# 1 INTRODUCTION

## 1.1 General Overview

The long-term management of used nuclear fuel is of great importance to many countries around the world. As a result, there is a need for permanent waste disposal solutions as a paramount component of long-term management strategies. In Canada, as of June 2008, there were 2.0 million used nuclear fuel bundles in storage at reactor sites, and the total used fuel for the end-of-life of the existing reactor fleet was estimated to be between 2.8 to 5.5 million used bundles (Garamszeghy 2008). The primary disposal solution being studied in Canada, and by other nations, is long-term isolation of spent nuclear fuel in a deep geologic repository (DGR). The goal of this disposal option is to ensure that no radioactive contamination is able to escape into the biosphere in concentrations that may cause unacceptable risk to human health and the environment (AECL 1994).

A Canadian DGR would be located between 500 m and 1000 m below the surface in suitable crystalline or sedimentary rock, and would consist of a network of tunnels leading to disposal rooms where the waste is stored. A schematic of a generic DGR is shown in Figure 1.1. The waste containers would be placed in boreholes with the annular gap between the container and rock filled with compacted bentonite-sand buffer (BSB) material. The rooms and tunnels would be backfilled with clay based material and sealed with concrete and bentonite-sand components. Since construction of the shafts and tunnels in a

DGR will create pathways for water flow through the repository, various seals would need to be constructed to limit flow to acceptable levels (AECL 1994). Typical seals are shown in Figure 1.2. Installing these seals would involve constructing tunnel seals as container placement is completed in each of the disposal rooms, and shaft seals at the time of repository closure. These seals may be of the composite type consisting of concrete components confining a bentonite-sand core. A diagram of a generic composite shaft seal is shown in Figure 1.3. After final closure of a DGR the various barriers in-place to limit contaminant movement would include the waste form itself, a corrosion resistant container, buffer, backfill, shaft/tunnel seals and the geosphere (overlying rock).

Following construction of tunnel and shaft seals it may be necessary to monitor the saturation and swelling of the bentonite-sand component, as well as stresses and strains within the concrete components. This would be accomplished by using remote instrument installations with data logging systems located on the surface hundreds of metres from the location being monitored. The instrument installation would need to be very robust, since after DGR closure access to the instruments for repair would be impossible.

To reliably ensure the performance of seals in a future DGR it is necessary to test methods for their construction, as well as determine what instrument technologies are appropriate to monitor them. This thesis will focus on the construction and monitoring of a full-scale shaft seal constructed as part of the closure of Atomic Energy of Canada Limited's (AECL) Underground Research

Laboratory (URL). The goal of this research is to provide valuable information for planning of future sealing studies, development of numerical models to evaluate repository seals and formal designs of repository seals.

## 1.2 Introduction to the Enhanced Sealing Project

The Enhanced Sealing Project (ESP) consists of the instrumentation and monitoring of a full-scale shaft seal that was installed as part of the closure of AECL's URL. The shaft seal is located at the intersection of the URL's access shaft (main shaft) and a low dipping ancient thrust fault, known as Fracture Zone 2 (FZ2). Fracture Zone 2 is a hydraulically active feature and serves as the boundary between deeper more saline groundwater (~90 g/L TDS) and shallower less saline groundwater (<2 g/L TDS). The shaft seal was installed to limit potential mixing of these two groundwater zones and return the area to its pre-development state.

The URL decommissioning, including construction of the shaft seal, is part of the Nuclear Legacy Liabilities Program (NLLP) funded by Natural Resources Canada (NRCan) and managed by AECL's Liability Management Unit (LMU). The NLLP monitoring program provides only basic hydrogeological monitoring of the surrounding rock mass. The ESP arose from the recognition of a unique opportunity to monitor the hydro-mechanical evolution of a full-scale repository-like shaft seal in well characterized conditions. The ESP is a joint venture between four (4) nuclear waste management organizations including Canada's Nuclear Waste Management Organization (NWMO), Sweden's Svensk

Kärnbränslehantering AB (SKB), France's Agence Nationale pour la gestion des Déchets Radioactifs (ANDRA) and Finland's Posiva Oy. The ESP consists of the installation and monitoring of a suite of sixty eight (68) instruments, containing a total of one hundred (100) sensors, in and in-close-proximity-to the URL's main shaft seal. The instruments monitor strain, temperature, total pressure, pore-water pressure, hydraulic pressure, soil suction/moisture content and displacement.

The author played a key role in many aspects of the ESP project, specifically in regards to the instrumentation layout design, instrument selection, preparation, calibration, modification, installation and monitoring. The author created the methods for, and performed, the in-house calibrations. The author oversaw all aspects of the implementation of the instrumentation plan during the construction and instrumentation phases of the project. This included creating many of the methods followed when installing the instruments in the field. The author personally installed the vast majority of the instruments, ensuring that the highest quality installation possible was achieved. The author also performed the initial set up on three of the five dataloggers, and has overseen all aspects of the data collection and data interpretation to date.

### 1.3 Hypothesis and Objectives

This thesis will examine the hypothesis that the performance of an engineered shaft seal installed at depth can be evaluated by remotely monitoring a key set of hydro-mechanical parameters using conventional instrumentation.

This thesis has four (4) objectives:

i. Comment on the materials and construction methods used to build the main shaft seal.
ii. Document the monitoring technologies and techniques used for the ESP.
iii. Comment on the performance and reliability of the various instrumentation technologies used.
iv. Interpret initial data collected from the ESP.

The ultimate goal of this research is to provide useful information for the design and monitoring of a future DGR in Canada.

## 1.4 Scope

This thesis will solely focus on the construction, instrumentation and monitoring of the main shaft seal at the URL. The ventilation raise seal installed at the URL and the hydrogeological monitoring of the URL site will not be examined.

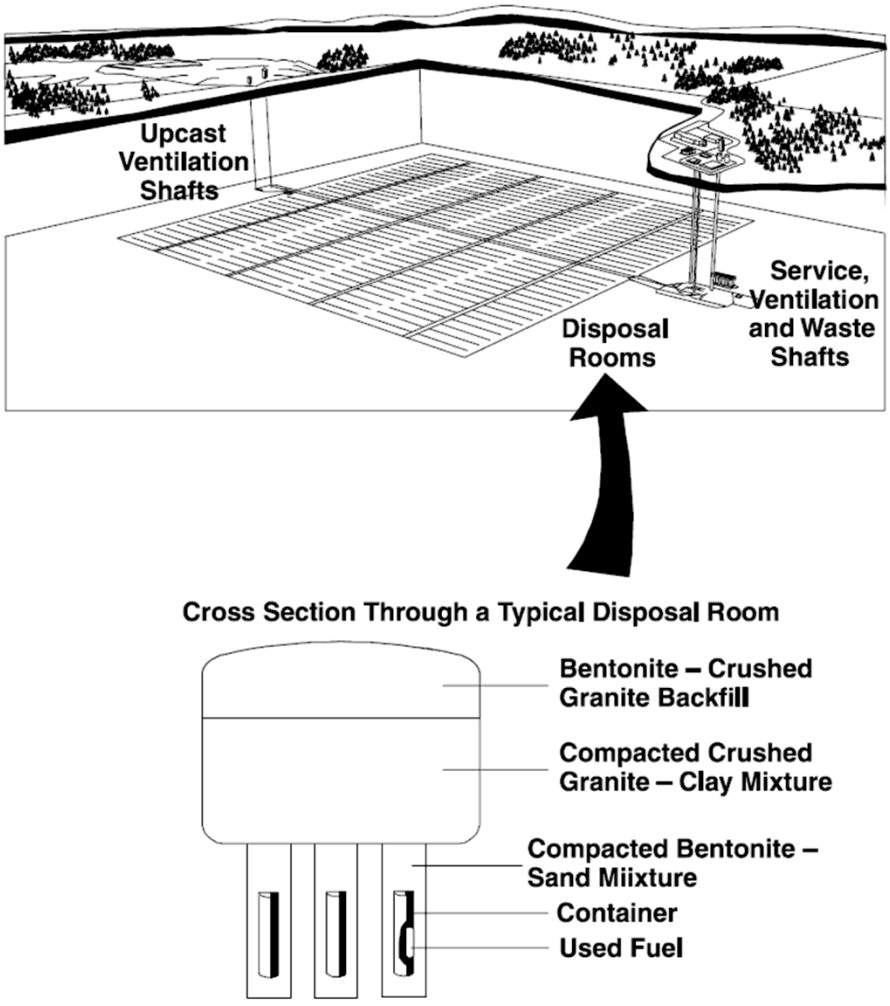


Figure 1.1: Schematic of a deep geologic repository and disposal rooms (AECL)

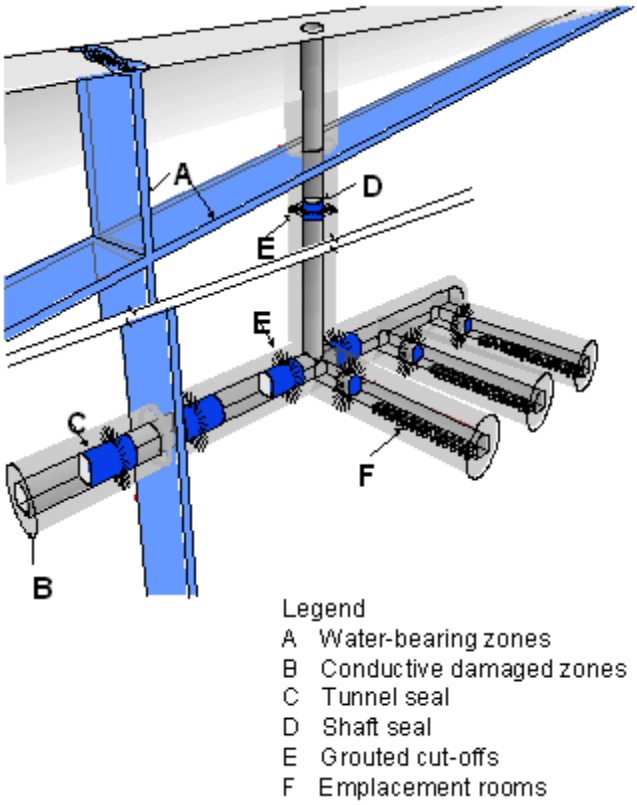


Figure 1.2: Potential pathways for water flow in a repository and the required seals (AECL)

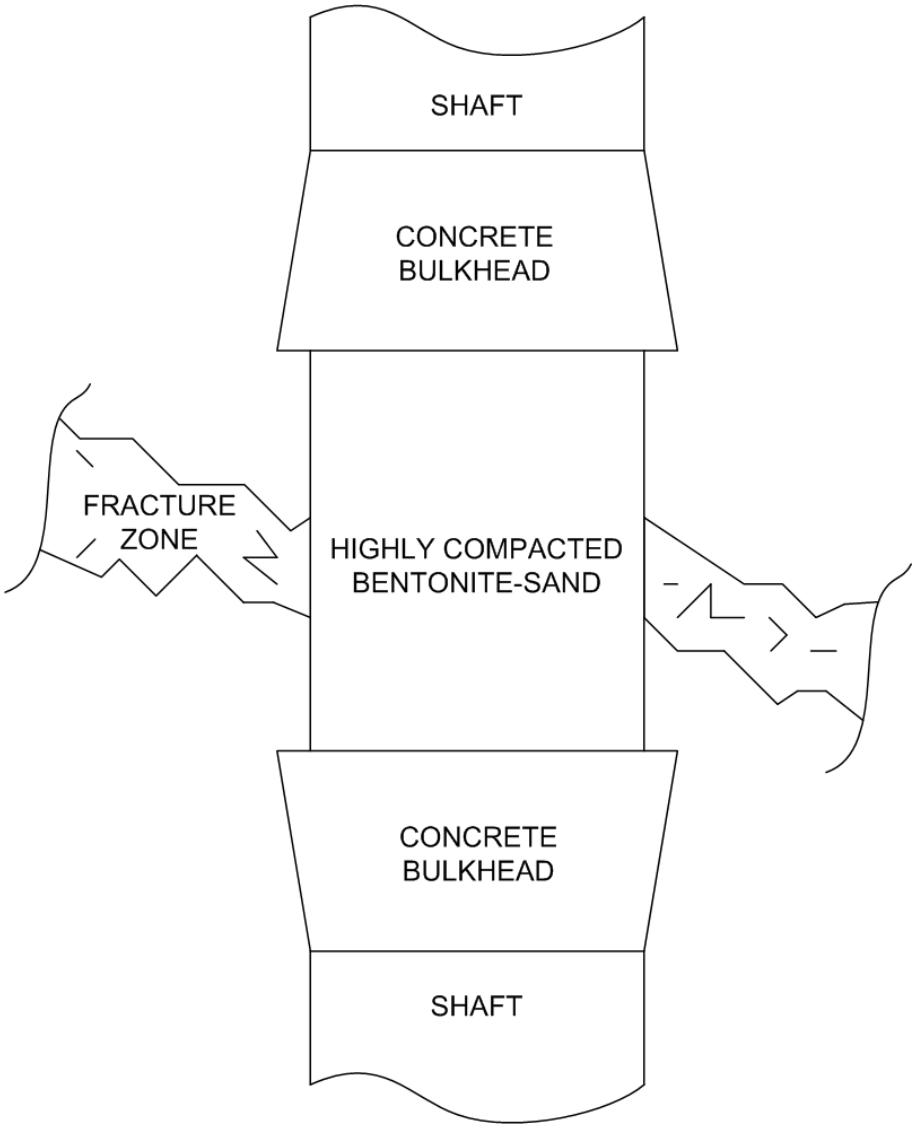


Figure 1.3: Example of a composite shaft seal

Figure 1.3 created by Blake Holowick

# 2 LITERATURE REVIEW

## 2.1 Introduction

In order to better understand the construction and monitoring processes studied in this thesis, some background knowledge is required regarding shaft sealing techniques and past experiments examining shaft and tunnel seals. Also, it is important to review soil suction to understand the use of thermocouple psychrometers for measuring suction in unsaturated soil.

Note that the terms *bentonite-sand* and *clay* are used interchangeably, and represent the same material.

## 2.2 Soil Suction

At the time of installation bentonite-sand material is unsaturated. It contains gas, liquid and solid particles, and is thereby governed by the theories of unsaturated soil mechanics. Unsaturated soil mechanics generally refers to soils that are a three-phase material and possess negative pore-water pressure, or suction (Fredlund and Rahardjo 1993). The suction in an unsaturated soil is commonly called total suction and is comprised of two components; these are matric suction and osmotic suction. Soil suction is related to the free energy of the soil water and can be measured in terms of the pore-water vapour pressure (Richards 1965).

Matric suction is attributed to capillary action caused by surface tension forces associated with the meniscus at the air-water interfaces within the pores of the soil. The small pore spaces in the soil act as capillary tubes drawing the water above the water table (Figure 2.1). The capillary water has a negative pressure with respect to the pore-air pressure, which is usually at atmospheric, because the capillary "tubes" are in hydrostatic equilibrium (Fredlund and Rahardjo 1993). The partial vapour pressure above the curved surface (meniscus) at the air-water interface decreases as the radius of curvature of the meniscus decrease. Therefore, at low degrees of saturation when the radius of the meniscus is small, the matric suction will be higher.

Osmotic suction exists due to variations in pore fluid chemistry. Pore-water usually contains dissolved salts, and the presence of dissolved materials lowers the escaping tendency of the solvent (pore-water) molecules, thereby lowering the vapour pressure and increasing suction (Edlefsen and Anderson 1943). This is the basis of osmotic suction. With increasing amounts of dissolved salts there is an increase in osmotic suction (Fredlund and Rahardjo 1993).

Using thermodynamics the relationship between soil suction and the partial vapour pressure of the soil water can be written as follows (Fredlund and Rahardjo 1993):

$$\psi = -\frac{RT}{v_{w0}\omega_v} ln\left(\frac{\bar{u}_v}{\bar{u}_{v0}}\right) \qquad [2.1]$$

Where $\psi$ is total soil suction, $R$ is the universal gas constant (8.31432 J/mol K), $T$ is the absolute temperature (K), $v_{w0}$ is the specific volume of water ($m^3$/kg), $\omega_v$ is the molecular mass of water vapour (18.016 kg/kmol), $\bar{u}_v$ is the partial pressure of pore water vapour (kPa) and $\bar{u}_{v0}$ is the saturation pressure of water vapour (kPa). Given that $\bar{u}_v/\bar{u}_{v0}$ is equal to the relative humidity (RH), Equation 2.1 can be simplified, at a temperature of 15°C, as:

$\psi$ (in kPa) = -132285$ln$(RH in %/100) [2.2]

The vapour pressure of soil water is a function of the soil's moisture content. When the soil is very wet the vapour pressure is close to that of free water, and as the moisture content decreases the vapour pressure also decreases (Edlefsen and Anderson 1943). This relationship allows indirect measurement of a soil's moisture content by measuring the partial vapour pressure (suction) of the pore-water, which can be done using thermocouple psychrometers, and using the soil-water characteristic curve (SWCC) to relate this to moisture content (Fredlund and Rahardjo 1993).

## 2.3 Shaft Sealing Technique

Sodium bentonite clays are used for the construction of shaft and tunnel seals because of their very low permeability and swelling capabilities (Pusch, Borgesson and Ramqvist 1987b). When an unsaturated montmorillonite dominated clay, such as sodium bentonite, is exposed to free water the water

molecules take the place of the cations in the diffuse double layer (DDL) leading to expansion (i.e. swelling) (Siemens 2006). With increasing water content there is further expansion and with decreasing water content there is shrinkage. The swelling behaviour of sodium bentonite based materials leads to self-sealing and self-healing properties that are desirable in shaft or tunnel seals (Chandler, et al. 2002).

The use of concrete bulkheads alone has been found to be less effective compared to bentonite based seals (Pusch, Borgesson and Ramqvist 1987b, Martino 2008). This is due to the concrete-rock interface not being watertight. A small gap may form at this interface due to concrete shrinkage during hydration and differing thermal expansion characteristics of the rock and concrete. In fact, during the construction of the URL main shaft seal the lower concrete component was found not to be watertight immediately following the concrete pour. A reduction in seepage along this interface can be accomplished by keying the bulkhead past the excavation disturbed zone (EDZ), installing bentonite gaskets around the concrete plug and grouting along the interface (Pusch and Borgesson 2003, Chandler, et al. 2002, Dahlstrom 2009). The EDZ is defined as the rock zone where rock properties have been changed due to excavation, such as fracturing due to blasting and stress redistribution.

The swelling properties of bentonite can be combined with the rigidity of concrete to create composite seals. By placing compacted bentonite-based material, for example a bentonite-sand mixture, between two concrete components a

synergistic improvement in the system can be accomplished (Kjartanson and Martino 2004). As the bentonite-sand takes up water from the fracture zone it swells while being rigidly confined by the concrete components and the surrounding host rock. This will allow significant swelling pressures to develop that will create a watertight seal at the clay-rock interface, assist in sealing circumferential fractures in the excavation disturbed zone (EDZ) and cause the bentonite-sand to self-inject up to several centimetres into fractures intersecting the seal (Kjartanson and Martino 2004, Pusch, Borgesson and Ramqvist 1987b, Chandler, et al. 2002). This type of composite seal has been identified as being effective and its construction is simple if it is installed in a vertical shaft.

## 2.4 Experiments on Shaft and Tunnel Seals

Over the past 30 years there have been a number of experiments conducted at underground research laboratories studying tunnel and shaft seals. Various demonstrations and experiments that incorporate seals as part of larger systems have also been conducted and either directly or indirectly provide useful information for advancing the design of seals.

This section of the thesis document outlines features of a number of experiments conducted around the world that either focused on seal performance, or incorporated seals into larger systems. The instrumentation and sealing performance of the experiments are discussed.

### 2.4.1 Experiments in Sweden

#### *2.4.1.1 Tunnel Sealing Test*

A tunnel sealing test was conducted by SKB as part of the Stripa Project in the mid-1980s. The test was conducted to examine the functionality of a tunnel seal designed to eliminate radial inflow from a strongly water-bearing rock zone (i.e. a fracture zone), while still permitting through-traffic during DGR construction and operation (Pusch, Borgesson and Ramqvist 1987c, Gray 1993). Such a seal would have an open passage through the middle and sealing components lining the perimeter of the tunnel (Figure 2.2). The general layout of the tunnel sealing test is shown in Figure 2.3. A saturated sand-filled chamber was employed as an analog to a water-bearing fracture zone. The water in the sand-filled chamber was pressurized at pressures up to 3 MPa during the test. Two O-ring seals comprised of highly compacted bentonite (HCB) blocks (dry density 1750 kg/m$^3$) were located at either end of the sand-filled chamber and completely filled the space between the steel casing and the host rock. Two concrete plugs confined the sand-filled chamber and bentonite O-rings. The plugs were connected by a central hollow steel casing and seven steel tie-rods. Testing the seal's performance involved measuring water outflow from the sand-filled chamber past the bentonite sealing components and the concrete plugs.

Monitoring of the tunnel sealing test included measurement of seepage, bentonite swelling pressure, pore-water pressure, displacement of the concrete plugs and displacement of the sand-bentonite interface.

Glötzl hydraulic total pressure cells were used to monitor the total pressure at the sand-bentonite, rock-bentonite and concrete-bentonite interfaces as well as in the sand fill. The total pressures increased irregularly with respect to time and location. A noted issue was compression of the nylon return tubes on the Glötzl cells at high water and swelling pressures. Also, incomplete saturation of the system led to non-uniform contact and erroneous values for total pressure at the concrete-bentonite interface. However, after 18 months the total pressure at the rock-bentonite interface stopped increasing, indicating that a high degree of saturation had been achieved. The swelling pressure (total pressure minus pore-water pressure) at the rock-bentonite interface was measured to be between 0.8 MPa and 5.2 MPa at the end of the test. The variation in swelling pressure was concluded to be due to the differing conditions at each total pressure cell.

Displacement of the concrete plug ends was measured using an adjustable micrometer. Four bolts were anchored to the corners of each concrete plug and four rock bolts were anchored to the rock wall approximately 1 m from each plug end. The rock bolts were assumed to be fixed points allowing the displacements of each bolt attached to the concrete plugs to be measured. Pre-stressing the tie-rods to 200 tonnes caused an inward movement of both concrete plugs of approximately 0.75 mm. Pressurizing the sand-filled chamber caused a temporary outward movement of approximately 0.25 mm for both concrete plugs.

The displacement of the sand-bentonite interface was monitored by installing Plexiglas tubes through the concrete plugs and bentonite into the sand fill. The

position of the sand-bentonite interface could then be measured directly by inserting a small TV camera or optical borehole inspection device into the Plexiglass tube and visually locating the interface. The measurements showed a uniform expansion of the HCB ranging from 5 mm to 7 mm during the 20 month testing period. The displacement of the sand-bentonite interface was inspected during decommissioning, and it was found that the HCB expanded outwards and around the corner of the concrete bulkhead while conforming to its geometry (Figure 2.4), which demonstrated the potential of bentonite to expand and seal existing gaps.

Seepage was measured by monitoring the amount of water injected into the sand-filled chamber and the amount of water seeping past the concrete plugs. It was found that water mainly flowed through the EDZ immediately adjacent to the ends of the plug. During the initial pressurization stage water rapidly leaked along the bentonite-rock interface for a few hours then the leakage decreased. During this stage it was assumed that the bentonite was taking up water and forming a clay gel along the bentonite-rock interface. During decommissioning it was noted that the HCB had swelled and was in complete contact with the rock wall (Figure 2.5). Leakage dropped by 60% during the 10 month test period from approximately 4800 L/day to 1800 L/day at pressure of 3 MPa. It was observed that outflow from a pegmatite zone and steep fractures intersecting the plug decreased substantially, indicating that swelling bentonite is effective at sealing such features. It was concluded that a concrete seal with no bentonite would have continued to leak at the rate observed during the initial pressurization of the

sand-filled chamber. At a pressure of 3 MPa the leakage would have been expected to be more than 24000 L/day.

#### *2.4.1.2 Shaft Sealing Test*

The shaft sealing test was conducted by SKB as part of the Stripa Project in the mid-1980s. The objective of the shaft sealing test was to compare the performance of a concrete-only seal to that of a seal comprised of HCB blocks (Pusch, Borgesson and Ramqvist 1987b, Gray 1993). The concrete and bentonite seals were known as the *reference seal* and *main seal* respectively.

The reference seal consisted of two concrete plugs, connected by steel tie-rods, that confined a sand-filled chamber. The concrete plugs were both 0.5 m thick and 1.2 m in diameter (Figure 2.6). Pressurized water, at 100 kPa to 200 kPa, was injected into the sand-filled chamber and the outflow rate was monitored. Tracer tests were also performed to determine the seepage path around the concrete plugs. Following completion of the reference test the concrete plugs were completely removed and the shaft walls were carefully cleaned so that no cement remained. No instrumentation was installed in the reference seal, as it was only monitored for seepage.

The main seal was constructed in the same location as the reference seal in order to ensure identical rock conditions. The main seal consisted of two bentonite sections that confined a sand-filled chamber. The bentonite sections were comprised of HCB blocks and were restrained by steel frames connected

by tie-rods (Figure 2.7). As shown in Figure 2.7, the lower bentonite seal had a 254 mm wide slot cut into the shaft wall. The location of the slot was chosen to cut off, and seal, a large open joint.

The main seal had four Glötzl total pressure cells installed in it; one in the top section and three in the bottom section. These total pressure cells gave valuable information regarding saturation rate and swelling pressures of the HCB. A maximum swelling pressure of 3 MPa was measured at the bentonite-rock interface in the bottom section and took 12 months to develop.

The test effectively demonstrated the sealing capabilities of swelling HCB. The outflow during the reference seal (concrete) test was ~200 L/day at an injection pressure of 100 kPa. At the end of the main seal (bentonite) test the outflow dropped to approximately 7.2 L/day at an injection pressure of 200 kPa. This result was attributed to the very low hydraulic conductivity of the HCB, the water-tight seal at the bentonite-rock interface, compression and partial closure of various nearby fractures due to swelling pressure, truncation of shallow flow paths by the slot, and clay intrusion into certain fractures (Figure 2.8).

#### *2.4.1.3 The Backfill and Plug Test*

The backfill and plug test (BPT) is currently installed at the SKB's Äspö Hard Rock Laboratory in Sweden. The objectives of the BPT are to test backfilling materials and emplacement methods, and develop techniques for constructing a full-scale tunnel plug and test its functionality (Gunnarsson, et al. 2001). The

general layout of the experiment is shown in Figure 2.9. The experiment was initiated in 1999 with hydration of the backfill taking place until 2003, at which point flow testing in the backfill was started (SKB 2005).

The experiment is installed in a 5 m diameter tunnel and is divided into three parts; the inner part, outer part and the plug. The inner part contains backfill with 30% bentonite and the outer part contains backfill with no bentonite, however bentonite blocks are installed at the roof. Permeable mats are installed throughout the backfill to facilitate the application of hydraulic gradients to study water flow in the backfill and near field rock. The plug is constructed of reinforced concrete and has an O-ring comprised of HCB blocks installed around its perimeter (Figure 2.10). The plug is keyed 1.5 m into the surrounding rock to provide mechanical support and cut off flow paths through the EDZ.

The backfill is instrumented for monitoring of total pressure, pore-water pressure and water saturation. Water pressure in the adjacent rock is also measured.

Total pressure in the backfill is measured by a total of 21 sensors, including Glötzl hydraulic total pressure cells (TPC) and Roctest vibrating wire total pressure cells. The Glötzl TPCs are connected via hydraulic lines to pressure transducers located outside of the test volume. One advantage of this type of installation is the transducer can be easily calibrated or replaced during the test (Gunnarsson, et al. 2001). The vibrating wire TPCs are typical to what is used in near surface applications, and are monitored by a Campbell Scientific CR10X datalogger.

Pore-water pressure in the backfill is monitored by 34 instruments, including Glötzl hydraulic piezometers and filter tips with tubing connected to Druck pressure transducers. The filters tips consists of a stainless steel filter connected to tubes that run outside of the test volume where the pressure transducers are located (Figure 2.11). The filter tip installation allows the pressure transducer to be calibrated or replaced during the experiment. Also, the filter tips can be used for tracer testing inside the backfill.

Water pressure in the adjacent rock is measured in 75 sections of core-drilled boreholes sealed by mechanical packers with bentonite rings. Mechanical packers with bentonite seals were used in the Stripa tests and were found to be advantageous due to the longevity of the bentonite seal (Pusch, Borgesson and Ramqvist 1987a). Two high pressure tubes run from the measuring section of the packers to Druck pressure transducers located outside the test volume.

The BPT contains 57 sensors for monitoring the saturation process of the backfill materials. The sensor types include electrical resistivity probes, Wescor thermocouple psychrometers and filter tips installed in both backfill materials. Electrical resistivity probes measure the resistivity of the soil, which is a function of the soil type, temperature, porosity and degree of saturation. The soil particles are poor electrical conductors, and therefore the soil's bulk electrical resistivity is dictated by water content and the concentration of dissolved salts. The resistivity of the soil decreases with increasing water content and increasing dissolved salt concentration. Thermocouple psychrometers measure the relative humidity in

the soil pore spaces, which can be related to the soil suction using principles of thermodynamics. Soil suction is a function of water content; with increasing water content soil suction decreases. The use of thermocouple psychrometers to measure soil suction has been studied extensively and their performance is well defined (Wan 1996, Dixon, el al. 2000).

During flow testing, seepage past the plug stabilized at approximately 28.8 L/day at a water pressure of 0.5 MPa (Pusch and Borgesson 2003). Pusch and Borgesson (2003) compared the performance of the tunnel plugs from the BPT and the Stripa tunnel sealing test and concluded that keying the plug 1.5 m into the tunnel wall effectively cut off the EDZ for the normally blasted rock.

#### *2.4.1.4 The Prototype Repository*

The Prototype Repository (PR) is installed at the 450 m level of SKB's Äspö Hard Rock Laboratory in Sweden. The PR was undertaken as a trial run for the actions required to construct a DGR, and involves detailed characterization of the resaturation of deposition holes and tunnel backfill (SKB 2009). The installation of the PR started in 2000 and ended in 2004; as of March 2010 monitoring and operation is still ongoing.

The Prototype Repository is divided into two sections, shown in Figure 2.12. The components of Section 1 include four (4) full-scale deposition holes with heated canisters and bentonite buffer, tunnel backfill comprised of bentonite and crushed rock, and a concrete plug. Section 2 consists of two (2) full-scale deposition

holes with tunnel backfill and is also capped with a concrete plug. The two sections are separated by a cast concrete plug, since Section 2 will be disassembled much earlier than Section 1 (Dahlstrom 1998).

The outermost plug was designed and constructed as an “arch plug” with a spherical front and a flat pressurized side and is designed to limit axial flow in the tunnel (Figure 2.13). It is a reinforced concrete structure made of low pH self-compacting concrete that required no vibration during placement. The plug does not contain any sealing bentonite, but contact grouting was performed at the concrete-rock interface using a special cooling technique. After curing, the plug was cooled to temperature of 4.5°C to increase the size of the gap at the concrete-rock interface; the gap was measured to be 0.15 mm to 0.24 mm wide. This larger gap allowed easier penetration of grout. After grouting, cooling of the plug ceased causing it to expand and tighten up the gap at the concrete-rock interface (Dahlstrom 2009).

In total there are more than 1000 instrument transducers installed in the rock, buffer, backfill and plugs of the Prototype Repository. Most of the instruments measure temperature, pore-water pressure and total pressure in different parts of the experiment. The water saturation process in the buffer and backfill is monitored by measuring the relative humidity in the soil pore spaces, which is then converted to soil suction. The relative humidity is monitored by Vaisala and Rotronic capacitive relative humidity sensors, and well as Wescor thermocouple psychrometers (Johannesson, et al. 2007).

The outermost concrete plug contains three types of instrumentation for measuring concrete strain and the gap width at the concrete-rock interface (Dahlstrom 2009). Geokon vibrating wire joint meters are installed at the concrete-rock interface to monitor the width of the gap. Geokon vibrating wire strain gauges are installed in the concrete parallel to each joint meter, and allow the total deformations of the joint meter to be separated into expansion or contraction of the joint (Figure 2.14). Geokon vibrating rebar strain gauges are also installed at the interior of the plug to measure internal strains.

The plug is controlling axial seepage in the PR tunnel and allows less than 7% of the total influx into the tunnel to exit (Dixon, et al. 2010). Also, with a tunnel pressure of 1 MPa no visible leakage is observed through the plug or at the concrete-rock interface, and most of the seepage seems to be coming from the rock (Dahlstrom 2009).

### 2.4.2 Experiments in Canada

#### *2.4.2.1 The Tunnel Sealing Experiment*

The Tunnel Sealing Experiment (TSX) was a full-scale experiment conducted by AECL to address construction and performance issues of seals for potential application in DGRs (Chandler, et al. 2002, Martino 2008). The experiment was installed at a depth of approximately 420 m at AECL's URL and consisted of the construction and monitoring of two types of seals (bulkheads); one comprised of entirely of concrete and the other of HCB blocks (Chandler, et al. 2002). The

seals confined a sand section that was injected with heated, pressurized water. The general layout of the TSX is shown in Figure 2.15.

The tunnel where the TSX bulkheads were installed is oval shaped, measuring 4.4 m wide by 3.5 m tall. The tunnel is aligned along the azimuth of the major principal stress ($\sigma_1$) and perpendicular to the intermediate principal stress ($\sigma_2$) in the host rock, and the oval shape was required to maintain tunnel stability. Both the major and intermediate principal stresses are sub-horizontal in this location.

The experiment was initiated in 1995 with construction finishing in 1998. It operated for 64 months under varying thermal and hydraulic conditions until 2004, with final decommissioning being completed in 2005. The experiment included tunnel pressurization phases up to 4 MPa with, and without, heating of the injected water. The water was heated to produce 50°C and 65°C temperatures at the concrete-sand and bentonite-sand interfaces.

*2.4.2.1.1 The TSX Concrete Bulkhead*

The concrete bulkhead was keyed 1.75 m into the surrounding rock (Figure 2.16). The key had an inclined downstream face and a vertical upstream face that provided a hydraulic cut off through the EDZ, as well as good rotational stability, and reduced potential for shear slippage along the concrete-rock interface. The bulkhead was an unreinforced concrete structure comprised of low heat high performance concrete. The concrete mix used had many desirable attributes, including low shrinkage, high strength, low permeability and good

workability; the same concrete mix was used for the construction of the URL shaft seals in 2009/2010. The concrete bulkhead was sealed along the concrete-rock interface using bentonite sealing strips and grout injection.

A total of 133 instruments were installed in the concrete bulkhead and at the concrete-rock interface. The instruments contained sensors for monitoring strain, interface water pressures, interface total pressures, EDZ pore-water pressure, temperature, interface displacement, bulkhead displacement and micro-seismic events. Since the concrete did not contain reinforcing rebar most of the instruments were suspended from glass fibre rods (Figure 2.17).

The thermal pulse due to initial concrete hydration was measured by 82 temperature sensors installed in and around the concrete bulkhead. The maximum temperature recorded was 45.1°C near the centre of the bulkhead. This indicated a maximum temperature rise of roughly 20°C above the initial temperature of the poured concrete.

The strain of the concrete was monitored continuously from initial curing to the end of tunnel pressurization by vibrating wire strain gauges and fibre optic strain gauges. The vibrating wire strain gauges were very rigid and required a temperature correction to be applied to their measurements, whereas the fibre optic strain gauges were more flexible and did not require temperature correction. Due to their rigidity, the vibrating wire gauges missed some of the initial shrinkage before the concrete had sufficiently hardened. However, after 48 hours of hydration both instrument types indicated approximately the same strain

rate. During the heating phases of the experiment all of the strain gauges showed expansion, as expected. Also, the strain in the concrete during tunnel pressurization was very low, only in the order of a few tens of microstrain.

The total displacement of the outer face of the concrete bulkhead was 0.2 mm during pressurization and 0.7 mm during heating. This indicated that thermal effects had a greater influence on the concrete displacement compared to tunnel pressurization. A substantial reduction in seepage was observed during the heating phase, since the aperture at the concrete-rock interface decreased in size due to thermal expansion of the bulkhead.

Seepage past the bulkhead was ~2.5 L/day with a tunnel pressure of 800 kPa. At 4 MPa the seepage stabilized at ~14.5 L/day prior to the heating, and dropped to ~2.9 L/day at the end of the 14 month long heating phase. It was found that grout injection along the concrete-rock interface was required for the concrete bulkhead to be an effective seal.

*2.4.2.1.2 The TSX Clay Bulkhead*

The clay bulkhead was 2 m long, and was keyed 1 m in to the surrounding rock (Figure 2.16) to provide a cut-off of the interconnected fractures around the tunnel's perimeter. The bulkhead was restrained on its downstream face by a steel support plate and the upstream face was in contact with the sand chamber (Figure 2.15). The clay bulkhead was constructed of pre-compacted bentonite-

sand blocks comprised of 70% Kunigel V1 bentonite and 30% silica sand (Figure 2.18), with shot-clay applied along the clay-rock interface.

A total of 234 instruments were installed in and around the clay bulkhead. These instruments monitored the moisture content, swelling pressure, clay pore-water pressure, EDZ pore-water pressure, and displacement of the bulkhead at various locations.

The moisture content of the clay bulkhead was monitored using thermocouple psychrometers, hygrometers and time domain reflectometry (TDR) probes A total of 132 psychrometers were installed, due to their relatively low cost and proven robustness in other AECL experiments (Dixon, et al. 2000). In comparison, only twelve (12) TDRs and fourteen (14) hygrometers were installed, and the TDRs were found to be problematic ceasing to function within a few months after their installation. The psychrometers provided the distribution of soil suction throughout the bulkhead. Water uptake was found to be controlled by the nature of the clay-rock interface and the construction related joints between the roughly 9000 pre-compacted bentonite-sand blocks used in the bulkhead. During initial hydration water was free to move along these joints providing saturating water to a large volume of the clay bulkhead. This served to expedite the hydration of the system before the material at these joints swelled and closed off the flow paths.

The total pressure within the bulkhead, and at the various interfaces, was measuring using vibrating wire total pressure cells and oil-filled flat-plate

pressure sensors. The pressure sensors indicated a maximum swelling pressure of approximately 1 MPa, and showed that the total pressure at the clay-steel support interface increased linearly with the applied tunnel pressure.

The displacement of the clay bulkhead was monitored at its top, interior, upstream interface and downstream interface. These measurements were facilitated by linear potentiometers installed in and around the bulkhead, and a sonic probe installed inside the clay mass. A total displacement of 54 mm was recorded at the upstream (clay-sand) face of the bulkhead, and was primarily attributed to compression due to the applied load. Only about 3 mm of displacement was recovered after tunnel depressurization, indication that non-recoverable compression of the clay mass had occurred.

Seepage past the clay bulkhead was found to stabilize at ~1.9 L/day at a tunnel pressure of 4 MPa. The seepage reduced to ~0.7 L/day once the tunnel pressure was lowered to 2 MPa. It was concluded that most of the seepage occurred along the clay-rock interface.

At the end of the test, full evolution of the bulkhead to an equilibrium state was found to be underway. However, it was estimated it could take up to several more years to reach full hydration and equilibrium of the hydraulic and mechanical pressures.

#### *2.4.2.2 The Composite Seal Experiment*

The Composite Seal Experiment (CSE) was an experiment conducted by AECL to examine the hydraulic and mechanical performance of an *in situ* composite seal comprised of swelling bentonite clay and concrete (Kjartanson and Martino 2004, Martino, et al. 2003).

The CSE was an intermediate scale experiment installed in an existing 1.24 m diameter borehole on the 240 m Level of AECL's URL. The layout of the CSE is shown in Figure 2.19. The borehole was 5 m deep, and allowed the seal to be installed below the EDZ induced by room excavation. The CSE arrangement included a 1-m-thick sand layer at the bottom of the borehole that supplied pressurized water to the seal. The seal consisted of a 0.5-m-thick layer of pre-compacted bentonite-sand (clay) blocks capped with a 0.5-m-thick layer of low heat high performance concrete. The clay block layer is comprised of three individual layers of blocks, each offset by 60° to each other. Construction of the CSE was completed in 2002 and it was never fully dismantled due to the subsequent closure of AECL's URL.

A total of 45 instruments were installed in the CSE that measure the pressure in the sand layer, soil suction (water content), swelling pressure, strain, concrete displacement and temperature.

Roctest vibrating wire piezometers were used to monitor the sand layer pressurization. Roctest vibrating wire total pressure cells and Kulite earth

pressure cells were installed in and around the clay component to measure swelling pressure. The Kulite cells are have a similar stiffness to the soil, and therefore were installed at the interior of the clay. Conversely the Roctest cells are much stiffer and were installed at the top and bottom of the clay layer. Concrete strain was monitored by two (2) Geokon vibrating wire strain gauges.

Soil moisture content was monitored using three types of soil moisture sensors including thermocouple psychrometers, soil water potential probes and thermoconductivity suction sensors. Psychrometers had been used successfully by AECL in past experiments (Martino 2008, Dixon, et al. 2000) and the CSE was seen as an opportunity to compare their measurements with other sensor technologies. The psychrometers provided suction measurement in the expected range (0 to 6 MPa) and showed gradual wetting of the system. However, the soil water potential probes and thermoconductivity suction sensors showed improbably high suction readings (up to 180 MPa). The very high readings were attributed to the instruments' inability to accurately measure the high soil suction present in bentonite-based materials. However, the instruments still provided an indication of the saturation rate.

Seepage past the seal was not observed until the applied hydraulic pressure exceeded 1.64 MPa. With an applied pressure of 2.4 MPa the seepage was initially ~0.058 L/day and dropped to ~0.036 L/day over a ten month period. This reduction is seepage was likely associated with the hydration and swelling of the bentonite-sand blocks (Kjartanson and Martino 2004). The CSE demonstrated

that a composite seal would be an effective means of sealing emplacement rooms and isolating regions of high groundwater flow.

### 2.4.3 Experiments in Switzerland

#### *2.4.3.1 The FEBEX Project*

The FEBEX project was a large-scale demonstration that simulated the horizontal emplacement of a waste container (Huertas, et al. 2000, Villar, et al. 2005). It was conducted at NAGRA's Grimsel Test Site in Switzerland, and was initiated in 1994 with dismantling beginning in the 2002. The experiment included two (2) heated containers that were surrounded by bentonite blocks in a tunnel capped with a massive concrete plug.

The test contained a total of 632 instruments that monitored temperature, total pressure, soil water content, strain and displacements. Vibrating wire based instruments were used in multiple applications including pore-water pressure, total pressures, strain and displacement measurements. The vibrating wire instruments were found to be accurate and reliable, except for the failure of some of their internal thermistors (Garcia-Sineriz and Barcena 2003).

Water content in the bentonite buffer was monitored using thermocouple psychrometers, time domain reflectometry probes and capacitive type sensors. The output from all of the instruments matched each other well, although the output from the psychrometers was difficult to interpret in some cases. The

difficultly in interpretation may have been due to the effect of salts in the bentonite contaminating the instruments (Garcia-Sineriz and Barcena 2003).

A concrete plug was installed at the entrance to the 1.79 m diameter circular borehole. It was 2.7 m long and was keyed 0.4 m into the rock along 1.57 m of its length. The plug was poured in three (3) sections and contained no steel reinforcement. It was designed to resists a total pressure of 5 MPa on its upstream face, but there were no requirements for it to be water tight. Substantial leakage past the plug occurred during the demonstration primarily through the instrument cable ports, however, it was not quantified (Dixon, et al. 2010).

#### *2.4.3.2 Mont Terri Project*

Switzerland also has the Mont Terri underground research facility that is located in sedimentary rock. The site is being used to study the potential for a DGR in sedimentary rock, and plans include the study of tunnel seals. Currently these studies are in the conceptual development stage and no field information is available (Dixon, et al. 2010).

### 2.4.4 Experiments in Germany

#### *2.4.4.1 Sondershausen Drift Sealing Experiment*

The Drift Sealing Experiment (DSE) was conducted at 700 m depth in a 34 year old drift (tunnel) of the former potash mine Sondershausen in Germany

(Sitz, Koch and Gruner 2003). The experiment was performed to test a sealing system installed in a salt deposit, which is proposed as a host rock for radioactive waste isolation in Germany. The project received support from the German Government from 1997 to 2003, with in situ testing taking place from 2000 to 2001.

The test plug was installed in a rectangular section measuring 3.5 m by 3.2 m and consisted of three (3) main components. These were a 5 m long section of pre-compacted bentonite-sand (clay) blocks (50%-60% bentonite), a 1.5 m long section containing bituminous asphalt and bentonite-sand blocks, and a prismatic static abutment constructed from compressed salt bricks. The abutment was keyed approximately 0.7 m into the rock wall in order restrain the clay bulkhead. Salt bricks were tested to assess their long term stability in a saline environment.

During seepage testing a pressurized brine solution was applied to the upstream face of the clay section at pressures up to 8 MPa. During the initial 1.5 MPa pressurization stage, seepage dropped from 72 L/day to approximately 10.8 L/day over a 30 day period. The drop in seepage was attributed to the swelling behaviour of the bentonite. Application of higher pressures (2.5 MPa, 4 MPa, 8 MPa) resulted in excessive axial displacement of the salt brick abutment, up to 20 mm/day and led to an increase in seepage that was too large to measure. It was concluded that a more stable abutment design was necessary to restrain the hydraulic and swelling pressures applied to the abutment.

### 2.4.5 Experiments in Belgium

#### *2.4.5.1 The PRACLAY Experiments*

The Belgium concept for the isolation of nuclear waste includes final deposition in the Boom Clay formation. The Boom Clay formation is a marine Oligocene deposit that is tens of metres thick. The thermal load generated by the waste is of particular importance since it will affect the temperature and stress profiles in the Boom Clay. The PRACLAY experiments at the HADES URL in Belgium are being performed to verify that Boom Clay is a suitable host medium for nuclear waste (SCK-CEN 2005). The experiment arrangement involves the installation of a heater in a 2.5 m diameter horizontal borehole that is capped with a plug. The *PRACLAY plug test* is one of the planned experiments and is aimed at demonstrating the possibility of cutting off the EDZ and sealing horizontal disposal galleries. The underground PRACLAY experiments are to be installed and operated from 2008 to 2013 (Dixon, et al. 2010).

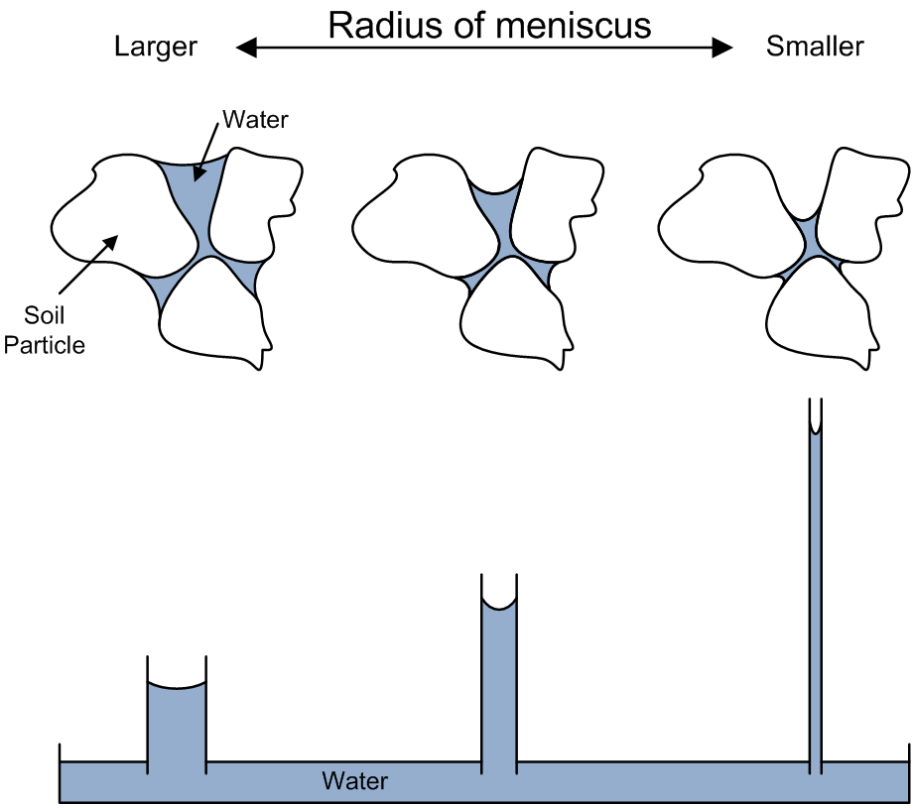


Figure 2.1: Diagram of capillary action in unsaturated soil (after Fredlund and Rahardjo 1993)

Figure 2.1 created by Blake Holowick

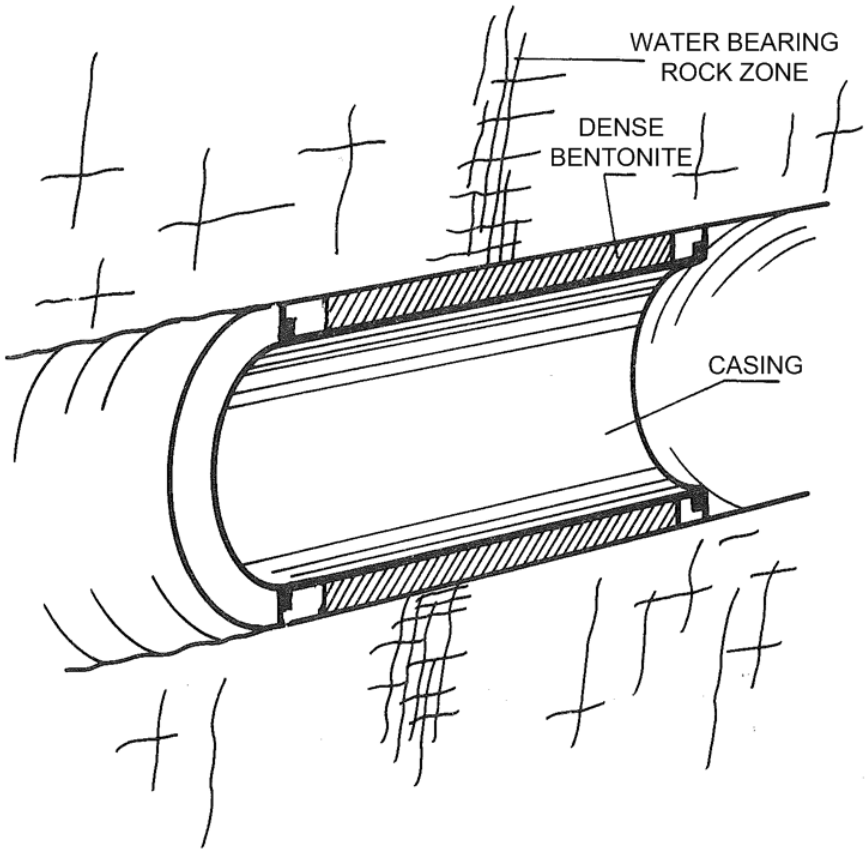


Figure 2.2: Conceptual layout of the Stripa tunnel seal (Pusch, Borgesson and Ramqvist 1987c)

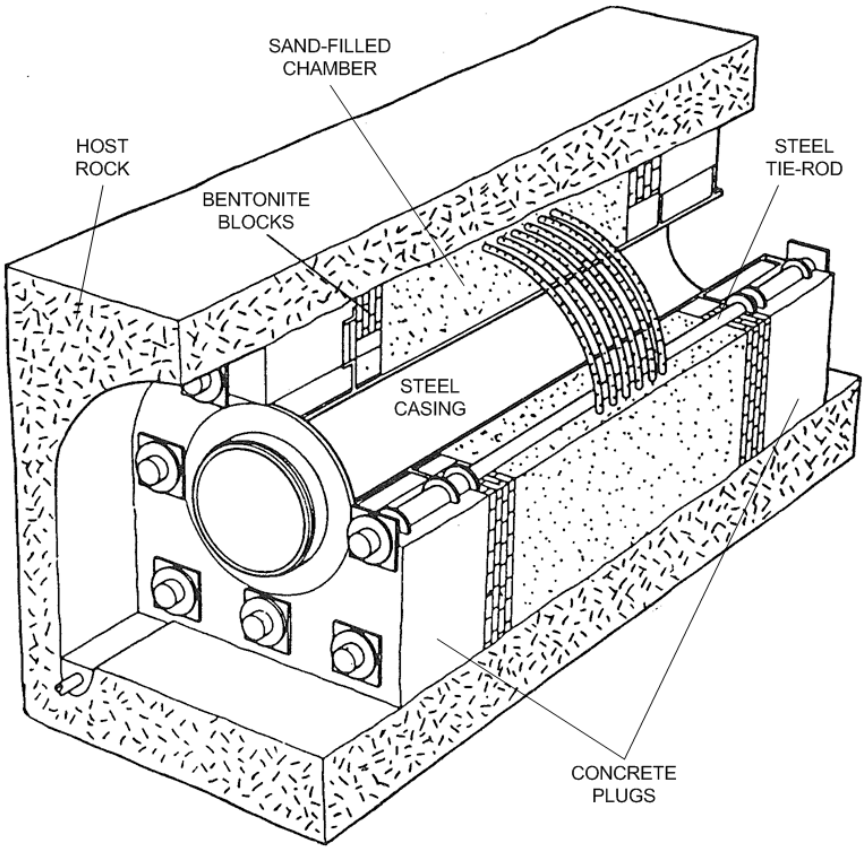


Figure 2.3: General layout of the Stripa tunnel sealing test (Pusch, Borgesson and Ramqvist 1987c)

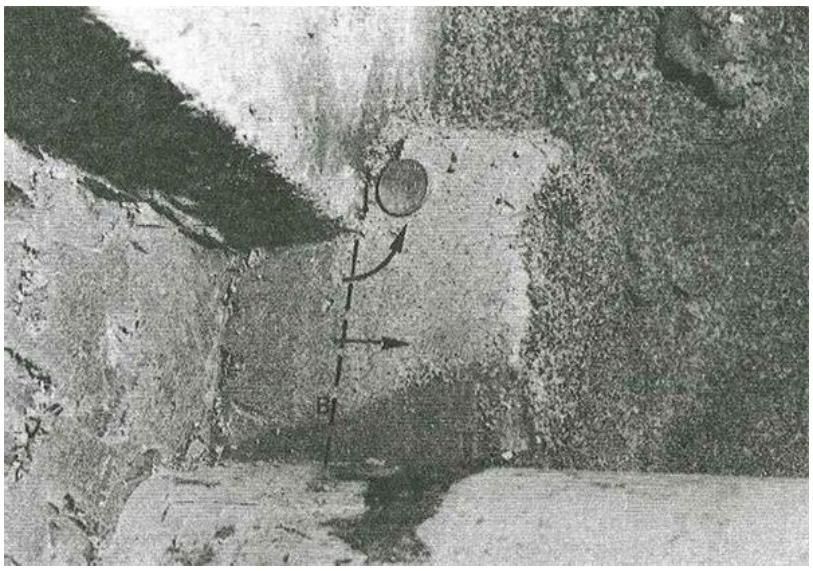

Figure 2.4: Expansion of HCB into sand while conforming to the concrete bulkhead (Pusch, Borgesson and Ramqvist 1987c)



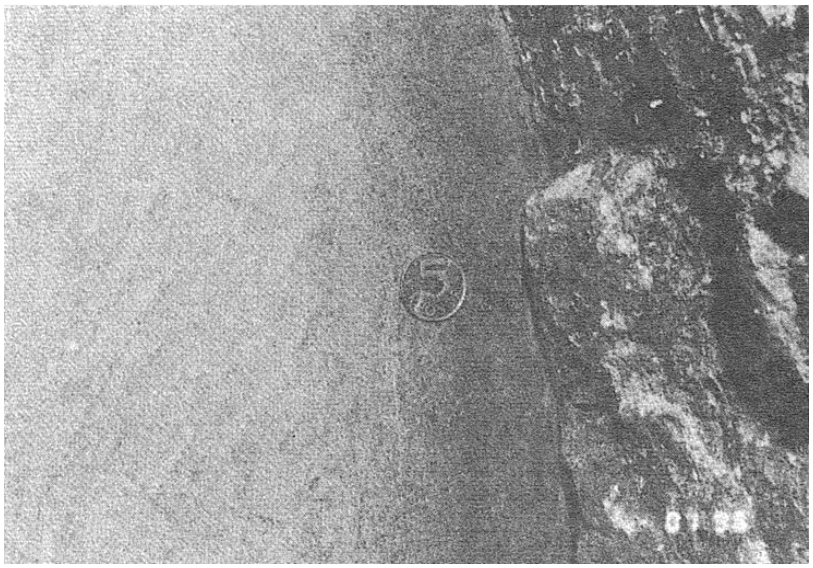

Figure 2.5: Complete contact at rock-bentonite interface (Pusch, Borgesson and Ramqvist 1987c)

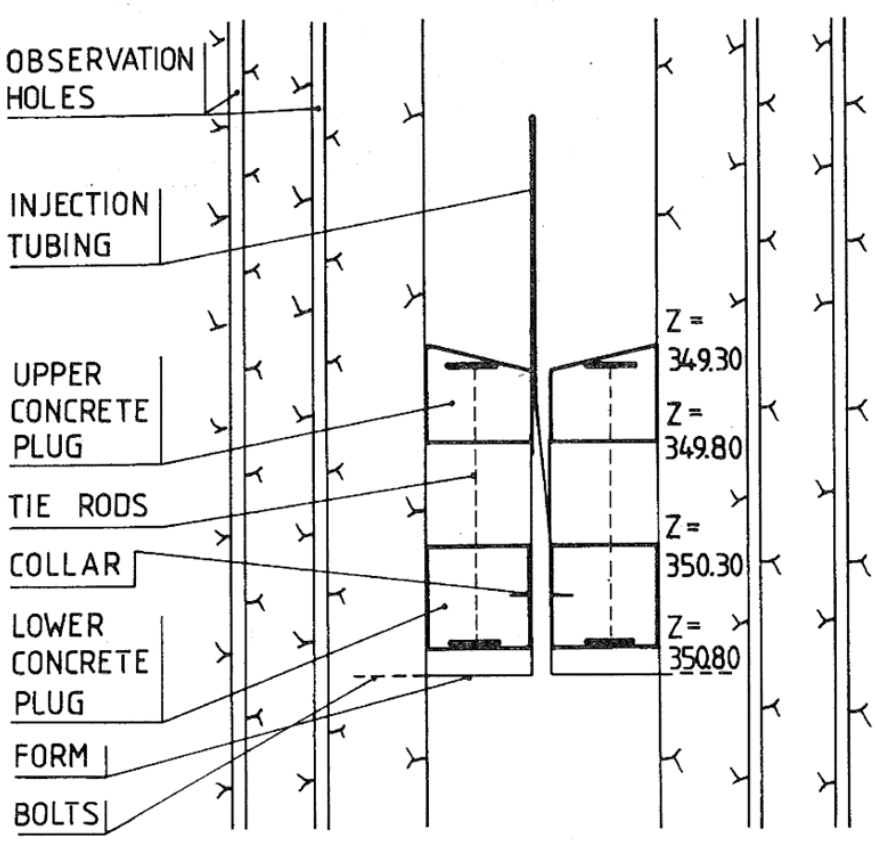


Figure 2.6: Layout of Stripa shaft sealing test concrete reference seal (Pusch, Borgesson and Ramqvist 1987b)

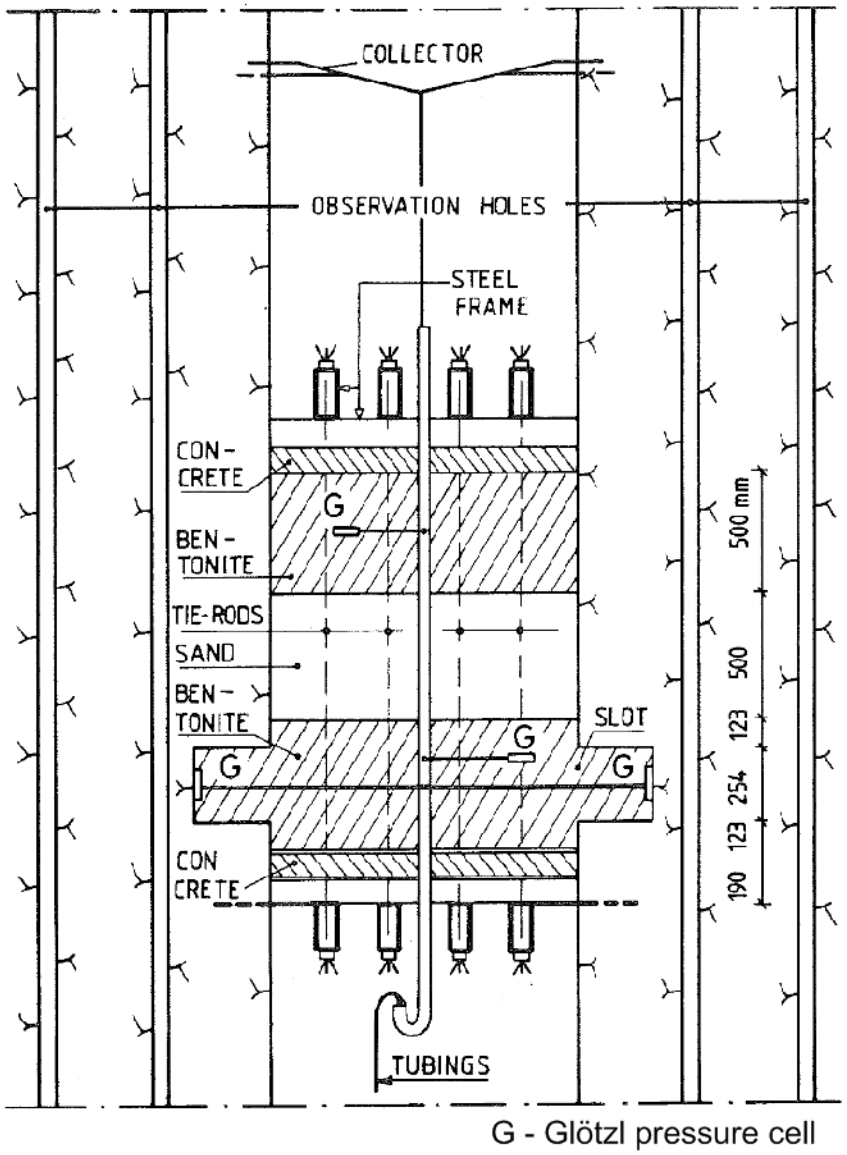


Figure 2.7: Layout of Stripa shaft sealing test HCB main seal (Pusch, Borgesson and Ramqvist 1987b)

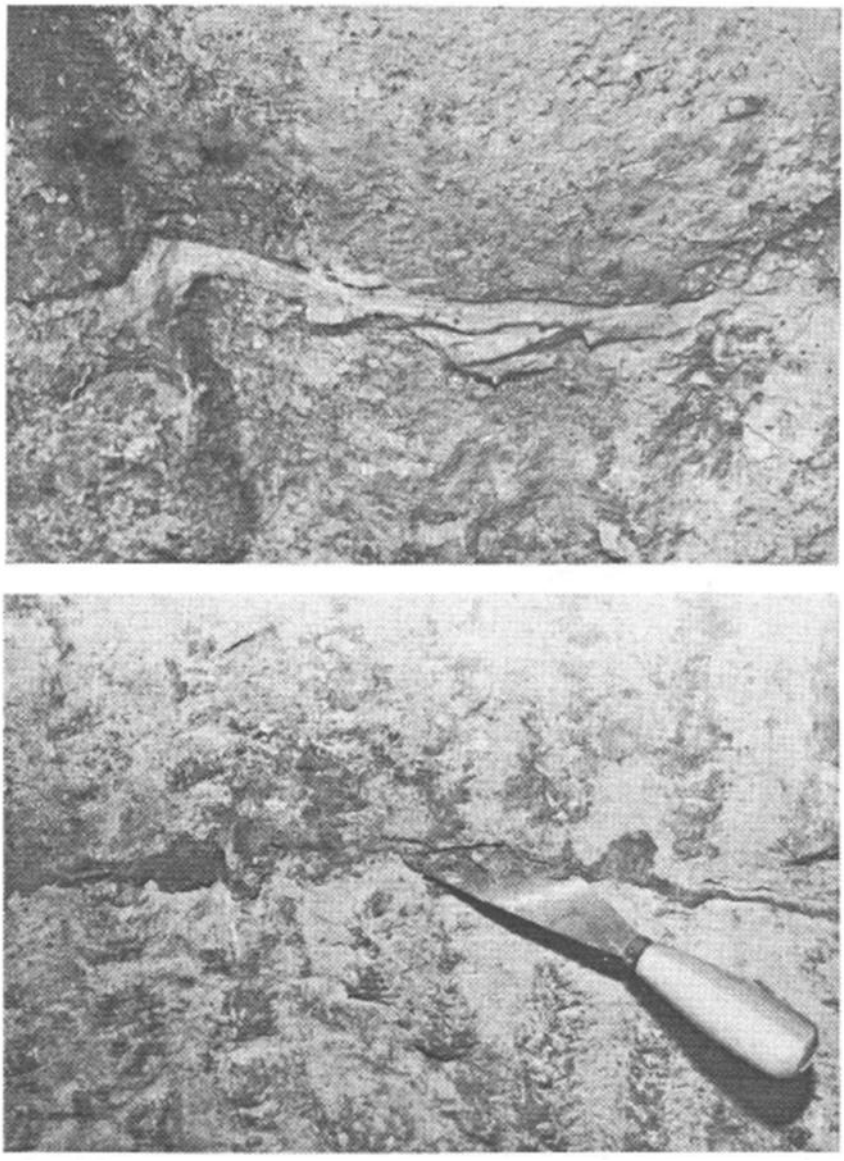

Figure 2.8: Bentonite intrusion into intersecting fractures (Pusch, Borgesson and Ramqvist 1987b)

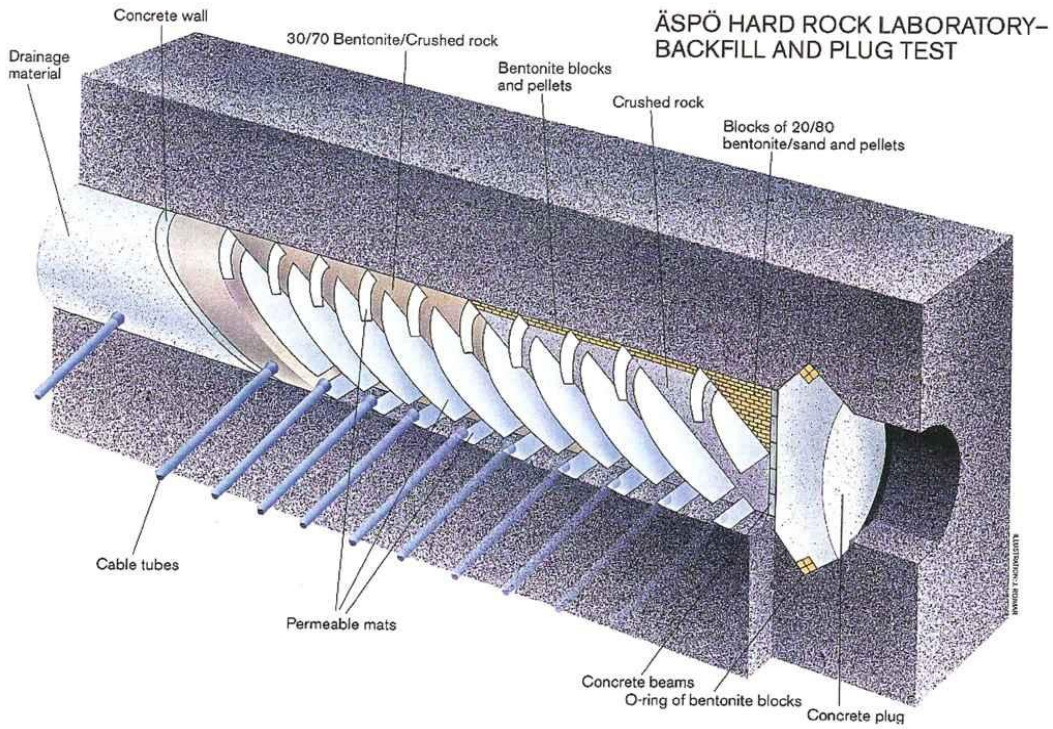


Figure 2.9: Layout of the Backfill and Plug Test (Gunnarsson, et al. 2001)



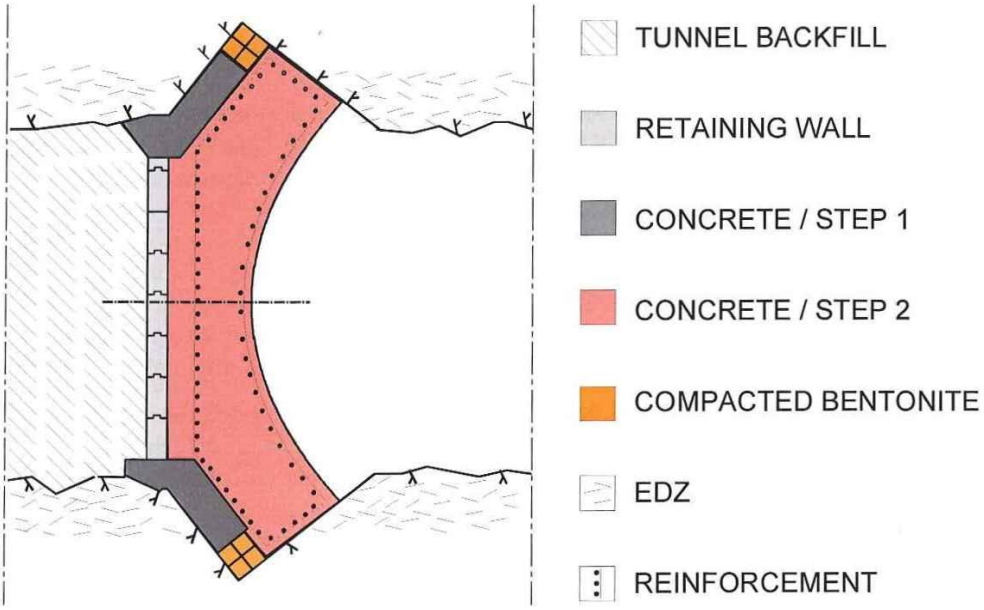


Figure 2.10: Schematic of the Backfill and Plug Test tunnel plug (Gunnarsson, et al. 2001)

Figure 2.11: Filter tip pore-water pressure measurement in the Backfill and Plug Test (Gunnarsson, et al. 2001)



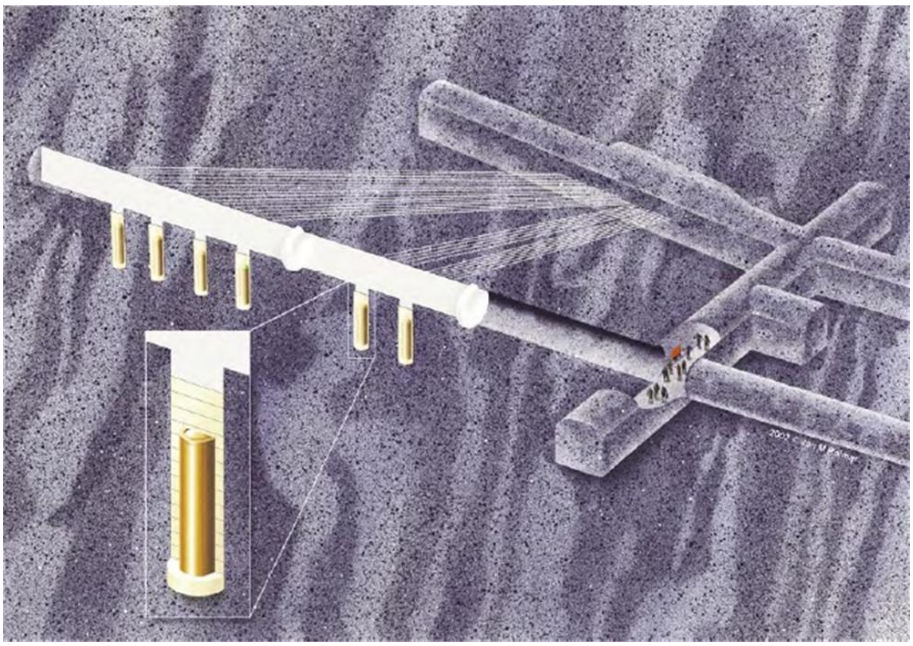

Figure 2.12: General layout of the Prototype Repository (SKB 2005)

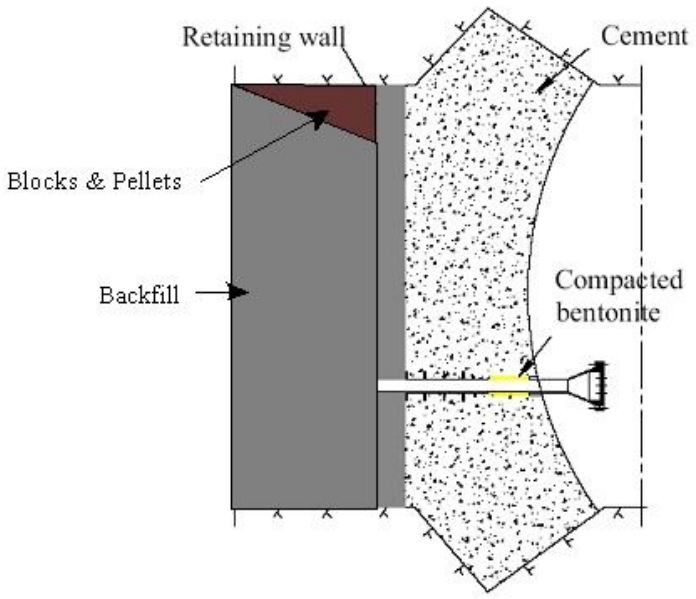


Figure 2.13: Cross section of the Prototype Repository tunnel plug (Johannesson, et al. 2004)



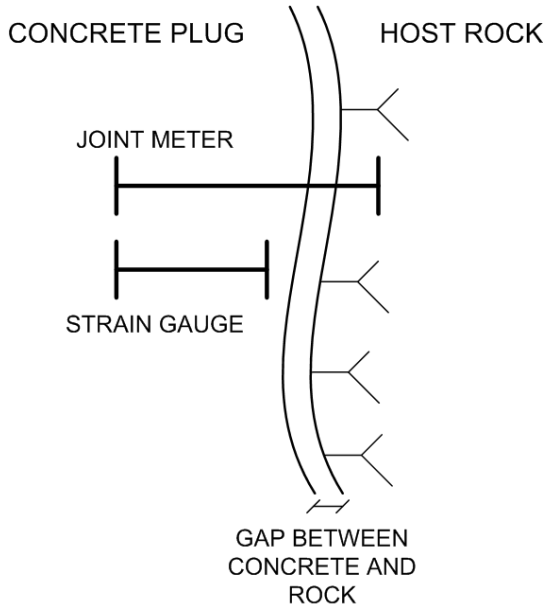


Figure 2.14: Installation of joint meter and strain gauge at the concrete-rock interface (Dahlstrom 2009)

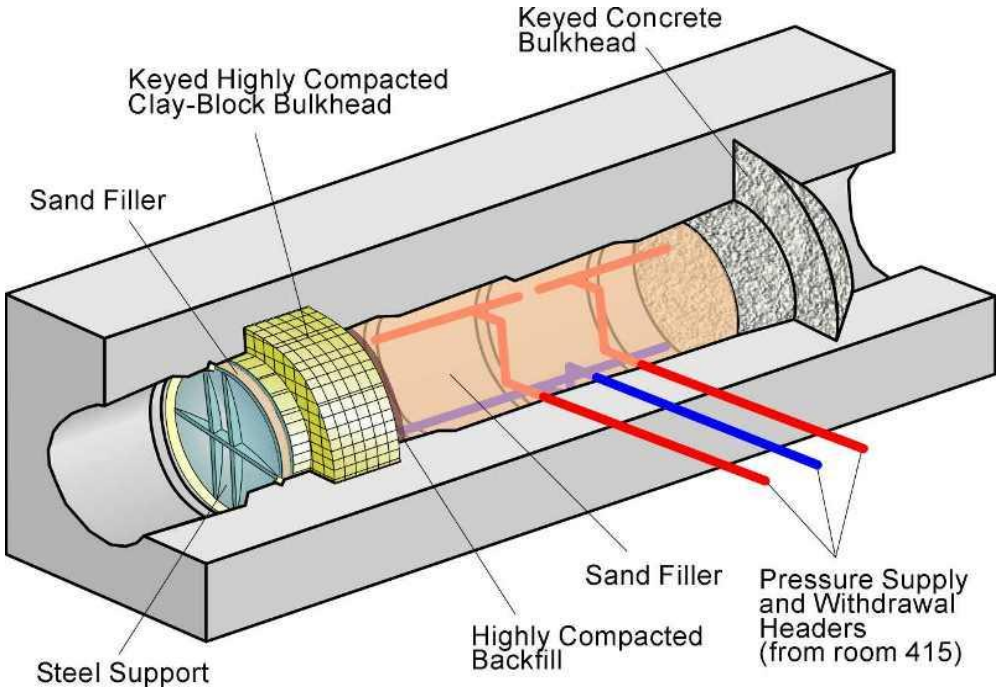


Figure 2.15: Layout of the Tunnel Sealing Experiment (Martino 2008)



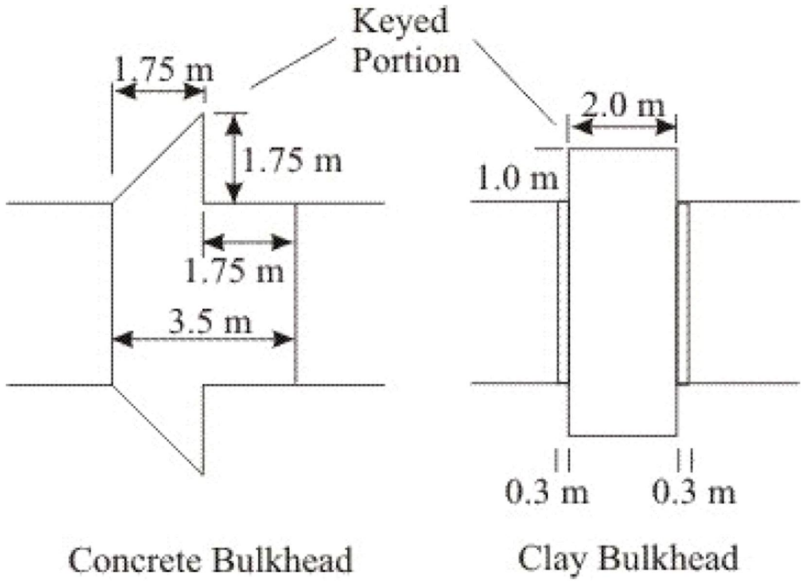


Figure 2.16: Cross section of the Tunnel Seal Experiment bulkheads (Chandler, et al. 2002)

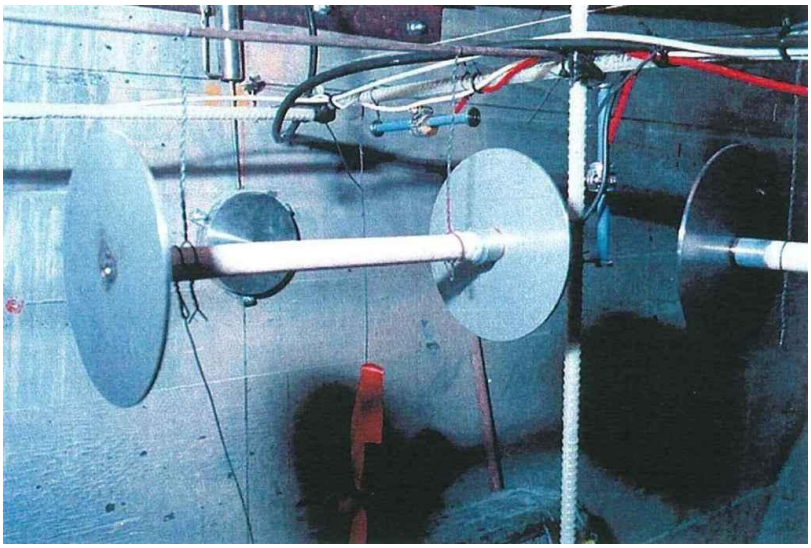

Figure 2.17: Instruments suspended from support rods in the Tunnel Sealing Experiment (Chandler, et al. 2002)



Figure 2.18: Pre-compacted block construction of the TSX clay bulkhead (Chandler, et al. 2002)

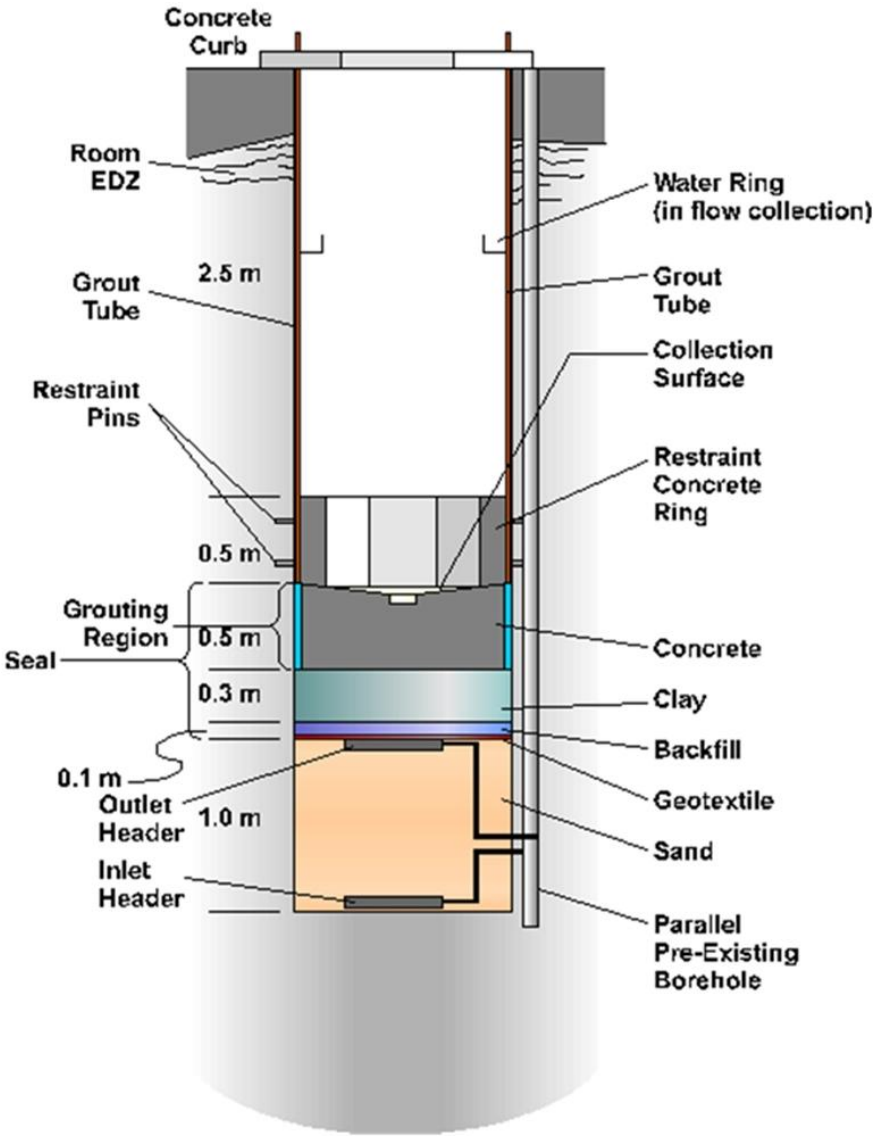


Figure 2.19: Layout of the Composite Seal Experiment (Kjartanson and Martino 2004)

# 3 THE UNDERGROUND RESEARCH LABORATORY: BACKGROUND AND GEOLOGIC SETTING

## 3.1 The Underground Research Laboratory

AECL's URL was constructed as a facility to study the mechanics of underground excavations and evaluate the effectiveness of various nuclear waste isolation concepts. The excavation of the shaft for the URL commenced in 1982, and numerous experiments and studies have been conducted since 1983 including studies of rock mass response to excavation, full-scale buffer experiments and full-scale sealing experiments (Read 2004). Currently the URL is being decommissioned, and the access shaft and vent raise shaft will be capped by the end of 2010.

## 3.2 URL Site Description and Geology

The URL is located in the granitic Lac Du Bonnet Batholith in south-eastern Manitoba, Canada (Figure 3.1). The URL consists of an access shaft, also known as the main shaft, and ventilation (vent) raise extending to a depth of 443 m. There are two main experimentation levels located at 240 m and 420 m depths, these are known as the 240 Level and the 420 Level respectively. The main shaft also has instrumentation levels at 130 m and 300 m depths. Years of experimentation and development have led to a complex underground network consisting of many kilometres of openings. The general layout of the URL is shown in Figure 3.2.

## 3.3 Fracture Zone 2

An important aspect of the URL geology is that the main shaft and vent raise both intersect two major low-dipping thrust faults (referred to as fracture zones). These thrust faults divide the geology of the URL into three primary stress domains as shown in Figure 3.3. Of these thrust faults, Fracture Zone 2 (FZ2) is the most prominent. Below FZ2 the granite is mostly intact and relatively unaltered, and from FZ2 to the surface there exist several sub-vertical fracture sets (Everitt, et al. 1996).

The fracture zones intersected by the URL excavations serve as the main pathways for groundwater movement in the surrounding rock and have surface discharge points to the west of the URL site. FZ2 also marks the boundary between younger (glacial age) groundwater that is less saline (< 2g/L total dissolved solids (TDS)) and deeper pre-glacial age groundwater that is more saline (up to 90 g/L TDS). The shafts intersecting FZ2 may allow for an enhanced rate of mixing of the deeper more saline groundwater with the shallower less saline groundwater (Dixon, Martino and Onagi 2009).

Groundwater seepage from FZ2 into the main shaft occurs at discrete points in the cataclastic zone of FZ2 with almost no seepage observed immediately adjacent to it (Figure 3.4). The flow from FZ2 into the main shaft is significant, and during construction of the main shaft seal the rate of flow was measured to be approximately 250 L/day.

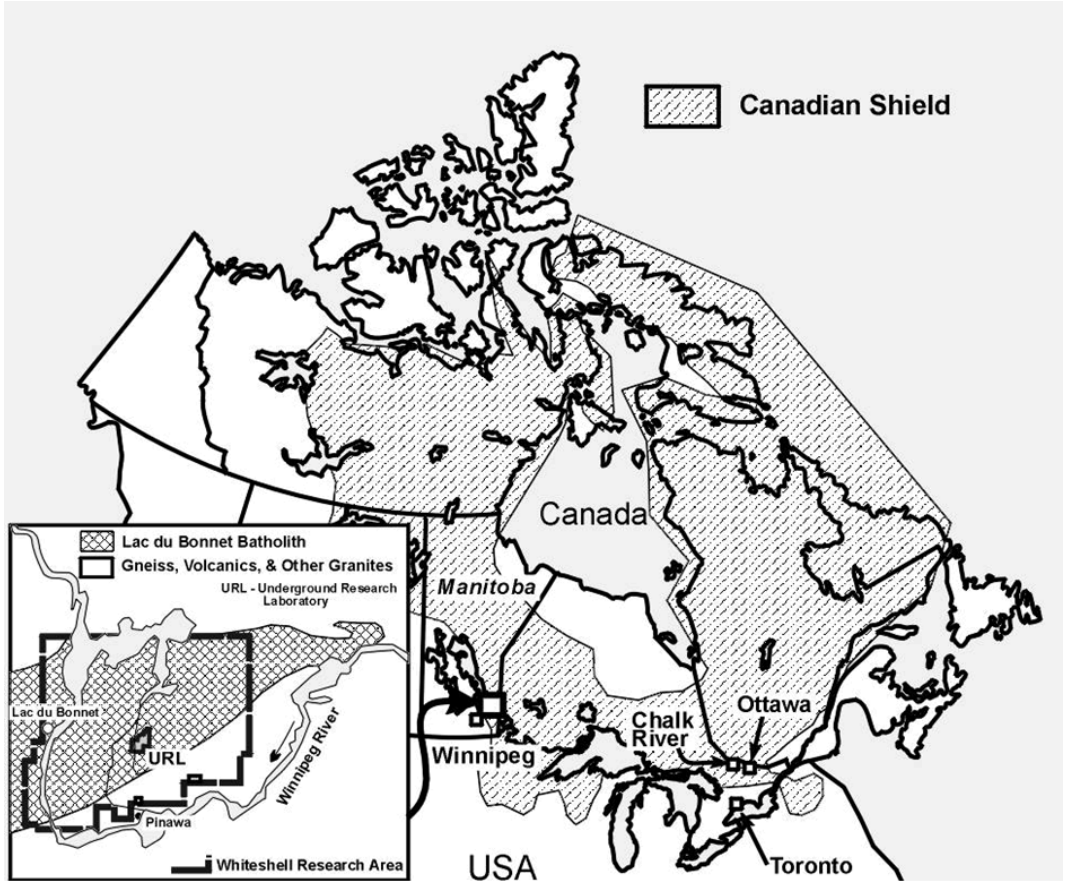


Figure 3.1: Map showing the location of the URL (AECL)

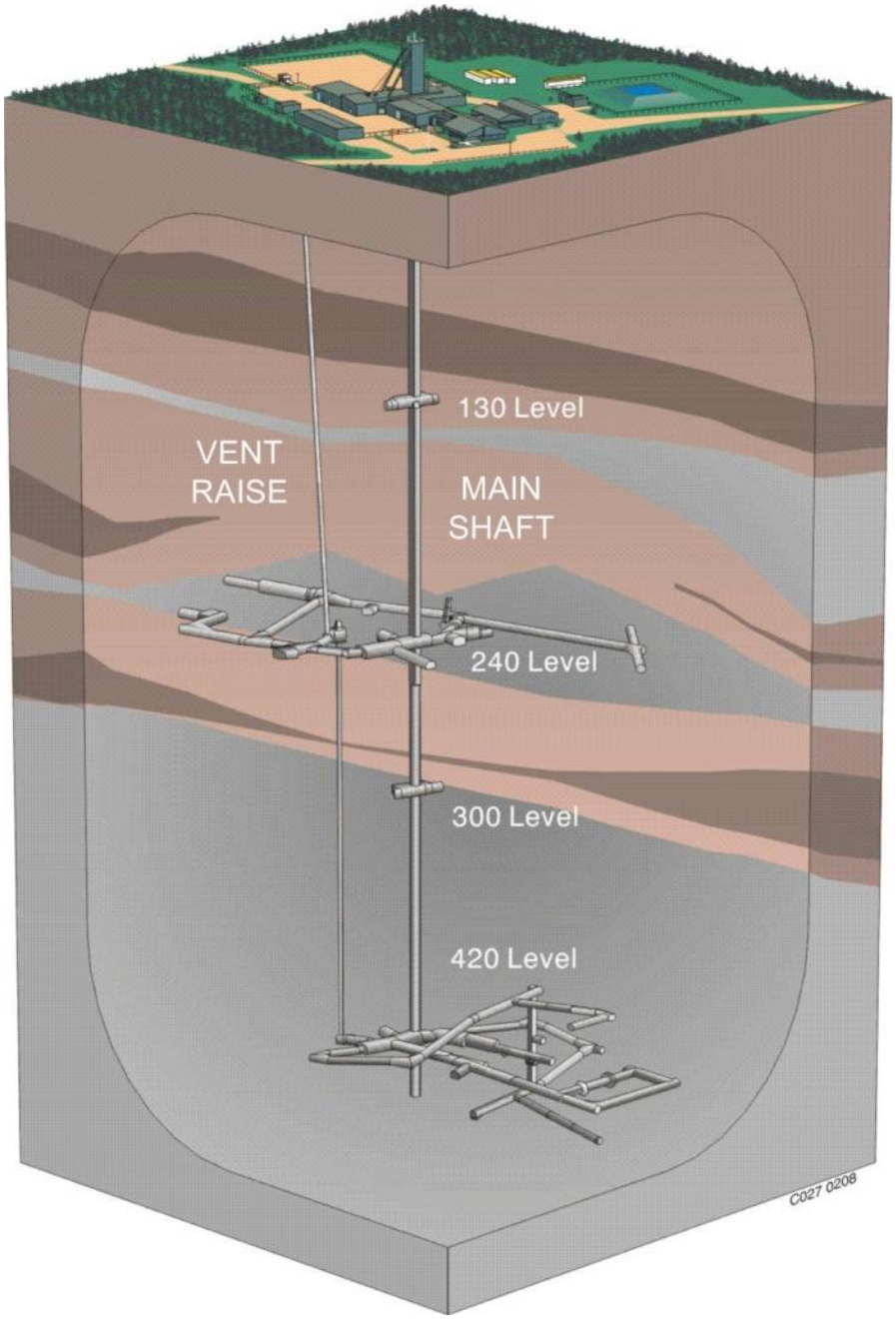


Figure 3.2: Layout of the URL (AECL)

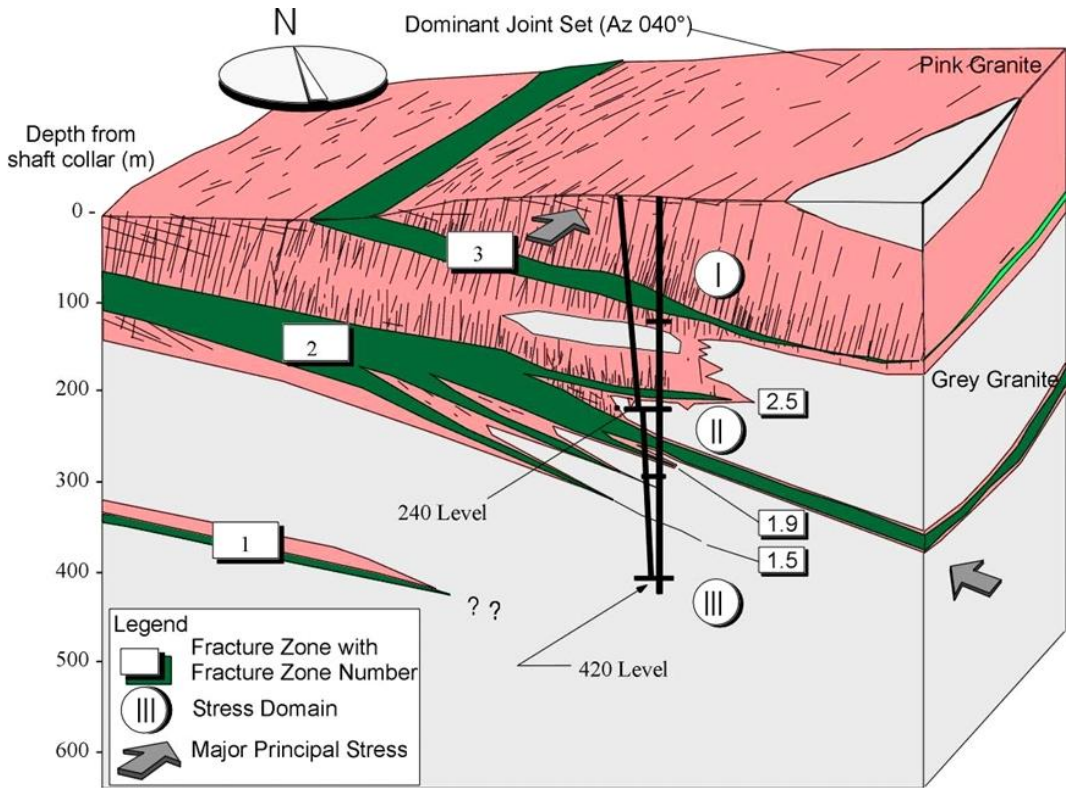


Figure 3.3: Local geology of the URL (AECL)

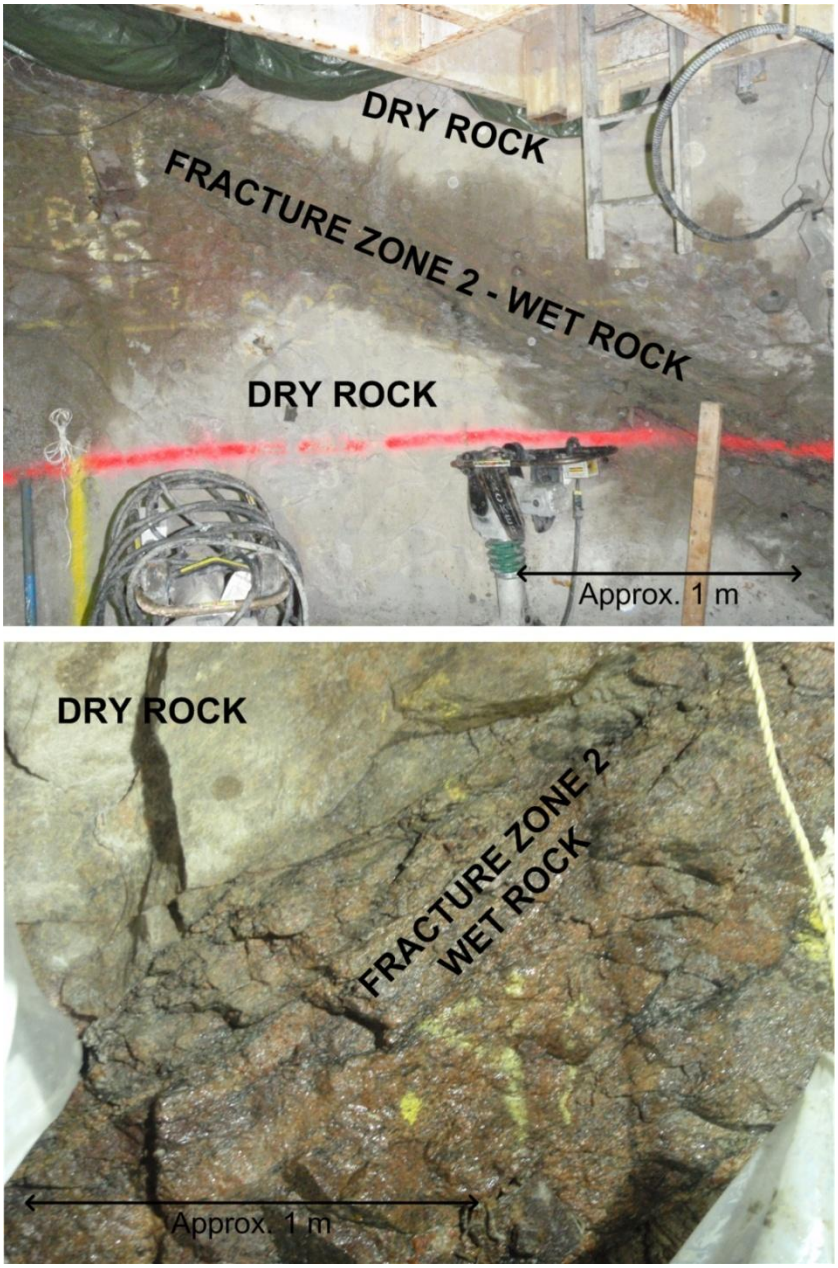


Figure 3.4: Examples of conspicuous groundwater flow into the main shaft from Fracture Zone 2 (AECL stock photographs)

# 4 SHAFT SEAL GEOMETRY, MATERIALS AND CONSTRUCTION

## 4.1 Shaft Seals at the Underground Research Laboratory

Two shaft seals were constructed as part of the decommissioning and closure of the URL to limit potential mixing of deeper saline groundwater with shallower less saline groundwater. One was constructed at the intersection of FZ2 and the vent raise, and the other was constructed at the intersection FZ2 and the main shaft. Both are located below the 240 Level at approximately 275 m depth (Figure 4.1). These shaft seals will from here forward be referred to as the *vent raise seal* and the *main shaft seal*, or simply the *shaft seal* in the case of the main shaft.

Both shaft seals are composite types, consisting of monolithic wedge shaped concrete components that are in direct contact with, and rigidly restrain, a swelling bentonite-sand core (Figure 1.3). FZ2 intersects the bentonite-sand core in both shaft seals. The high strength and rigidity of the concrete combined with the swelling capabilities of the compacted bentonite-sand provides a synergistic improvement in the performance of the seals (Kjartanson and Martino 2004). The bentonite-sand component provides *all* of the hydraulic sealing capabilities of the shaft and vent raise seals, as the concrete components were observed not to be water-tight along the concrete-rock interface due to concrete shrinkage during hydration.

### 4.1.1 The Main Shaft Seal

The main shaft seal consists of three primary components. These components are the lower 3-m-thick reinforced concrete component, the 6-m-thick *in situ* compacted bentonite-sand component, and the upper 3-m-thick unreinforced concrete component (Figure 4.2). The concrete components are keyed into the shaft walls to anchor them in place and restrain the swelling bentonite-sand component as it saturates. The keys were excavated 0.5 m into the shaft wall, and give the concrete components a conical frustum shape. The shaft diameter at the location of the seal is approximately 4.8 m with some variation due to breakout around the circumference of the shaft, especially in the area near FZ2. An isometric drawing of the completed main shaft seal is shown in Figure 4.3.

The main shaft seal contains sixty eight (68) monitoring instruments and is the focus of this thesis.

### 4.1.2 The Ventilation Raise Seal

The URL's vent raise is 1.8 m in diameter and it extends to the same depth as the main shaft, approximately 443m. The vent raise shaft seal consists of a lower 2-m-thick reinforced concrete component, a 5-m-thick compacted bentonite-sand component, and an upper 2-m-thick unreinforced concrete component. Similar to the main shaft seal, the concrete components have a 0.5 m key into the vent raise shaft wall and have a conical frustum shape. Unlike the main shaft seal, the bentonite-sand component is comprised of pre-fabricated

highly compacted bentonite-sand blocks. The bentonite-sand blocks were the same as those used in AECL's Tunnel Sealing Experiment.

The vent raise seal contains no instrumentation and will not be monitored following construction. Subsequently, the vent raise seal will not be discussed further in this thesis.

## 4.2 Shaft Seal Materials

### 4.2.1 Lower Concrete Component Materials

The lower concrete component of the shaft seal is composed of low heat (of hydration) high performance concrete (LHHPC) using of the same basic mix design as the concrete in AECL's Tunnel Sealing Experiment (Dixon, Martino and Onagi 2009). The low heat of hydration is desirable when placing high-mass structures and minimizes the effects of high curing temperature on the performance of the components, the host rock and the bentonite-sand barrier (Chandler, et al. 2002). The maximum temperature increase at the centre of the lower concrete component during hydration was approximately 16°C; which is typical for this concrete mix. Laboratory test results on cylindrical samples taken during the pour of the lower concrete component show an average 28-day strength of 49.2 MPa with a standard deviation of 5.5 MPa. The LHHPC concrete has a lower pH compared to conventional concrete and has little to no free lime ($Ca(OH)_2$, calcium hydroxide). This is advantageous since it will not have the adverse chemical reactions with the bentonite clay that occur with

contact with conventional concretes (Chandler, et al. 2002). The low heat of hydration, high strength and low pH make LHHPC an ideal material for shaft and tunnel seal construction. The lower component is comprised of approximately 75 $m^3$ of LHHPC

Two steel I-Beams (W410 x 132) are notched into the rock at the base of the shaft seal to hold the formwork that supported the weight of the lower concrete section as it cured. The formwork is based on the “sacrificial” bottom deck of the decommissioning Galloway stage (Figure 4.4) that was detached and secured to the steel beams as well as bolted to the shaft wall.

The lower concrete component contains a dense pattern of reinforcing bar. Three sizes of rebar were used, including 25M (25.2 mm), 30M (29.9 mm) and 35M (35.7 mm). The reinforcement was installed resting on top of the bottom formwork and is not anchored to the rock. However, the reinforcement does extend into the key blasted into the rock to create the conical shape of the concrete component. This reinforcement was designed using safety factors and assuming the bottom concrete component will support the entire weight of the bentonite-sand, the top concrete component and a 270 m column of water after the shaft has flooded (Dixon, Martino and Onagi 2009). Figure 4.5 shows a top view of the completed rebar for the lower concrete component.

### 4.2.2 Bentonite-Sand Component Materials

The bentonite-sand material used to construct the core of the shaft seal is a mixture, by mass, of 40% Wyoming sodium bentonite and 60% washed quartz sand aggregate (40-60 blend). Blending of the 40-60 material was accomplished on the URL site using a concrete batching truck (Figure 4.6). The blended material was placed into lined bags in quantities of approximately 1 Mg and stored until required for the shaft seal construction (Figure 4.7). Approximately 250 Mg of material was blended and bagged in a two day period.

Previous research at AECL (Dixon, Gray and Thomas 1985) has shown the attainable dry density (~1800 kg/m$^3$) of a 40-60 blend is relatively insensitive to water content if the water content is less than the “optimum”. This property was very desirable when placing the large quantity of bentonite-sand in the shaft seal, since moisture reconditioning (drying/wettings of the material) was not required. Also, having a 60% sand fraction will not adversely affect the maximum swelling pressure achievable by the material, which is expected to be between 400 and 800 kPa.

### 4.2.3 Upper Concrete Component Materials

The upper concrete component contains no reinforcement. It is a massive concrete structure comprised of approximately 72 m$^3$ of LHHPC of the same mix design used for the lower concrete component. The maximum temperature rise during hydration in the centre of the upper concrete component was 18.6°C.

Laboratory test results on cylindrical samples taken during the pour of the lower concrete section show an average 28-day strength of 52.2 MPa with a standard deviation of 4.5 MPa. The use of LHHPC offers the same benefits mentioned in Section 4.2.1.

The upper concrete component did not require any formwork since it was confined by the top of the bentonite-sand component and the shaft wall.

## 4.3 Shaft Seal Construction

### 4.3.2 Lower Concrete Component Construction

The first step was to excavate the key for the lower concrete component. This was done by line drilling a 0.5 m deep ring around the top of the key. Then drill and blast techniques were use to excavate the rock and create the conical frustum shape of the component. Line drilling allowed for minimal amounts of explosives to be used, thereby minimizing the generation of, and subsequent influence of, an EDZ in the area near the shaft seal.

Following excavation of the key, the two support beams for the steel formwork were notched into the rock and the sacrificial bottom deck of the Galloway stage was bolted to them; the Galloway stage is attached to the bottom of the support beams and served as the formwork for the concrete pour. Then LHHPC was poured on top of the formwork until the support beams were completely covered.

This provided a level surface on which to construct the reinforcement for the lower concrete component.

The reinforcement was installed after the levelling pour of LHHPC had sufficiently hardened to allow standing on it. The reinforcement was designed by a structural engineer and installed by a contractor.

After the installation of the reinforcement was complete, the concrete was poured continuously over a 28 hour period starting on September 1, 2009. Having one continuous pour ensured that no joints were present in the finished concrete component. The concrete was mixed on surface using the mixer located in the URL's Concrete Lab, then transported down the shaft in a concrete delivery bucket. The bucket was outfitted with a flexible rubber chute that extended through the centre of the Galloway stage and allowed the concrete to be evenly poured across the rebar (Figure 4.8). It was important to distribute the concrete evenly during the pour because the rebar is very closely spaced and inhibited its flow. The rubber chute also made it possible to pour the concrete precisely in order to avoid areas where instruments were installed, and thereby avoiding potential damage to them (Figure 4.9). The concrete cured for 36 days before commencing the installation of the bentonite-sand component.

### 4.3.2 Bentonite-Sand Component Construction

The bentonite-sand component was installed in lifts using *in situ* compaction. The bulk material was transported to the shaft seal using the URL's concrete

delivery bucket. This bucket has a lever-actuated door at its base, which allowed the material to be dumped in a loose pile (Figure 4.10). The material was then manually spread and levelled before compaction (Figure 4.11). Compaction was accomplished using two electric Wacker vibratory rammer compactors (Figure 4.12) for the majority of the area, and a smaller Hilti impact hammer (Figure 4.13) in tighter areas. The Hilti impact hammer had interchangeable compaction feet and was especially useful around the perimeter of the seal and near the instrument cables (Figure 4.14). Each load of material was approximately 2000 kg, which resulted in a final compacted height of approximately 5 cm per lift.

After each lift was completed the diameter of the shaft at that elevation was measured in four (4) directions, and the final lift thickness was measured at five (5) points using elevation reference lines (Figure 4.15). Taking these measurements allowed the final compacted density of each lift to be estimated.

The bentonite-sand component of the seal contains a total of 217.2 Mg of bentonite-sand material, and has a volume of approximately 107.1 $m^3$. This leads to an estimated bulk density of 2028.3 $kg/m^3$ and a dry density of 1810 $kg/m^3$, assuming an average gravimetric water content of 12.1%. The target dry density of the bentonite-sand core material was 1800 $kg/m^3$. At top view of the completed bentonite-sand component is shown in Figure 4.16.

### 4.3.2 Upper Concrete Component Construction

Similarly to the lower concrete component, the first stage in constructing the upper concrete component was to excavate the 0.5 m key around the circumference of the shaft; excavation of the keys was completed at the same time for both concrete components. This was again done by line drilling to 0.5 m depth followed by drill and blast excavation.

The construction of the upper concrete component was very simple compared to the lower component. The upper component contains no rebar and did not require a formwork, since the top of the bentonite-sand component and the shaft wall define the edges of the upper component.

The concrete was poured continuously over a 24 hour period starting on November 25, 2009. Having one continuous pour ensured that no joints would be present in the finished component. A flexible rubber chute was used to direct the flow of concrete out of the bucket, creating an even pour and avoiding causing damage to the instruments (Figure 4.17). Construction of the main shaft seal was complete at the end of this pour.

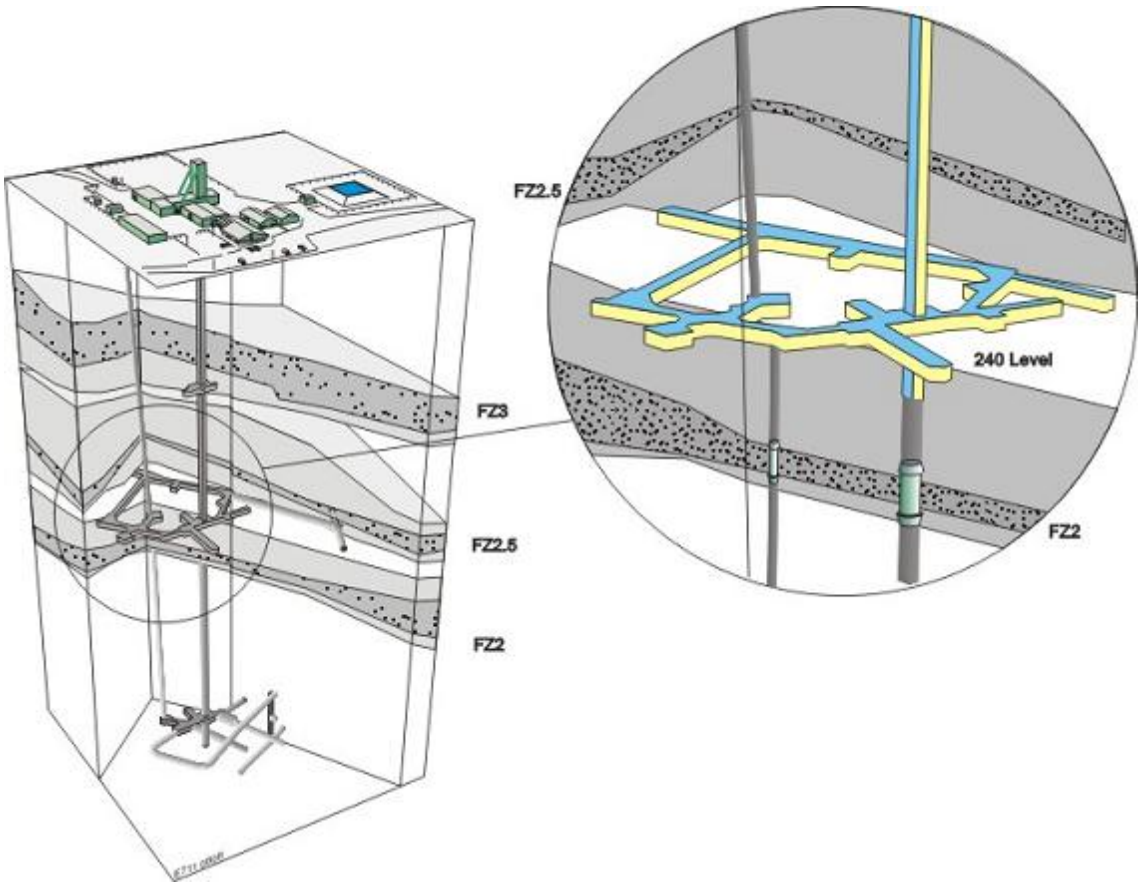


Figure 4.1: Location of the URL shaft seals (AECL)

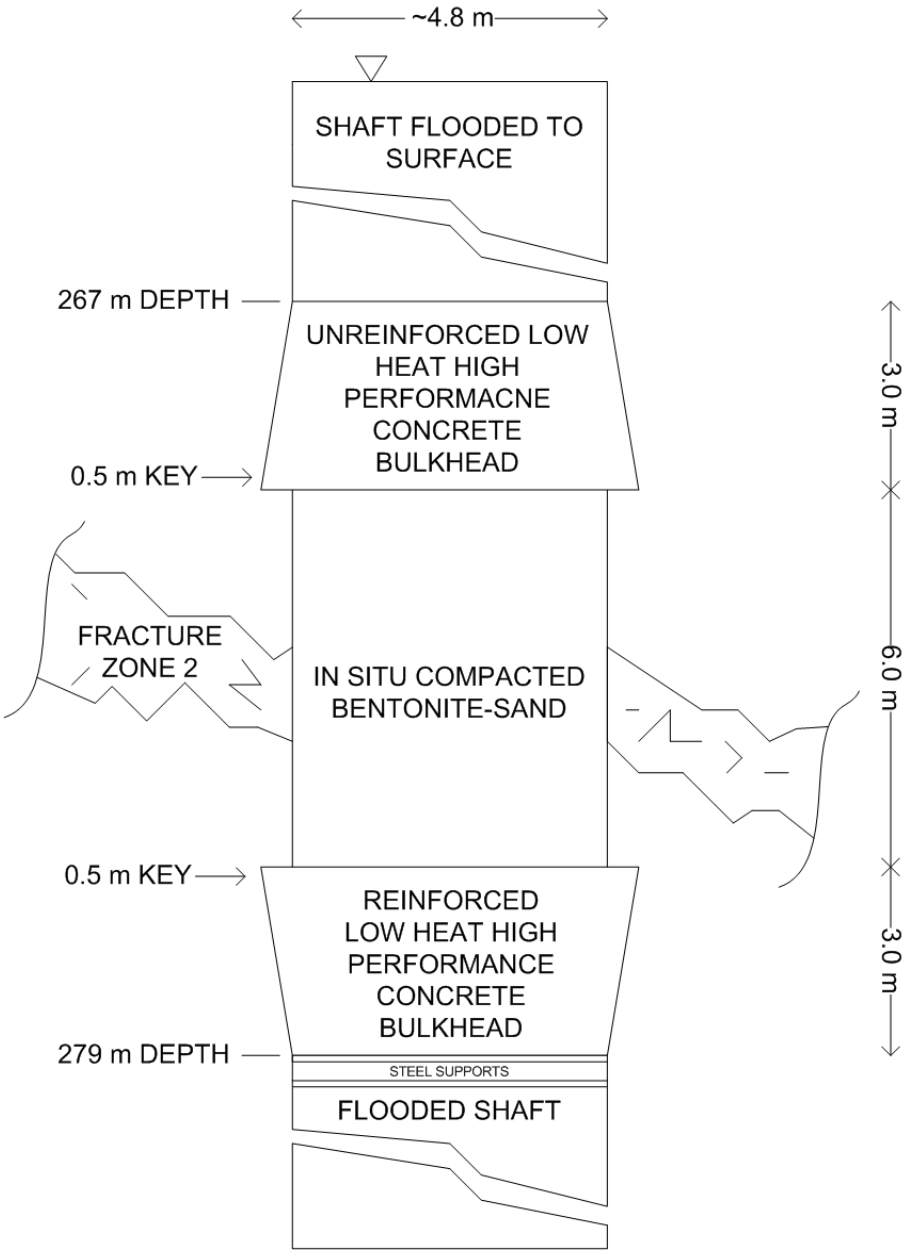


Figure 4.2: Schematic of the Main Shaft Seal

Figure 4.2 created by Blake Holowick

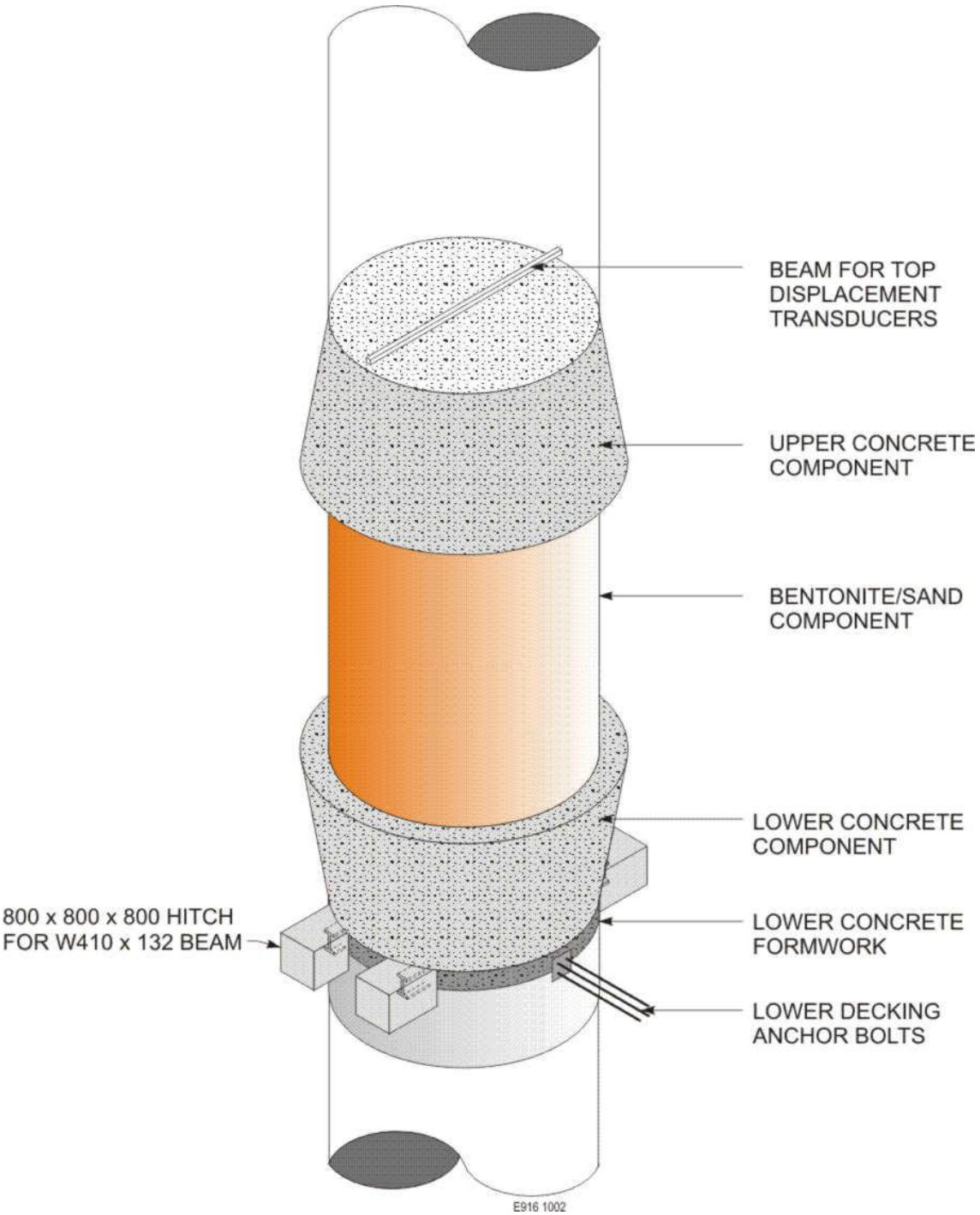


Figure 4.3: Isometric view of the main shaft seal (AECL)

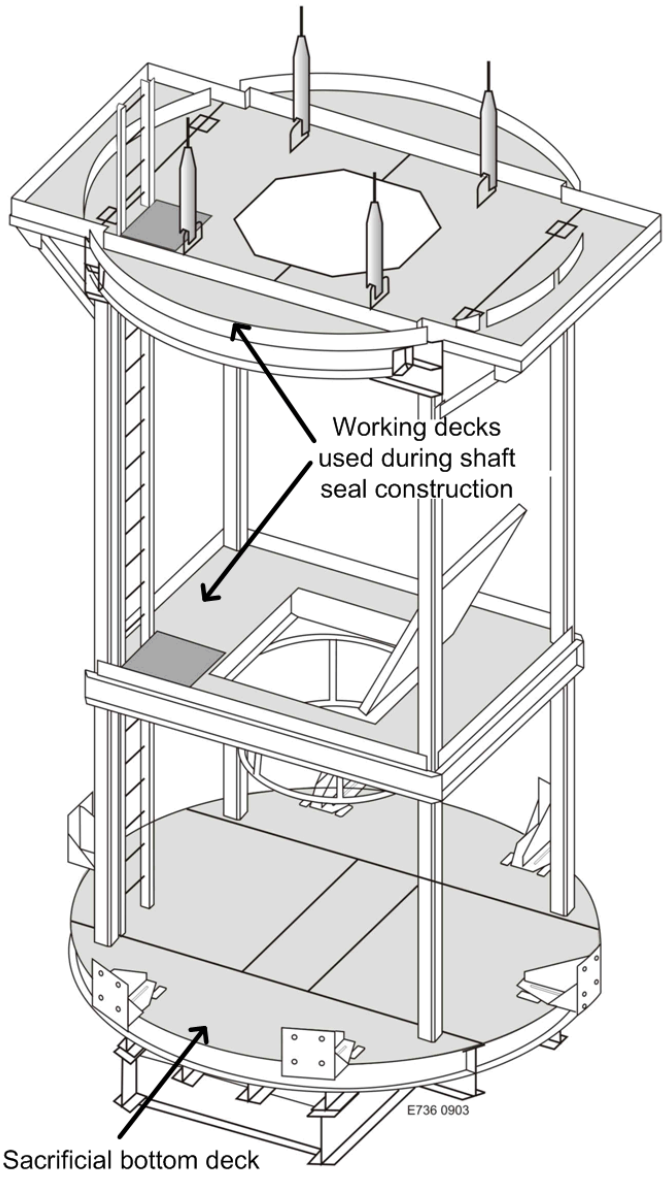


Figure 4.4: Galloway stage showing sacrificial bottom deck and working decks (AECL)


Figure 4.5: Top view of rebar in the bottom concrete component (AECL stock photograph)


Figure 4.6: Loading the batching truck used to mix bentonite-sand material (AECL stock photograph)



Figure 4.7: Storage of bentonite-sand material (AECL stock photograph)

Figure 4.8: Lowering the concrete bucket with flexible rubber chute through the Galloway stage (AECL stock photograph)



Figure 4.9: Pouring concrete using the flexible rubber chute (AECL stock photograph)

Figure 4.10: Dumping a load of bentonite-sand material (AECL stock photograph)



Figure 4.11: Spreading and leveling bentonite-sand material (AECL stock photograph)

Figure 4.12: Wacker vibratory rammer compactor (AECL stock photograph)



Figure 4.13: Hilti impact hammer used for compaction (AECL stock photograph)


Figure 4.14: Impact hammer compaction foot used near instrument cables (AECL stock photograph)



Figure 4.15: Surveying elevation reference lines during bentonite-sand construction (AECL stock photograph)

Figure 4.16: Top view of the completed bentonite-sand component (AECL stock photograph)



Figure 4.17: Partially completed pour of the upper concrete component showing instrument support cables (AECL stock photograph)

# 5 INSTRUMENTATION AND MONITORING

## 5.1 Introduction

A total of sixty eight (68) monitoring instruments were installed in and around the shaft seal. These instruments comprise a total of one hundred (100) sensors, as some instruments contain a primary sensor plus a temperature sensor. The instruments were installed in the upper and lower concrete components, the bentonite-sand component and in the rock adjacent to the shaft seal. Parameters being monitored include temperature, pore-water pressure, total pressure, soil suction/water content, concrete strain and vertical displacement.

The shaft seal presents a situation similar to that of a seal installed in a future post-closure deep geologic repository (DGR), and therefore provides an opportunity to test instrumentation and monitoring techniques that may be employed in a future DGR. The shaft seal at the URL is the first functional full-scale composite seal to be instrumented, and provides an excellent opportunity to assess the robustness and functionality of a large number of instruments installed at depth under high confining (swelling) pressures and high hydraulic head.

The instruments were chosen, and the layout designed, with four primary focuses in mind:

- Maintain the ability to monitor the shaft seal after the URL is fully decommissioned.
- Monitor the hydration temperatures and shrinkage of the concrete segments.
- Monitor the saturation and swelling of the bentonite-sand sealing component.
- Monitor the pore-water pressures in the nearby rock.

Table 5.1 shows a complete list of the instrument technologies installed.

The instruments installed in the ESP are mostly conventional geotechnical instrumentation used in typical near-surface applications. The major difference with the ESP is the instruments need to maintain functionality under high hydraulic (2.7 MPa) and swelling pressures (up to 800 kPa), and there had to be mechanisms in place to monitor and control them at an installed depth of approximately 275 m. These difficulties were overcome by choosing instruments capable of operating under high pressure (5 MPa), using instruments capable of operating with long cables (>300 m) and installing remote dataloggers at 240 m depth with communications to the surface.

## 5.2 Instrument Locations

Tables and diagrams detailing the location of each installed instrument can be found in Appendix A and Appendix B, respectively.

### 5.2.1 Methodology for Placing the Instruments

The instruments installed in the shaft seal are divided into four main groups, those installed in the lower concrete component, the bentonite-sand component, the upper concrete component and the adjacent rock. This section of the report describes the parameters being monitored and the methodology used when designing the instrument layout.

#### *5.2.1.1 Instrument Placement in the Lower Concrete Section*

The lower concrete component is instrumented to allow for monitoring of:

- The temperature rise during concrete hydration.
- The concrete strain. Shrinkage of the concrete as it hydrates, and strain caused by the subsequent bentonite swelling load.
- Water pressure along the concrete-rock interface.

The hydration temperature rise was monitored by five (5) thermocouples installed at the interior of the lower concrete component, as well as the three (3) vibrating wire piezometers installed around its perimeter; note that vibrating wire piezometers contain thermistors. The thermocouples and vibrating wire piezometers were placed in a pattern that allowed the thermal gradient from the centre of the concrete to its periphery to be measured.

The concrete strain is monitored in the horizontal and vertical directions. The horizontal strain is measured approximately 0.5 m from the top and bottom of the

lower concrete component, and is facilitated by strain gauges oriented along both horizontal axes. A horizontally oriented strain gauge with a 1 m active length is located 0.62 m from the base of the concrete, and two (2) horizontal strain gauges with 3 m active lengths are oriented perpendicular to each other 0.5 m from the top of the concrete. The vertical strain is measured by two (2) vertically oriented strain gauges with 1 m active lengths. They are located 0.15 m and 2.0 m from the shaft centreline, and are centre about the mid-height of the lower concrete component.

The water pressure along the concrete-rock interface is monitored by three (3) vibrating wire piezometers. They are placed at different elevations with roughly 120° angular spacing between them around the circumference of the shaft. This placement should provide a good understanding of the hydraulic pressures along this interface.

#### *5.2.1.2 Instrument Placement in the Bentonite-Sand Component*

The bentonite-sand component is instrumented to allow for the monitoring of:

- Wetting up of the bentonite-sand resulting from the inflow of groundwater.
- Swelling pressures at the clay-concrete and clay-rock interfaces.
- Swelling pressures at the interior of the bentonite-sand.
- Pore-water pressures at the bentonite-sands interior and near its edges.

The degree of saturation of the bentonite-sand component is monitored by measuring suction and volumetric water content. The suction of the bentonite-sand is monitored by fourteen (14) thermocouple psychrometers (or simply psychrometers); suction is related to the relative humidity in the soil. The psychrometers are monitored by a datalogger located on the 240 Level that will no longer be operational once the 240 Level has flooded. Therefore the operational lifespan of the psychrometers will be limited to an estimated 10 to 14 years, which is the estimated time for passive flooding of the 240 Level (Dixon, Martino and Onagi 2009). Based on these estimates, the psychrometers were placed mainly around the periphery of the bentonite-sand component since this area will be the first to saturate. Located closer to the core of the bentonite-sand component are four (4) time domain reflectometry (TDR) probes that provide direct measurement of the volumetric water content of the material. The TDRs are monitored by a datalogger located on the 240 Level that is encased in a watertight steel caisson that will allow it to operate indefinitely. Since the TDRs are expected to be operational past the lifespan of the psychrometers they were placed in locations that should saturate later in the evolution of the seal.

The total pressure exerted by the swelling bentonite-sand is measured at the edges of the bentonite-sand component (i.e. the clay-rock and clay-concrete interfaces). This is accomplished by installing total pressure cells (TPC) at these interfaces. The TPCs located at the upper and lower clay-concrete interfaces are of the vibrating wire type, since these instruments can also collect data regarding

the temperature of the concrete. One vibrating wire TPC is located at the centre of the lower clay-concrete interface, and two (2) are located at the upper clay-concrete interface. All of them are rigidly attached to the concrete components.

The swelling pressure at the clay-rock interface is measured by three (3) fibre optic TPCs located at 1 m, 3 m and 5 m heights from the base of the bentonite-sand component. They are positioned above one another, and will provide an understanding of the horizontal swelling pressure distribution along a vertical line. Fibre optic TPCs (with no temperature monitoring) were installed at the clay-rock interface because it is expected to be thermally stable and temperature measurement is therefore not required.

The swelling pressure at the interior of the bentonite-sand component is measured by two (2) fibre optic TPCs. These are located near the centreline of the shaft at 3 m and 5 m elevations above the base of the bentonite-sand component. These locations will provide an understanding of how the swelling pressure varies from the centre of the bentonite-sand component to its edge.

The pore-water pressure in the bentonite-sand is measured by eight (8) piezometers (5 fibre optic, 3 vibrating wire). The piezometers are placed throughout the bentonite-sand component to give an indication of the pore-water pressure gradients in both the horizontal and vertical directions. The vibrating wire piezometers were placed close to the concrete components to provide information about heat transfer to the bentonite-sand during concrete hydration.

The fibre optic piezometers are located farther away from the concrete in thermally stable locations.

#### *5.2.1.3 Instrument Placement in the Upper Concrete Component*

The upper concrete component is instrumented to allow for the monitoring of:

- The temperature rise during concrete hydration.
- The concrete strain. Shrinkage of the concrete as it hydrates, and strain cause by the subsequent bentonite swelling and shaft flooding loads.
- Water pressure along the concrete-rock interface.
- Total pressure at the concrete-rock interface.
- Vertical displacement of the upper concrete component.
- The head of water above the shaft seal.

The temperature rise caused by concrete hydration was monitored by five (5) thermocouples installed at the interior of the lower concrete component, as well as the five (5) vibrating wire piezometers, four (4) vibrating wire TPCs and a psychrometer. The instruments that are not thermocouples were installed at or near the concrete perimeter, and provide temperature data since vibrating wire instruments contain thermistors and psychrometers contain thermocouples. The thermocouples and other instruments allow the thermal gradient from the centre of the concrete to its periphery to be measured. The large number of instruments

monitoring the temperature of the upper concrete provided a very clear picture of the temperature rise during hydration.

The concrete strain is monitored in the horizontal and vertical directions. A horizontally oriented strain gauge with a 3 m active length is located 0.5 m from the base of the concrete, and two (2) horizontal strain gauges with 3 m active lengths are oriented perpendicular to each other 0.5 m from the top of the concrete. The vertical strain is measured by two (2) vertically oriented strain gauges with 1 m active lengths, located 0.5 m and 1.5 m from the shaft centreline. The vertical strain gauges are located at approximately mid-height of the upper concrete component. One of the vertical strain gauges was originally planned to be at the centre of the upper concrete component, but was moved to allow concrete to be poured at this location.

The water pressure along the concrete-rock interface is monitored by three (3) vibrating wire piezometers. The piezometers were placed at different elevations with 120° spacing between them around the circumference of the shaft. This placement should provide a good understanding of the hydraulic pressure along this interface.

The head of water above the shaft seal is measured by a single vibrating wire piezometer mounted on the top surface of the upper concrete component. This instrument will provide useful data for estimating the time until the 240 Level floods and indicate when the shaft is fully flooded.

The total pressure at the concrete-rock interface is measured by two (2) vibrating wire TPCs. They are located at mid-height of the upper concrete component and are positioned 90° apart. The TPCs are rigidly mounted to the rock wall. The placement of the instruments will allow the total pressure on the upper concrete key to be monitored as the bentonite-sand swells.

The vertical displacement of the upper concrete component is monitored by two (2) fibre optic displacement transducers installed on a rigid beam directly above the shaft seal. The moveable plungers on the displacement transducers are secured to the top surface of the upper concrete component and allow for very fine measurement of its vertical displacement. One of the instruments is located near the centre of the shaft seal and the other is located close to its edge. This placement makes it possible to monitor any tilting of the upper concrete component as it displaces.

#### *5.2.1.4 Instrument Placement in the Adjacent Rock*

The rock immediately adjacent to the shaft seal is only monitored for pore-water pressure. This is accomplished by vibrating wire piezometers attached to three (3) horizontal borehole packers located 4.5 m from the base of the bentonite-sand section. The packers extend 0.5 m, 1.0 m and 1.85 m horizontally into the host rock. They are located above FZ2 and do not intersect it. These instruments will provide insight into the pore-water pressure response in the near

field rock as the regional groundwater table rebounds and the bentonite-sand component saturates and swells.

### 5.2.2 Deviation from the Instrument Layout Design

A detailed instrumentation layout was created by Dixon, Martino and Onagi (2009) that specified the design location for each instrument to be installed in the shaft seal. However, the instrument layout was changed after the first day of instrument installations in the bentonite-sand component due to the excessive water inflow in the southern portion of the shaft. The water inflow made it difficult to install the instruments near the south wall of the shaft. Also, if psychrometers were installed in the areas experiencing high inflow of water there was a risk they could be saturated immediately after installation. During the initial construction of the bentonite-sand component it was noticed that there was substantially less water inflow along the northern shaft wall. Therefore, the instrument layout in the bentonite-sand component was mirrored along the east-west shaft axis, with the instruments in the southern half of the shaft moved to the northern half. Having the instruments installed in the northern half of the bentonite-sand component made their installation easier and will allow the gradual evolution of the shaft seal to be monitored more effectively.

The design locations by Dixon, Martino and Onagi (2009) assumed a circular 5 m diameter shaft and concrete keys blasted precisely to 0.5 m depth. Due to the method of shaft excavation and the nature of the host rock, the shaft is not exactly circular and its diameter generally varies from 4.8 m to 5.0 m. Also, in

the time since the main shaft was first excavated, rock has spalled off the walls and has made the diameter up 0.30 m greater in some areas. More significantly, the area with the greatest loss of rock is in close proximity to FZ2 at the location of the shaft seal. This rock is highly fractured and in some cases rubblized, allowing the shaft diameter to increase as the result of rocks gradually falling out of these regions over the 30 years since the shaft was originally constructed. Therefore, when installing the instruments the relative *position* of each modified design location was followed. For example, if an instrument was specified for installation 2.4 m from the shaft centreline (i.e. 0.1 m from the shaft wall in an ideal 5 m wide shaft) then it was installed 0.1 m from the shaft wall, even though this may have resulted in it being 2.3 m from the shaft centreline.

The location of each instrument was accurately measured to the centreline of the main shaft after installation because of the necessary deviations from the design layout. These measurements were then used to create the as-built layout drawings included in Appendix B.

### 5.3 Instrument Type and Operation Principle

The section will describe the principle of operation for each instrument type and comment on why it is suited for use in the ESP.

### 5.3.1 Thermocouples

The thermocouples used in the ESP are model TH-TC Type T (copper-constantan) supplied by Roctest. They have 60 m extension wires consisting of 24 AWG solid conductors and were supplied in stainless steel housings with 3/8" Swagelok fittings (Figure 5.1).

Thermocouples measure temperature using the Seebeck effect (McGee 1988). When a conductor is subjected to a thermal gradient it will produce a voltage, and if two different metals are subjected to the same thermal gradient they will produce different voltages. By joining these two different conductors a circuit is created with two junctions that produces a measurable microvolt output (Figure 5.2). The magnitude of the voltage produced is directly related to the temperature difference between the reference junction, located in the datalogger, and the sensing junction located in the instrument. If the temperature of the reference junction is known the temperature at the sensing junction can be calculated using a standard relationship for Type T thermocouples.

### 5.3.2 Vibrating Wire Piezometers

The vibrating wire piezometers (VWPZ) installed in the ESP are Roctest model PWF with thick-wall stainless steel housings and stainless steel filters. They are designed with an operating range up to 5 MPa. All of the VWPZs were delivered from the manufacturer complete with 350 m of stainless steel jacketed 22 AWG two shielded pair cable.

Vibrating wire piezometers measure hydraulic pressure and operate by measuring the resonant frequency of a “piano wire” under tension (Roctest Ltd. 2005a). The piano wire is attached to a flexible stainless steel diaphragm at one end and rigidly held in place by wire grips at the other end (Figure 5.3). The fluid surrounding the instrument (i.e. soil pore-fluid or water) is in contact with the diaphragm and causes it to flex with changing fluid pressures. As the diaphragm flexes the tension in the piano wire will change. This tension is directly proportional to the square of the resonant frequency of the wire. Plucking voltages spanning the piano wire’s natural frequencies are applied to an electromagnetic coil located near the wire and cause it to vibrate. Once the application of the plucking voltage is stopped the wire will continue to vibrate at its resonant frequency. This vibration generates a voltage in the electromagnetic coil which is read by the datalogger. This signal can be related to the hydraulic pressure contacting the diaphragm by applying the instrument’s calibration equation to the raw frequency reading.

Roctest model PWF vibrating wire piezometers contain a 3 kΩ thermistor. The resistance of the thermistor varies with its temperature and can be converted to a temperature reading using a standard equation. The temperature of the vibrating wire piezometer must be recorded since it is required to apply a correction for the temperature of the instrument to the pressure data.

A major advantage to using vibrating wire technology in the ESP is the signal frequency is not affected by line impedance and long cable lengths can be used with limited signal degradation (Roctest Ltd. 2005a).

### 5.3.3 Vibrating Wire Total Pressure Cells

The vibrating wire total pressure cells (VWTPC) installed in the ESP are Roctest model TPC with stainless steel housings and a 229 mm diameter sensing pad (Figure 5.4). They are designed with an operating range up to 5 MPa and have 350 m of stainless steel jacketed 22 AWG two shielded pair cable.

Vibrating wire total pressure cells measure the total pressures (swelling pressure plus pore-water pressure) acting at the clay-concrete and concrete-rock interfaces of the shaft seal. The VWTPCs consist of a sensing pad connected to a vibrating wire pressure transducer via a stainless steel tube. The sensing pad is comprised of two welded stainless steel discs. The sensing pad and the stainless steel tube are filled with oil that is in contact with the diaphragm of the vibrating wire pressure sensor. As pressure is applied to the sensing pad both of the steel discs deform and thereby transmit pressure to the oil and hence to the vibrating wire sensor diaphragm. The operation of the vibrating wire sensor on the VWTPCs is exactly the same as in vibrating wire piezometers. It involves plucking a piano wire and measuring its resonant frequency (Roctest Ltd. 2005b). Using the instruments calibration equation this frequency can be related to the total pressure applied to the sensing pad.

One advantage of using this technology is the pressure measured by the device is the average pressure over the surface area of a relatively large sensing pad. This avoids any artificially high readings that may be measured by devices with smaller sensing pads, because the large sensing surface gives a more representative value for total pressure. For example, the high pressures from point contacts with aggregate in the bentonite-sand are averaged with the lower contact pressure from the clay portion of the material.

Roctest model TPC vibrating wire total pressure cells contain a 3 kΩ thermistor. The resistance of the thermistor varies with its temperature and can be converted to a temperature reading using a standard equation. The temperature of the instrument must be recorded since it is used to temperature correct the data when applying the calibration equation.

A major advantage to using vibrating wire technology in the ESP is the signal frequency is not affected by line impedance and long cable lengths can be used with no signal degradation (Roctest Ltd. 2005b).

### 5.3.4 Packers with Vibrating Wire Piezometers

The measurement of pore-water pressures in the rock adjacent to the shaft seal is accomplished using mechanical packers with attached Geokon model 4500 vibrating wire piezometers. The Geokon 4500s originally had 3 m long cables. These were extended to 350 m using a Geokon cable splicing kit and 22 AWG two shielded pair extension cable. The piezometers feature a 1/4" Swagelok

fitting on the sensing end which allowed them to be easily connected to the borehole packers.

The Geokon vibrating wire piezometers measure hydraulic pressure by monitoring the resonant frequency of a steel wire under tension (Geokon Inc. 1993). Their principle of operation is the exact same as described in Section 5.3.2

Mechanical packers are used to isolate areas of rock at different depths for pore-water pressure measurement; Figure 5.5 shows a diagram of a packer installation. A mechanical packer is installed by inserting it into a borehole and turning the tightening nut to move the thrust pipe and compress the rubber gland, which causes it to expand radially. The tightening nut is turned until the rubber gland is in complete contact with the borehole wall and provides a watertight seal. There are three packers installed in three boreholes with horizontal depths of 0.5 m, 1.0 m and 1.85 m In the ESP. These packers and piezometers will provide a view of the horizontal pore-water pressure gradient in close proximity to the shaft seal. The packers were designed, constructed and installed by URL technical staff (Figure 5.6).

### 5.3.5 Fibre Optic Piezometers

The fibre optic piezometers (FOPZ) installed in the ESP are Roctest model FOP-F with thick-wall stainless steel housings and stainless steel filters. They are designed with an operating range up to 5 MPa. All of the FOPZs were delivered

from the manufacturer complete with 350 m Kevlar reinforced polyurethane jacketed cable.

The fibre optic piezometers in the ESP measure the pore-water pressure in the bentonite-sand component. FOPZs operate by measuring the length of a Fabry-Perot cavity created by the inner surface of a stainless steel diaphragm and the tip of a cleaved optical fibre (Figure 5.7). A light signal is sent from the signal conditioner and when it reaches the end of the optical fibre in the instrument, part of it is reflected by the end of the fibre and part is transmitted into the Fabry-Perot cavity and then reflected by the stainless steel diaphragm. These two reflected signals interfere with each other and create an interferometric signal that is related to the length of the Fabry-Perot cavity (Rao, et al. 1994). This signal is then interpreted by the signal conditioner and the displacement of the stainless steel diaphragm is determined. The displacement of the diaphragm is then related to the applied pressure using a calibration equation (Roctest Ltd. 2000a).

A major advantage of fibre optic instruments is they are not affected by electromagnetic interference. They are not affected by lightning strikes and their cables can be run in close proximity to power cables. They are also capable of operating with very long cable lengths (up to 2 km). These properties were very desirable for the ESP.

One disadvantage is that they do not measure temperature. The pressure readings are slightly affected by temperature and Roctest does supply a temperature correction factor. However, since the actual temperature of the

instrument is not measured, the application of a temperature correction can be difficult in applications with varying temperatures. That being said, the temperature of the shaft seal will reach equilibrium with the surrounding rock soon after construction and is expected to remain essentially stable.

### 5.3.6 Fibre Optic Total Pressure Cells

The fibre optic total pressure cells (FOTPC) installed are Roctest model FO-TPC with stainless steel housings and 229 mm sensing pads. They are designed with an operating range up to 5 MPa. All of the FOTPCs were delivered from the manufacturer complete with 350 m Kevlar reinforced polyurethane jacketed cable.

Fibre optic total pressure cells are used to measure the total pressure (swelling pressure and pore-water pressure) acting in the bentonite-sand and at the clay-rock interface. The FOTPCs consist of a sensing pad connected to a fibre optic pressure sensor via a stainless steel tube. The sensing pad is comprised of two welded stainless steel discs. The sensing pad and the stainless steel tube are filled with oil that is in contact with the diaphragm of the fibre optic pressure sensor. As pressure is applied to the sensing pad both of the steel discs will deform transmitting pressure to the oil and then to the diaphragm. The operation of the fibre optic pressure sensor on the FOTPCs is the same as the FOPZs, with the Fabry-Perot cavity length being related to applied total pressure (Roctest Ltd. 2000b).

One advantage of using this technology is the pressure measured by the device is averaged over the surface area a relatively large sensing pad. This avoids any artificially high readings that may be measured by devices with smaller sensing pads, since the large sensing surface gives a more representative value for total pressure. For example, the high pressures from point contacts with aggregate in the bentonite-sand are averaged with the lower contact pressure from the clay portion of the material.

A major advantage of fibre optic instruments is that they are immune to electromagnetic interference. They are not affected by lightning strikes and their cables can be run in close proximity to power cables. They are also capable of operating with very long cable lengths (up to 2 km). These properties were very desirable for the ESP.

Similar to the FOPZs, the FOTPCs do not contain an internal temperature sensor and therefore corrections for temperature effects cannot be made. However, the shaft seal is expected to be thermally stable.

### 5.3.7 Thermocouple Psychrometers

The thermocouple psychrometers installed in the ESP are Wescor model PST-55 with stainless steel filters protecting the thermocouple junction. They have either 50 m or 55 m long cables, depending on their location in the shaft seal. Figure 5.8 shows a diagram of a Wescor PST-55 thermocouple psychrometer.

Thermocouple psychrometers are used to measure the in situ water content of soil. This is done by measuring the partial vapour pressure of the pore-water. The vapour pressure of the pore-water can be related to *total* suction, and total suction is related to soil water content. Using thermodynamics the relationship between total suction and the partial vapour pressure of the pore-water can be written as follows (Fredlund and Rahardjo 1993):

$$\psi = -\frac{RT}{v_{w0}\omega_v} ln\left(\frac{\bar{u}_v}{\bar{u}_{v0}}\right) \quad [5.1]$$

Where $R$ is the universal gas constant (8.31432 J/mol K), $T$ is the absolute temperature (K), $v_{w0}$ is the specific volume of water ($m^3$/kg), $\omega_v$ is the molecular mass of water vapour (18.016 kg/kmol), $\bar{u}_v$ is the partial pressure of pore water vapour (kPa) and $\bar{u}_{v0}$ is the saturation pressure of water vapour (kPa). Given that $\bar{u}_v/\bar{u}_{v0}$ is equal to the relative humidity (RH) Equation 5.1 can be simplified, at a temperature of 15°C, as:

$\psi$ (in kPa) = -132285$ln$(RH in %/100) [5.2]

Psychrometers contain two thermocouple junctions, known as the sensing junction and the reference junction, as shown in Figure 5.8. The sensing junction is exposed to the soil pore spaces, while the reference junction measures the ambient temperature of the soil. Psychrometers operate by passing an electrical current through the sensing junction that causes the junction to cool due to the

Peltier effect; this in turn causes water to condense on the sensing junction. Once the cooling is stopped, the instruments microvolt output during warming of the junction back to ambient temperature is logged as a function of time. The microvolt output from a psychrometer, which is related to the temperature of the sensing junction, is generated in the same manner as a standard thermocouple and is created via the Seebeck effect by the temperature gradient between the sensing junction and the reference junction. The microvolt output changes, due to the changing thermal gradient, as the sensing junction heats up. The recorded output during this re-warming can be interpreted to determine the vapour pressure in the soil pore spaces (Wan 1996).

A typical psychrometer output is shown in Figure 5.9; note that a positive microvolt output indicates the temperature at the sensing junction is below ambient temperature. At point A, in Figure 5.9, the sensing junction is at ambient temperature (dry bulb temperature). A cooling current is applied from A to B, which causes the sensing junction to cool. This results in water condensing on the junction surface. Application of the cooling current is stopped at B. Here the temperature of the sensing junction is below the dew point within the pore-spaces of the soil. From B to C the temperature of the sensing junction rises until the dew point (wet bulb temperature) is reached. The plateau from C to D indicates adiabatic evaporation of water from the sensing junction. In theory the temperature from C to D should remain constant as the condensed water evaporates; however the output may have a slight slope since this is not an idealized situation. At D all of the water has been evaporated and the

temperature of the junction sharply rises back to ambient at E. The microvolt output at C is taken to the reading produced by the psychrometer (Berkeley Lab 2000). This reading can be converted into suction using the instrument's calibration curve which is explained in Section 5.4.2.

Another temperature reference junction is located in the datalogger and is used to determine the temperature of the reference junction inside the psychrometers tip. Psychrometers also provide temperature data for the surrounding soil.

Typically the outputs from psychrometers are normalized to 25°C to account for temperature effects on the instrument. This is done using the ambient temperature measured by the psychrometer's reference junction and the following equation (Wescor Environmental Products Division n.d.):

$$\text{Corrected Reading} = (\text{Measure Reading})/(0.325+0.027*T) \qquad [5.3]$$

Where T is the temperature of the reference junction in °C.

Psychrometers can only provide meaningful suction measurements when the total suction is less than approximately 8 MPa. Based on this operational limit, the psychrometers installed in the ESP can only be expected to provide meaningful data for 40:60 bentonite-sand material having a gravimetric water content higher than approximately 15% (Dixon, et al. 2000). The 40:60 material installed in the shaft plug had an initial water content of approximately 12%, which is outside the operating range of the psychrometers. This limitation of the

instrument could result in a plateau of initial suction measurements at the upper operating range of the psychrometers.

Also, changes in the soil's density and stress field can affect psychrometers' outputs even when there is no change in water content (Martino, Dixon and Thompson 2001). Due to the uncertainties in converting the psychrometer readings from suction to water content, the data from these instruments is simply reported as soil water suction.

Despite these limitations, psychrometers have been used in multiple experiments performed by AECL and have proven to be a reliable way of recording semi-quantitative measurements of water uptake in bentonite-based materials (Dixon, et al. 2000, Martino, Dixon and Thompson, 2000).

### 5.3.8 Time Domain Reflectometry Probes

The time domain reflectometry (TDR) probes used in the ESP are manufactured by SDEC France and were supplied to AECL by ANDRA and Guigues Environnment (France). They are equipped with 50 m long watertight high durability coaxial cables. They also have insulated brass probe rods (antennas) with polyurethane filled cable connection boxes to help prevent corrosion (Figure 5.10).

TDR probes can be used to measure the in situ water content of soils (Ekblad and Isacsson 2007). This is accomplished by surrounding the TDR probe, which

consists of two brass rods, with soil and transmitting a pulsed electromagnetic signal through the probe. The time required for the pulse to propagate down the probe rods and be reflected back is measured; this is called the pulse travel time and is measured in nanoseconds. If the length of the probe is known, the propagation velocity of the electromagnetic pulse can be calculated. This propagation velocity is dependent on the dielectric constant of the material surrounding the probe (i.e. the soil). The dielectric constant of water is high relative to other soil constituents, which means water content dominates the dielectric constant of soil. Therefore, the water content of the soil can be directly related to the bulk dielectric constant of the surrounding material, and hence the pulse travel time along the probe (Campbell Scientific Inc. 2008).

The pulse travel time for each TDR reading is automatically interpreted by datalogging software supplied to AECL by Guigues Environment. The computer algorithm used by the software determines the inflection points in the TDR signal that represent the beginning and end of the probe, and then calculates the pulse travel time between these two points (Figure 5.11). The pulse travel time is then related to the volumetric water content of the surrounding material. For monitoring the TDRs installed in the shaft seal an in-house calibration was performed at the URL to define a relationship between the pulse travel time and the volumetric water content of 40:60 bentonite-sand material, see Section 5.4.3.

There are three main disadvantages associated with using TDRs. The first is that the signal will be attenuated if ionic conduction occurs in the soil. Ions

provide a conductive path between the two probe rods and can alter the shape of the signal. This affects the accuracy and resolution of the water content measurements (Campbell Scientific Inc. 2008). This limitation has implications in the ESP since both the sodium bentonite used in the shaft seal and the infiltrating groundwater contains ions. Therefore, since no correction will be applied to account for ionic conduction, the readings should be interpreted carefully.

The second major disadvantage is the size of the sensor, it is very large making its installation potentially problematic. It needs to be pre-installed in a precompacted block of clay so that the rods remain parallel and in close contact with the soil. This means that the initial state of the soil surrounding the probe may not be the same as the medium in which it is installed.

The third disadvantage is that the readings provided by the sensor are representative of a fairly large volume of soil. This may make identification of wetting front movement problematic.

### 5.3.9 Fibre Optic Displacement Transducers

The fibre optic displacement transducers (FODT) installed in the ESP are Roctest model FOD-F. They have stainless steel housings, and are designed for a working hydraulic pressure of 2.7 MPa (the maximum hydraulic pressure at the shaft seal once the URL is fully flooded). They are connected to 350 m of high durability PVC jackets fibre optic cable.

Fibre optic displacement transducers measure the relative displacement of a surface in relation to a fixed anchor point, and are used to monitor the vertical displacement of the upper concrete component in the shaft seal. This is done by measuring the position of the plunger protruding from the instrument (Figure 5.12), and is accomplished by the use of a Thin Film Fizeau Interferometer (TFFI) that is mounted on the plunger shaft inside the instrument housing. According to the FOD-F instruction manual (Roctest Ltd. 2000):

> *The TFFI can be seen as a spatially distributed Fabry-Perot cavity where the cavity length varies along the lateral position. The optical fibre is mounted in a manner that the tip is facing the surface of the TFFI, which is moved relative to the optical fibre extremity.*

Essentially, a varying interferometric signal is received by the signal conditioner as the position of the plunger changes. Using the supplied calibration equation this signal can be converted into displacement of the plunger tip.

A major advantage of fibre optic instruments is they are immune to electromagnetic interference. They are not affected by lightning strikes and their cables can be run in close proximity to power cables. They are also capable of operating with very long cable lengths (up to 2 km). These properties were very desirable for the ESP.

No temperature correction needs to be applied to the displacement readings.

### 5.3.10 Fibre Optic Deformation Sensors

The fibre optic deformation sensors (strain gauges) installed in the ESP are Standard Deformation Sensors manufactured by Smartec. They were ordered with either 3 m or 1 m active measuring lengths and are each connected to 350 m of stainless steel reinforced PVC jacketed fibre optic cable.

The fibre optic deformation sensors measure the elongation or shortening of an optical fibre mounted inside a plastic tube, and are installed in the concrete components of the shaft seal. When a deformation sensor is mounted to structure it measures the relative axial deformation between the sensor's two anchor points. If the active length of the sensor is known, this measurement can be converted into strain. The measurement is based on the principle of low-coherence interferometry and is interpreted by a SOFO structural monitoring readout unit. Diagrams of the fibre optic deformation gauge and the SOFO monitoring system can be found on Smartec's website (www.smartec.ch).

Two optical fibres are mounted inside the sensor tube that is embedded in the structure, in the case of the ESP the sensors are cast into the concrete components. One of the internal fibres is connected to the structure via anchors and deforms (lengthens/shortens) with the structure, while the other is installed freely in the sensor tube. These are called the measurement fibre and the reference fibre, respectively. Mirrors are placed at the end of both of these fibres. They reflect the light signal back to the readout unit where the beams are recombined by a coupler and directed to an analyzer. The analyzer also

contains two fibres, as well as a mobile mirror. When taking a reading the mobile mirror in the analyzer is moved, and an interference signal is obtained only when the length difference between the fibres in the sensor tube is compensated by the length difference between the fibres in the analyzer. By taking successive readings the change in length of the measurement fibre can be calculated, and this directly relates to the deformation (strain) of the structure.

The standard deformation sensors have the following advantages: they are insensitive to temperature fluctuations, measure thermal expansion/contraction accurately, have very fine measurement resolution (2 μm), do not require calibration, are immune to electromagnetic interference, and can operate with very long cable lengths (up to 2 km). Also, since the sensor bodies are made from flexible plastic tubes, they are capable of measuring the strain of concrete during initial setting.

## 5.4 Instrument Calibrations

### 5.4.1 Introduction

Factory calibrations were used for all of the vibrating wire and fibre optic based instruments but functionality checks were done on all the sensors before they were installed. The reasons for not conducting in-house recalibrations are associated with the nature of the sensors received. The 350 m long cables attached to the vibrating wire and fibre optic instrumentation meant that for in-house calibration to be performed the entire 350 m length of each instrument

cable would need to be run through small ports in the high pressure calibration chamber located at the URL, this was not a feasible method for calibration as the risk of damaging the cabling during this process was substantial. Also, the shaft seal is expected to be in an isothermal condition and calibration of the instruments under varying thermal conditions was not required. Previous experience with these types of sensors at the URL established that the factory calibrations were very comparable to anything that could be obtained by in-house recalibration.

In-house calibrations were needed for, and performed on, the thermocouple psychrometers and time domain reflectometry (TDR) probes. These in-house calibrations were required since this application is not the typical scenario where these instruments are used or signal output was very dependent on the unique behaviour of each sensor. These sensors had either been physically modified (e.g. sensor tips and cable lengths) in case of psychrometers or required special installation processes to be followed. This section will describe the calibration methods, and the calibrations curves produced, for the psychrometers and TDRs.

In-house calibration checks were also feasible to verify the manufacturer calibrations on the thermocouples, Geokon vibrating wire piezometers and fibre optic displacement transducers.

### 5.4.2 Calibration of Thermocouple Psychrometers

#### *5.4.2.1 Selection of Cooling Parameters*

Determination of the cooling parameters to be used for the operation of the psychrometers was required prior to calibration of the instruments. There are two parameters that affect the output of psychrometers; these are the cooling current and the cooling time. Proper selection of these parameters is crucial if meaningful data are to be collected from the instruments. If the cooling current is too low, or the cooling time too short, the sensing junction may not reach the dew point of the surrounding air and/or insufficient volumes of water may condense on the sensing junction. This will lead to a poorly defined wet-bulb depression and lack of a plateau in the reading. Conversely if the cooling current is too high, or the cooling time too long, excessive amounts of water may condense on the sensing junction leading to a poorly defined “peak” at the point when cooling is stopped (Wan 1996). A range of cooling currents was tested prior to calibration. Figure 5.13 shows typical outputs from overcooled and undercooled psychrometer operation.

The selection of cooling time is based on judgment and experience. Consequently a cooling time of 30 seconds was selected based on past experiments at the URL, for example in the Buffer Container Experiment and the Tunnel Sealing Experiment (Johnston 2009).

The methodology for determining the proper cooling current was to hold the cooling time constant at 30 seconds and vary the cooling current until an acceptable output was received. The required cooling current is affected by the combined electrical resistant of the sensing junction and the constantan lead in the psychrometers cable. Typically the total resistance is 15 ohms for psychrometers with 1 m lead lengths, and this resistance increases by 2.4 ohms per meter for psychrometers with longer leads (Campbell Scientific Inc. 1992). When monitoring psychrometers using a Campbell Scientific CR7X datalogger and A3497 Cooling Current Interface, the cooling current is controlled by inputting a cooling *voltage* into the data logger programming. This cooling voltage is determined by using a modified version of Ohm's Law (Campbell Scientific Inc. 1992):

$$V = I(249 + R_S) + 700 \qquad [5.4]$$

Where V is the voltage (mV) required to produce the desired cooling current, I (mA), with a specific total resistance, $R_S$ (Ω).

Using Equation 5.1 the required cooling voltage to produce a 6 mA cooling current for a psychrometer with 50 m long leads is approximately 3000 mV, this cooling voltage was used as a starting point to determine the optimal cooling voltage for calibration and monitoring. A number of psychrometers were installed in airtight calibration cells above a 0.5 molal KCl solution (Figure 5.14) to find the optimal cooling voltage (cooling current); molality is defined as the number of moles of solute per kilogram of solvent. A 0.5 molal KCl solution in an airtight

vessel creates a suction of 2.2 MPa, which is approximately the mid-range of suctions expected in the bentonite-sand material in the shaft seal. Next, cooling voltages ranging from 1500 mV to 3500 mV were applied to the psychrometers in 250 mV increments, this made it possible to track the changing response from the psychrometers. The optimal cooling voltage was determined from these tests to be 2500 mV, since it created consistently acceptable output curves; typical examples of good and bad output curves are shown in Figure 5.13. This cooling voltage was used to both calibrate and monitor the psychrometers in the ESP.

#### *5.4.2.2 Calibration Method of Thermocouple Psychrometer*

All of the psychrometers were calibrated prior to their installation in the shaft seal using the optimal cooling parameters determined in Section 5.4.2.1. The calibration provides a relationship between the microvolt output of the instrument and the vapour pressure, suction, in the air void surrounding the sensing junction of the psychrometer. This vapour pressure can be related to the total suction of the surrounding soil.

Each psychrometer was calibrated by suspending its sensing tip in an airtight calibration cell above a potassium chloride (KCl) solution with a known molal (*m*) concentration (Figure 5.14). The KCl solution is used to control the vapour pressure in the air void surrounding the sensing tip of the psychrometer. The standard relationship between the molality of a KCl solution and the equilibrium vapour pressure, suction, in the sealed container is shown in Table 5.2. The calibration cells were constructed using stainless steel Swagelok tube fittings

(Figure 5.15) so that the solution would not react with the metal and potentially change the suction conditions present. A three-point calibration was performed for each psychrometer using 0.3, 0.5 and 1.1 molal KCl solutions at a constant temperature of 15°C. After equilibrium was reached, a calibrated data point was recorded for each psychrometer with the three different KCl solutions. These data points were then used to create a calibration equation for each psychrometer that is used to convert the raw output to soil suction (Figure 5.16).

During calibration, the psychrometers were connected to the same Campbell Scientific CR7X data logger and cooling current interfaces that were finally installed at the 240 Level for the monitoring of the shaft seal. This was done to avoid any errors that may be introduced by using different cooling current interfaces for the calibration and real-life monitoring. Using the CR7X for the calibration also made it possible to ensure that thermal and vapour equilibrium had been reached in the calibration cells, since data could be recorded over the entire calibration period.

Psychrometer output is highly dependent on the temperature of the instrument (Wan 1996). The ambient temperature in the completed shaft seal was expected to be approximately 15°C, therefore the psychrometers were calibrated at 15°C to reduce temperature effects. In reality, the ambient temperature of the shaft seal is closer to 12°C. The constant 15°C environment for the calibrations was created by performing them in the environmental chamber located at the URL (Figure 5.17). However, since temperature fluctuations are expected in the field

it is standard procedure to temperature correct the output voltage of each measurement and calibration point to 25°C (Berkeley Lab 2000). The temperature correction is performed by applying Equation 5.3.

### 5.4.3 Calibration of Time Domain Reflectometry Probes

A single calibration curve relating the TDR pulse travel time to the volumetric water content of the 40:60 bentonite-sand material was created to process the readings from all of the TDR probes. The calibration was performed using the 'spare' TDR probe that was not installed in the shaft seal. However, based on the manufacturers' instructions, all the TDR probes should give approximately the same reading in identical materials and water contents. The four TDR probes in the shaft seal were installed before the TDR automatic interpretation software was received, and therefore individual calibrations could not be performed for each sensor. Conduct of a multi-point calibration process involving each sensor was also a potentially risky activity. The probes need to be straight and parallel and it is important that the coating on each antenna not be damaged during installation. Repeated installations in large calibration blocks ran the unnecessary risk of doing damage to these very expensive probes and so calibrations using the "spare" probe and then preparing each "to-be-installed" probe at slightly different water contents provided a considerable body of calibration information.

The calibration was performed by inserting the spare TDR probe into five (5) precompacted bentonite-sand cylinders with varying, and known, volumetric

water contents (Figure 5.18). The cylinders were comprised of material taken from the bulk bags of bentonite-sand material used to construct the shaft seal, and were compacted in a cylindrical steel mould using a hydraulic press (Figure 5.19) to dry densities of 1825 kg/m$^3$ +/- 15 kg/m$^3$; the target dry density for the clay component of the shaft seal was 1800 kg/m$^3$, and the installed density is roughly 1810 kg/m$^3$. The compacted bentonite-sand cylinders measured 35 cm tall with 28 cm diameters. This size of cylinder was used because 90% the soil affecting the TDR signal is contained in a cylinder surrounding the sensor having a length equal to the probe rods (30 cm), and a diameter three times the distance between the probe rods (16 cm). Having a large bentonite-sand cylinder ensured that representatives readings were taken for the calibration.

The calibration points were collected by taking ten (10) successive readings in each calibration cylinder using the automatic interpretation software supplied to AECL by Guigues Environnment. After ten (10) acceptable readings were recorded, the TDR cylinders were broken apart and water content analysis was performed on the central portion of each cylinder (Figure 5.20). Each water content sample had a mass of approximately 8 kg, roughly 18% of the material from one cylinder. This ensured that a representative water content measurement was taken for each calibration point.

Also, included in the calibration curve is the average of the first ten (10) readings taken by each TDR sensor installed in the shaft seal; these are the “as-built” points on the calibration curve. Each TDR probe installed in the shaft seal was

inserted into a precompacted bentonite-sand brick with a known water content before installation (Figure 5.21). Also, the approximate initial water content of the material surrounding the bricks in the shaft seal is known. The TDR installation bricks measure 10 cm wide by 10 cm tall and are 33 cm long, therefore the volume affecting the TDR readings includes the TDR installation brick and a portion of the surrounding material. This means that a volume-corrected average of the water content of the TDR installation brick and the surrounding material had to be calculated to estimate the as-built water contents. Even though the exact volumetric water content for each as-built reading is unknown, these points served to increase confidence in the calibration curve. The TDR calibration curve is shown in Figure 5.22.

The data points on the calibration curve do not demonstrate a perfectly linear relationship between pulse travel time and volumetric water content. Therefore, the relationship should be viewed as a trend. That is, with increased water content the pulse travel time increases. The data from the TDRs should only be considered as an indication of the stage of saturation and saturation rate, not as an exact measurement of volumetric water content.

## 5.5 Instrument and Cable Armouring

Most of the instruments were available from the factory in high pressure housings (5 MPa) and heavy duty cables. High pressure instrument housings were necessary given the high swelling pressures and high hydraulic head to which the instruments will be subjected. Heavy duty instrument cables were necessary

since the cables were susceptible to damage during the shaft seal construction, and post-construction from falling debris and decommissioning activities. The instrument cables that required special in-house armouring were for the psychrometers and thermocouples, since these instruments were only available with thin wire leads. The psychrometers were also potted with polyurethane resin to be water tight, and had additional armouring placed around the tips of the instruments.

### 5.5.1 Psychrometer Waterproofing and Armouring

The psychrometers required special armouring and water proofing around the tip of the instruments. Leakage of water can occur at the psychrometer tip, after the instrument is saturated, and water can be forced up the instrument cable into the datalogger. This can lead to completed failure of the datalogger due to water damage. To limit this leakage, the ends of the psychrometers were encapsulated in polyurethane resin (it is important to note that encapsulating the tip of the instrument will only reduce the possibility of leakage, since internal leakage past the sensing junction leads cannot be prevented). The method for waterproofing and armouring the psychrometer tip involved inserting the instrument through a 3/8” stainless steel tube, with the metal filter tip protruding, and filling the tube with polyurethane resin (Figure 5.23). This completely encapsulated the entire instrument except for the sensing tip, and should effectively prevent leakage of water directly into the instrument cable at the junction of the cable and the instrument body. The stainless steel tube also protects the instrument from

mechanical damage and makes it easy to connect the cable armouring via a Swagelok union.

One of the potted-and-armoured psychrometers was pressure tested to failure. Water leaked past the potting at approximately 2 MPa of hydraulic pressure.

Additional leakage protection for the CR7X datalogger was added by creating a break in the psychrometer cable insulation that allows water to drip away before it reaches the datalogger. This was accomplished by removing the cable jacket to expose the three insulated conductors inside, then cutting a small slip in the insulation around each wire. Since the wire insulation acts like a small pipe, this slit provides a break in the water flow path preventing it from reaching the datalogger (Figure 5.24). All of the psychrometers cables run through a box located next to the datalogger, known as the *psychrometer drip box* (Figure 5.25), and this is where the wires are slit. Holes are drilled in the bottom of the psychrometer drip box to allow water to escape.

### 5.5.2 Cable Armouring

The instrument cables supplied with the psychrometers and thermocouples are thin wires that could have be easily damaged if installed unprotected in the shaft seal. Possible causes of damage include compaction of overlying material after installation of in the instruments, falling debris after closure of the URL, and damage from Galloway movements up and down the shaft (i.e. cutting or

crushing of cables). Therefore, the full length of these instrument cables exposed in the shaft had to be armoured.

The chosen method for armouring the cables was to run their entire length through 3/8” nylon Synflex high pressure tubing. This tubing helps protect the instrument leads from the crushing and abrasion to which they might otherwise be subjected.

The 3/8” Synflex tubing was easily connected to the armoured psychrometer using a 3/8” Swagelok union (Figure 5.26). The thermocouples were supplied from Roctest with a 3/8” Swagelok connection at the back of the instruments, making connection of the armouring very simple (Figure 5.1). These Swagelok connections provided a strong and watertight connection of the armouring to the instrument.

The tubing that protects the cables may cause a pathway for water flow into the datalogger if the instruments leak when they are pressurized, therefore the cable armouring (tubing) was terminated outside the datalogger boxes.

## 5.6 Installation of Shaft Cabling

There are a total of seventy one (71) cables installed in the URL main shaft as part of the ESP, including communications, instrument and power cables. These cables are divided into three groups: cables that run from surface to the shaft seal (40 instrument cables), cables that run from surface to the 240 Level (3

power/communications cables), and cables that run from the 240 Level to the shaft seal (28 instrument cables). These cables required different installation methods depending on which group they fell into. See Table 5.3 for the complete list of cables.

### 5.6.1 Installation of Cables from Surface to the 240 Level

There are forty three (43) cables installed in the shaft from surface to the 240 Level, including forty (40) that continue to the shaft seal. These cables are grouped into two bundles. One bundle contains all of the fibre optic instrument cables, power cables and communications cables, while the other bundle contains only vibrating wire instrument cables. The vibrating wire instrument cables are separated from the power cables since the power cables may cause interference with the vibrating wire signals. However, the fibre optic instrument cables are immune to electromagnetic interference and can be bundled with the power cables. All of the cables are located in the counterweight compartment in the "south-east" corner of the URL main shaft (Figure 5.27).

The majority of the cables are supported in the shaft by two 3/16" steel messenger wires (one for each bundle), so they do not self-support their full hanging weight. The messenger wires were anchored to shaft timbers for the initial shaft cabling installation, and were relocated and anchored to the shaft wall as the shaft was decommissioned. Each bundle was installed separately. The installation process is described below.

The messenger wire and the cables were lowered down the shaft at the same time. The messenger wire was initially spooled on an electric cable tugger (winch) with a hand brake that allowed easy control of its rate of decent. The messenger wire ran from the tugger over a shiv wheel hanging above the counterweight compartment of the shaft. The cables to be installed were initially on cable stands (Figure 5.28) with their ends routed to a cable guide mounted below the shiv wheel that supports the messenger wire (Figure 5.29). The instruments were attached to their cables at the factory, which meant they would be hanging from the cables as they were lowered down the shaft. To protect the instruments the piezometers were wrapped with foam padding and the TPCs were mounted on a plywood backing supported by the instruments cables, this helped minimize the stress on the cable connection of the TPCs (Figure 5.30). The cables and instruments were then attached to the messenger wire, which was lowered down the shaft. The cables were reeled out manually while keeping some tension on them (Figure 5.31), this helped to maintain a compact bundle hanging in the shaft. The cables were attached to the messenger wire using Kellum® grips and Crosby® clips (Figure 5.32) at set intervals ranging from every 30 m to 120 m, depending on the cable type. Because the instrument cables needed to eventually reach the shaft seal, 35 m below the 240 Level, the cable bundles were lowered until 50 m excess length for each instrument cable was on the 240 Level. After the cable lowering was complete the messenger wire was anchored to a steel I-beam located at the surface above the shaft, and secured shaft to timbers at 60 m intervals (Figure 5.33). This method of installation

imposed minimal stress on the cables during initial installation and relocation to the shaft walls, and will provide excellent support for the duration of the ESP.

The method of installation described above was used to install most of the cables in the shaft. The exceptions are the TDR power/communications cable and the FODT instrument cables, which were installed afterwards and hang freely in the shaft. These cables are sufficiently strong to support themselves with a hanging length of 270 m. In order to keep the cables organized, they were tie wrapped to the bundle of fibre optic and power cables after installation.

### 5.6.2 Installation of Cables from the 240 Level to the Shaft Seal

There were sixty eight (68) instrument cables that needed to be lowered from the 240 Level to the shaft seal, including the forty (40) instrument cables that were previously run from the surface to the 240 Level. Each instrument cable hangs freely only from the 240 Level to the shaft seal; a distance of approximately 30 m. The shorter cables for the instruments with dataloggers located on the 240 Level (i.e. psychrometers, thermocouples and TDRs) are supported at the 240 Level with cable ties. The instruments and cables were stored on the 240 Level and lowered down the shaft manually at the time of their installation. One exception was the TDR cables, which were raised from the shaft seal to the 240 Level using a rope. This was done since suspending the TDR probes might have damaged them.

### 5.6.3 Protection of Shaft Cabling

The cables are susceptible to damage from falling debris during shaft decommissioning and after closure. Therefore protection had to be installed up the entire length of the shaft.

Plywood armouring was installed covering all the instrument cables exiting the top of the shaft seal (Figure 5.34). Since the cables exit the shaft seal over a wide arc, the plywood was installed covering approximately three quarters of the circumference of the shaft at this location. The plywood was installed at a steep angle in order to deflect falling debris, rather than stop it.

The cable bundles running up the shaft wall also have armour covering them. This involved building a wooden box consisting of two-by-fours and plywood around the cable bundles as the shaft decommissioning progresses. The box has two compartments in order to maintain separation of the vibrating wire cables from the power cables, and is anchored to the shaft wall with Hilti bolts approximately every 3 m (Figure 5.35).

The cables have extra protection where they cross the 240 Level, since this area is likely more susceptible to direct impact from falling debris. This cable protection is anchored to an existing steel column that runs from the floor to the roof of the 240 Level; the column was not removed during decommissioning activities. Steel plating was bolted to this column, and the instrument cable

bundles were run behind the steel plate. This protects the cable bundles from any falling or ricocheting objects near the 240 Level.

## 5.7 Instrument Installation Methods

This section provides details on the installation methods used for the various instruments in the shaft seal.

It is important to note that not all of the instruments are installed in the exact position specified in the instrument layout plan by Dixon, Martino and Onagi (2009). This was due to the variable diameter and shape of the shaft as installation of the bentonite-sand component progressed, whereas in the instrument layout plan the shaft was assumed to be circular and 5.0 m in diameter. After each instrument was installed its position relative to the centreline of the shaft was accurately measured and recorded.

Tables listing the coordinates of each instrument and drawings showing their final installation locations and are included in Appendix A and Appendix B, respectively.

### 5.7.1 Instruments Installed in the Lower Concrete Component

The lower concrete component of the shaft seal contains steel reinforcing bar. This rebar provided mounting locations for nearly all of the instruments installed in the lower concrete section. The instrument design locations were predetermined, and at the time of installation a suitable location on the rebar

close to the design location was chosen. After installing the instruments, the coordinates of the as-built locations were accurately measured.

Even though the dense reinforcing bar (rebar) made it easy to install the instruments close to the design location, it also made it very difficult to physically reach the locations to install the instruments (Figure 5.36). In some instances mechanical reach extenders or grabbers were used to mount the instruments.

The cables for each instrument were tie wrapped to the rebar and run to a suitable location at the shaft wall. The cables were then run vertically out of the area of the lower concrete component and attached to the shaft screening. This held them securely in place during the pour of the lower concrete component. To avoid damaging the instruments during the concrete pour the locations of each instrument and instrument cable routing were marked with spray paint and marking tape (Figure 5.37) so concrete would not be poured directly onto them.

#### *5.7.1.1 Installation of Thermocouples*

There are five (5) thermocouples located in the lower concrete component. All the thermocouples were attached to the rebar using multiple heavy duty tie wraps. The tie wraps were tensioned using a tie wrap gun to ensure the instruments did not come loose during the subsequent concrete pour. The cables for each thermocouple are also tie wrapped to the rebar in multiple locations. Figure 5.38 shows an example of a finished thermocouple installation.

#### *5.7.1.2 Installation of Fibre Optic Deformation Sensors*

There are five (5) fibre optic deformation sensors (strain gauges) installed in the lower concrete component. Three (3) were installed oriented horizontally and two (2) vertically.

The horizontally oriented deformation sensors were installed by attaching them to the rebar using heavy duty tie wraps (Figure 5.39). The installation was simple and could be carried out for each sensor when the progression of the rebar installation was at the proper elevation. The cables of each sensor were also attached to the rebar and routed to a suitable location along the shaft wall.

The vertically oriented deformation sensors were much more difficult to install. They needed to be installed after the rebar installation was complete; since one anchor is close to the top of the rebar and the other is close to the bottom. To accomplish this, a steel wire was looped around a lower horizontal rebar, and then pulled back up using a reach extending grabber. The lower anchor of the strain gauge was then attached to the wire, which was used to pull down the end of the strain gauge. Finally, the upper anchor of the strain gauge and the steel wire were attached to an upper horizontal rebar (Figure 5.40). See Figure 5.41 for a pictorial description of the process. The cables of each sensor were then tie wrapped to the rebar and routed to suitable locations along the shaft wall.

#### *5.7.1.3 Installation of Vibrating Wire Piezometers*

There are three (3) vibrating wire piezometers installed around the perimeter of the lower concrete component. They measure the hydraulic pressure at the concrete-rock interface.

The tips of the vibrating wire piezometers were wrapped with a nonwoven geotextile sock prior to installation (Figure 5.42). This was done to prevent concrete from completely encasing the filters of the instruments, and increase the likelihood of the instruments intersecting the concrete-rock interface.

Two of the vibrating wire piezometers (VWPZ01 and VWPZ03) were mounted onto short pieces of fibre glass rod, which were then secured to the lower concrete component rebar using heavy duty tie wraps (Figure 5.43). The third vibrating wire piezometer (VWPZ02) was installed directly onto an existing I-bolt that was anchored to the rock (Figure 5.44). The sensing tips of the instruments were ensured to be in good contact with the rock when they were installed. The cables for all three instruments were routed to a suitable location and attached to the rebar with tie wraps.

### 5.7.2 Instruments Installed in the Bentonite-Sand Component

The instruments in the bentonite-sand component of the shaft seal were installed as the construction progressed, and are installed in groups at 1 m intervals. Typically the construction of the bentonite-sand component would be allowed to

progress approximately 0.2 m past the elevation where instruments were to be installed. Then holes were drilled down to the desired elevation, or an opening would be excavated, and the instruments inserted and backfilled. This provided a 0.2 m cover of compacted material above the instruments which served to protect them from the compaction of subsequent bentonite-sand lifts. This ensured that compacted bentonite-sand material of the proper density surrounded the installed instruments.

The instrument cables in the bentonite-sand component of the shaft were installed as follows. Firstly, a shallow trench was excavated to the locations where each instrument was to be installed. The instrument cables were laid into these trenches then covered with bentonite-sand material and compacted with a Hilti impact hammer. A good example is seen in the TDR installation shown in Figure 5.56. The cables were run to the shaft wall and separated with plywood guides in order to maintain an individual run for each cable through the bentonite-sand component (Figure 5.45). This was done to reduce the chance of water piping along a cluster of instrument cables.

#### *5.7.2.1 Installation of Piezometers*

There are three (3) vibrating wire piezometers and five (5) fibre optic piezometers installed in the bentonite-sand component of the shaft seal. They measure the pore-water pressure at various locations ranging from the centreline of the seal to the clay-rock interface.

The vibrating wire piezometers and fibre optic piezometers in the bentonite-sand component were installed in the exact same manner. Firstly, a shallow trench for the instrument cable was excavated. Then a hole was drilled, at a 45° angle, to a depth sufficient to place the sensing tip of the instrument in the desired location. The filter tip of each instrument was smeared with saturated bentonite-sand material before insertion into the hole to ensure the instrument was in direct contact with the host material (Figure 5.46). Then the piezometer was inserted into the hole, and the void behind it filled with loose material and gently compacted (Figure 5.47). The cable was then run to a suitable location along the shaft wall, and the cable trench backfilled and compacted by hand.

#### *5.7.2.2 Installation of Total Pressure Cells*

There are three (3) vibrating wire total pressure cells and five (5) fibre optic total pressure cells installed in the bentonite-sand component of the shaft seal. They measure swelling pressures inside the bentonite-sand, at the clay-concrete interfaces and the clay-rock interface.

##### *5.7.2.2.1 Installation of Vibrating Wire Total Pressure Cells*

The vibrating wire total pressure cells are installed at either the lower clay-concrete interface or the upper clay-concrete interface. This was done since the VWTPCs contain a thermistor and are able to collect valuable temperature information regarding the temperature rise during concrete hydration.

The VWTPC installed at the lower clay-concrete interface (VWTPC01) is anchored to the top surface of the lower concrete component. Firstly bentonite-sand material was installed to 0.2 m thickness and a hole was excavated down to the concrete surface. Then, two 1/4" Hilti bolts were anchored to the concrete aligning with the anchoring tabs on the VWTPC. A globule of hydraulic cement was placed underneath the pressure pad of the VWTPC and the instrument was pushed into it (Figure 5.48). This ensured the pressure pad was in direct contact with the lower concrete component. The VWTPC was then secured to the Hilti bolts and the hole was backfilled with bentonite-sand and compacted to the proper density.

There are two VWTPCs installed at the upper clay-concrete interface (VWTPC02 and VWTPC03). The first step of the installation was to create a smooth and level surface on top of the bentonite-sand where the instruments were to be placed. Next, 15 cm long threaded steel rods were attached to two of the anchoring tabs on the pressure pad. The threaded rods are installed pointing upwards and anchor the VWTPCs to the base of the upper concrete component. The instrument was then placed on top of the bentonite-sand and secured in place by hammering 15 cm long steel spikes into the bentonite-sand through the two remaining anchor tabs (Figure 5.49). These spikes securely held the instruments in place during pouring of the upper concrete component. The final installation of VWTPC02 and VWTPC03 is shown in Figure 5.50.

*5.7.2.2.2 Installation of Fibre Optic Total Pressure Cells*

All of the fibre optic total pressure cells are installed in the bentonite-sand component or at the clay-rock interface. They do not provide temperature measurement, and were therefore deemed adequate for use in the bentonite-sand. There are two installation orientations for the FOTPCs, either they measure the horizontal swelling pressure at the clay-rock interface, or the vertical swelling pressure at the interior of the bentonite-sand component.

The FOTPCs measuring horizontal swelling pressure at the clay-rock interface are installed with their sensing pads pointing towards the centre of the shaft plug (i.e. they are oriented on a vertical plane). Bentonite-sand was installed to an elevation approximately 0.2 m above the installation location on the instrument. Then a hole was excavated at the shaft wall to the required depth. A globule of hydraulic cement was then placed on the back of the sensing pad and the instrument was pressed into place on the shaft wall. The cement ensured direct contact was made between the sensing pad and the shaft wall. Finally, the excavated hole was backfilled manually ensuring that all excavated material was re-compacted into place, thereby guaranteeing that bentonite-sand of the proper density is in contact with the sensing pad. See Figure 5.51 for a typical installation.

The FOTPCs measuring swelling pressure at the interior of the bentonite-sand are installed with their sensing pads facing upwards (i.e. oriented on a horizontal plane). Bentonite-sand was installed to 0.2 m above the installation elevation,

and then a hole was excavated down to the desired elevation. A smooth and level surface was then created using loose bentonite-sand material at the site of installation and compacted with a flat compaction foot. The instrument was then set in place, making sure the sensing pad was in complete contact with the underlying bentonite-sand (Figure 5.52). The hole was finally backfilled with all of the excavated material and compacted to the proper density (Figure 5.53).

#### *5.7.2.3 Installation of Thermocouple Psychrometers*

There are total of fourteen (14) psychrometers installed in the bentonite-sand component of the shaft seal. They measure the suction of the material at various locations ranging from the centreline of the shaft seal to near the clay-rock interface.

Firstly, bentonite-sand material was installed to an elevation 0.2 m above the desired installation elevation. Then a 3/4" diameter hole was drilled at a 45° angle to an elevation just above the final installation point. The hole was then extended to the final installation elevation using a 3/8” auger bit. The 3/4" diameter hole accommodates the Swagelok union behind the psychrometer that attaches it to the Synflex cable armouring, and the 3/8" diameter hole snugly fits the steel tube that protects the psychrometer, see Figure 5.26. The psychrometer was then gently inserted into the hole making sure the stainless steel filter tip was not crushed or damaged. Following this, the rest of the hole was filled with loose material and gently compacted. This installation method

creates a minimal air void around tip of the psychrometer and ensures that bentonite-sand material of the proper density surrounds the instrument. See Figure 5.54 for a typical installation.

#### *5.7.2.4 Installation of Time Domain Reflectometry Probes*

There are four (4) TDR probes installed in the bentonite-sand component of the shaft seal. They measure the volumetric water content of the material.

When installed, the TDR probe robs are required to be completely surrounded by bentonite-sand material of the proper density. Drilling insertion holes in the field for installation of the TDRs would have been extremely difficult, since the holes are required to be parallel, less than 1 mm longer than the probe robs, and only 0.2 mm larger than the rod in diameter. Also, in situ compaction immediately adjacent to the TDR probes was not an option, since the probe rods are required to be parallel and could be damaged by compaction. Therefore, prior to installation each TDR was inserted into a drilled precompacted bentonite-sand brick, as shown in Figure 5.21. These bricks allowed for a high quality installation since they could be carefully manufactured to the proper density (~1800 kg/m$^3$ dry density) then precisely drilled (Figure 5.55) to snugly fit the TDR probe robs without causing them to bend.

For the installation in the shaft seal, bentonite-sand material was installed to an elevation 0.2 m higher than the instrument installation elevation. A hole roughly the size of the TDR installation block was then excavated. The precompacted

TDR installation brick, with the TDR probe inserted, was then placed in the hole and ensured to be level. The TDR probes were installed so that the probe robs are vertically aligned with each other, this will help to better capture the radial inflow of groundwater as it passes the TDR probes. Finally, the installation hole was backfilled and compacted. A typical installation is shown in Figures 5.56 and 5.57.

### 5.7.3 Instruments Installed in the Rock Adjacent to the Shaft Seal

The only monitoring instruments installed in the rock adjacent to the shaft seal are three (3) horizontal borehole packers with vibrating wire piezometers that measure the pore-water pressure in the rock.

#### *5.7.3.1 Installation of Horizontal Borehole Packers with Piezometers*

There are three (3) mechanical packers installed in horizontal boreholes in the rock adjacent to the bentonite-sand component of the shaft seal. These packers isolate areas of rock for pore-water pressure measurement and have vibrating wire piezometers (Geokon 4500 series) connected to them for this purpose. The horizontal boreholes are of three different depths (0.5 m, 1.0 m, 1.85 m) and allow the hydraulic gradient in the rock adjacent to the shaft seal to be monitored.

The mechanical packers were designed and constructed by URL technical staff; an example is shown in Figure 5.6. They are typical mechanical packers consisting of a tightening nut, thrust pipe and expandable rubber gland.

The first step was to identify a suitable location and drill the monitoring boreholes (Figure 5.58). A location was chosen at a depth of 271.5 m (4.5 m above the base of the bentonite-sand component of the shaft seal). This site provided competent rock and does not intersect Fracture Zone 2. After identifying the locations, the boreholes were drilled with 0.5 m horizontal spacing between them to depths of 0.5 m, 1.0 m and 1.85 m.

The first step in packer installation involved connecting a short rubber tube to the angled end of the piezometer line before insertion into the borehole. The packer was inserted with the piezometer line angled upwards with this rubber tube in contact with the top of the borehole (Figure 5.59), doing this ensured that no air bubbles remained in the isolated zone upon filling the packer and borehole with water. The packers were each inserted to the required depth and tightened into place. Then the annular gap between the packer thrust pipe and the borehole wall was filled with cemetitous grout. Next a vibrating wire piezometer was connected to the piezometer line on each packer. Water was then injected into the fill line until it started to leak out of the drain line plug, at which point the fill valve was closed and the drain line plug tightened. This ensured the isolated zone at the end of the borehole, the piezometer line and the fill line are entirely full with water. A completed packer installation is shown in Figure 5.60.

### 5.7.4 Instruments Installed in the Upper Concrete Component

The upper concrete component of the shaft seal does not contain any steel reinforcement. It is a monolithic structure composed entirely of low-heat high-

performance concrete. This meant that a support system was required to suspend some of the instruments in their final location before the concrete pour. This was accomplished by stringing 1/4" stainless steel cables across the shaft in a various locations. The instruments along the perimeter of the upper concrete component were simply anchored directly to shaft wall.

The instruments cables for each instrument were tie wrapped to the steel support cables and run to a suitable location at the shaft wall. The instrument cables were then run vertically out of the area of the shaft seal and attached to the shaft screening above the shaft seal. This held them securely in place during the upper concrete component pour.

There are also instruments mounted to the top surface of the upper concrete component. These include a vibrating wire piezometer and two fibre optic displacement transducers.

#### *5.7.4.1 Installation of Instrumentation Support Cables*

All of the thermocouples and deformation sensors installed in the upper concrete component were supported by 1/4" stainless steel cables prior to the pouring of the upper concrete component (Figure 5.61). There are two types of support cable installation; horizontal and vertical.

The horizontal support cables are anchored to the rock wall with 1/4" Hilti bolts, I-bolts and turnbuckles. Firstly, the locations for the cable anchor points were

accurately surveyed. Care was taken to ensure the support cables would run exactly level across the shaft. Then 1/4" Hilti bolt were anchored to the rock in the identified locations. The horizontal cables were then strung up and tightened using the turnbuckles (Figure 5.62). The turnbuckles were tightened until the cables we deemed sufficiently taut by the field inspector.

The two vertical support cables each span three horizontal support cables, and are clipped to the horizontal cables at each intersection point via Crosby® clips (Figure 5.63). An effort was made apply minimal tension to the vertical support cables in order to maintain the alignment of the horizontal cables.

#### *5.7.4.2 Installation of Thermocouples*

There are five (5) thermocouples installed in the upper concrete component. They are simply attached to the horizontal instrument support cables using heavy duty tie wraps. An example of an installed thermocouple is shown in Figure 5.64.

#### *5.7.4.3 Installation of Fibre Optic Deformation Sensors*

There are five (5) fibre optic deformation sensors (strain gauges) installed in the upper concrete component. Three (3) are oriented horizontally and two (2) are oriented vertically.

Whether installed vertically or horizontally, the deformation sensors were anchored to the appropriate support cable using heavy duty tie wraps. The deformation sensor tubes and support cables were also wrapped with electrical

tape in areas where the tube was bulging away from the support cables. This allowed the deformation sensors to be installed essentially straight, which is the ideal installation. The accurate positioning of the instrument support cables allowed the sensors to be installed in the exact positions prescribed in the instrument layout design. The final installation of the deformation sensors is shown in Figures 5.65 and 5.66.

#### *5.7.4.4 Installation of Vibrating Wire Piezometers*

There are a total of four (4) vibrating wire piezometers installed in the upper concrete component. Three (3) are installed around the perimeter of the upper concrete component and measure the hydraulic pressure at the concrete-rock interface. The fourth is installed on the top surface of the upper concrete component and measures the head of water above the shaft seal.

The three (3) piezometers installed at the concrete-rock interface have a nonwoven geotextile sock wrapped around their sensing tip, similar to the piezometers in the lower concrete component. This sock was put in place to prevent concrete from completely encasing the sensing tip (i.e. filter) of the instruments. It also served to increase the likelihood that water at the concrete-rock interface would reach the sensors, since the sock essentially increases the size of the instruments' filters. Each piezometer is held in place with two Hilti bolts that are anchored to the shaft wall. Multiple tie wraps were used to attach the instruments to the Hilti bolts to ensure they did not come loose during the

concrete pour of the upper concrete component. An example of an installed piezometer is shown in Figure 5.67.

The fourth piezometer is installed on the stop surface of the concrete and was secured in place using two clamps fastened to the concrete surface with Hilti bolts (Figure 5.68).

#### *5.7.4.5 Installation of Vibrating Wire Total Pressure Cells*

There are two (2) vibrating wire total pressure cells installed along the perimeter of the upper concrete component. They measure the total pressure at the concrete-rock interface.

After the installation location was identified, two Hilti bolts that align with the VWTPCs anchor tabs where attached to the rock. Hydraulic cement was then placed on the back of the sensing pad and the instrument was pushed into place. The nuts on the Hilti bolts were tightened until the hydraulic cement began to squeeze out from the back of the sensing pad (Figure 5.69). This ensured that solid contact was made between the sensing pad and the rock surface. Finally, the pressure transducer was secured to the rock using a clamp. A finished installation of a VWTPC is shown in Figure 5.70.

#### *5.7.4.6 Installation of Fibre Optic Displacement Transducers*

There are two FOSTs installed on a beam located directly above the top surface of the upper concrete component. The bodies of the instruments are mounted to

the rigid beam and the tips of their plungers are attached to the top surface of the upper concrete component (Figure 5.71). These displacement transducers measure the vertical movement of the upper concrete component of the shaft seal.

Firstly, the mounting beam was installed above the upper concrete component. The beam consists of a 4”x4” steel box section measuring 4.90 m long and is located approximately 0.30 m above the top surface of the shaft seal. It is anchored to the shaft wall using half inch steel plating and two 3/4" Hilti bolts at each end (Figure 5.72). The steel plates were first bolted to the shaft wall, and then the beam was levelled along both the lateral and longitudinal axes and welded to the steel plates.

The first step in installing the FODTs was to secure 1/2" female concrete drop-in anchors to the top surface of the upper concrete component. Next, steel tabs were connected to the concrete anchors. These tabs had threaded holes that the tips of the FODTs’ plungers could screw into. A threaded rod was also screwed into the back of the FODTs’ housings. These rods were used to attach the FODTs to mounting pates welded to the steel beam. The mounting plates were then aligned with the threaded rods connected to the FODTs and welded into place on the mounting beam. When positioning the mounting plates the FODTs were ensured to be positioned as close to vertical as possible. Finally, the FODTs were adjusted to their zero positions and tightened to the mounting plates using two nuts. The FODTs have a total displacement range of 20 mm

and were installed allowing for 10 mm of displace up or down (i.e. at their zero point). See Figure 5.73 for an example of an installed FODT.

Temperature fluctuations may cause the mounting beam to flex leading to false displacement readings for the upper concrete component. However, the shaft plug is expected to be thermally stable, and this will likely not be an issue.

It is expected that up to several meters of muck and fine debris will accumulate on top the shaft seal as the URL access shaft is decommissioned. This debris may include dirt, dust, pieces of shaft timber and loose rock. A wooden box was constructed covering the entire FODT mounting beam (Figure 5.74) to protect the FODTs from this debris. This box will kept the FODT plungers free of debris and prevent debris from settling on top of the mounting beam, as this may cause the beam to flex.

### 5.7.5 Instrument Cable Water Stops

There are sixty five (65) instrument cables routed through the top concrete component of the shaft seal. Once the shaft seal is pressurized by FZ2 it is possible that water may try to travel along these instrument cables and leak out of the top of the shaft seal. Therefore, in order to disrupt any potential flow paths, rubber water stops were installed on each instrument cable as they pass through the upper concrete component (Figure 5.75). Each rubber stopper was drilled out with a properly sized hole to provide a snug fit around each cable diameter, then slit along its edge. The rubber stoppers were then wrapped

around each instrument cable and secured in place using RTV adhesive sealant (Figure 5.76). These water stops should provide an adequate seal interrupt the flow path and prevent water flow along the instrument cables. This type of installation was successfully used in the Tunnel Sealing Experiment (Chandler, et al. 2002).

## 5.8 The ESP Data Acquisition System

The instrument logging and data acquisition system used for the ESP is comprised of multiple independent data acquisition systems. Multiple data acquisition systems are required for the excitation and monitoring of the various instrument technologies employed in the ESP. The entire system can be broken down into five sections. These sections include monitoring of: 1) vibrating wire pressure transducers, 2) interferometer-based fibre optic instruments, 3) fibre optic deformation sensors, 4) thermocouples/psychrometers, and 5) time domain reflectometry probes. The major components of the system, and the instruments they monitor, are listed in Table 5.4. A simplified schematic showing the major components of the data acquisition system is shown in Figure 5.77.

All of the instrument and communications cables are routed into the Geotechnical Science and Engineering Branch Laboratory (GSEB Lab) at the URL. The GSEB Lab houses all of the surface dataloggers, signal conditions and logging computers (Figure 5.78). Once the data are collected and interpreted by the equipment in the GSEB Lab it is sent on to the URL network database where it is stored and made available for analysis.

### 5.8.1 Instrument Cable Length Limitations

Vibrating wire and fibre optic technologies were used for sensor output transmission whenever possible because of their ability to operate with long cables lengths (>350 m). However, the cable lengths for some instrument technologies cannot exceed a certain length because line impedance will affect their measurements. The time domain reflectometry probes, psychrometers and thermocouples were limited to maximum cable lengths of approximately 60 m. Cables longer than this would result in voltage lose that significantly affect the psychrometer and thermocouple outputs, and cause the TDR waveform to be degraded.

Dataloggers for the instruments with limited maximum cable length were installed near the roof of the 240 Level (Figure 5.79). This way cables 60 m in length, or less in some cases, could be used to monitor these instruments since they were only required to reach from the shaft seal to the 240 Level. Communications lines running up the shaft transmit the data from these dataloggers to surface PCs. Installing dataloggers at the 240 Level raises some issues related to their long-term operation and this is discussed in Section 5.8.3.

### 5.8.2 Data Acquisition, Sensor Interfaces and Signal Conditioning

This section of the report describes the various interfaces and signal conditioners used to monitor the instruments. The data acquisition process, including communications to the URL network database, will also be discussed.

#### *5.8.2.1 Vibrating Wire Instruments*

The vibrating wire instruments (VWTPC and VWPZ) have cables that extend from the shaft seal to the GSEB Lab. They are monitored using a Campbell Scientific CR10X datalogger equipped with a Campbell Scientific AVW4 vibrating wire interface. The CR10X automatically takes readings and stores the data internally. These data are then backed up to the URL network database daily.

#### *5.8.2.2 Fibre Optic Piezometers, Total Pressure Cells and Displacement Transducers*

The fibre optic pressure sensors (FOPZs and FOTPCs) and displacement transducers (FODTs) are based on fibre optic interferometry and can be monitored using the same signal conditioner. All twelve (12) of these instruments have cables that extend from the shaft seal directly to the GSEB Lab and are connected to a FISO Technologies DMI signal conditioner. The DMI interfaces with the instruments and takes the readings. The DMI signal condition is connected to a personal computer running FISO Commander 2 software that allows configuration of the DMI signal conditioner and retrieves the data. The data is backed up the URL network database.

#### *5.8.2.3 Fibre Optic Deformation Sensors*

The ten (10) fibre optic deformations sensors installed in the concrete components of the shaft seal have instrument cables that are run from the shaft

seal to the GSEB Lab. The deformation sensors are connected to a SOFO V reading unit that is connected to a personal computer running SOFOSBD software. The SOFO V analyzes the signal from the sensors, and determines the deformation. The SOFOSBD software allows configuration of the SOFO V and records the data. The data is then backed up to the URL network database daily.

#### *5.8.2.4 Thermocouples and Thermocouple Psychrometers*

The ten (10) thermocouples and fourteen (14) psychrometers installed in the shaft seal have cables that are only long enough to reach the 240 Level. Therefore, a CR7X is located at the 240 Level to monitor these instruments. The CR7X is supplied power from a TECK90 power cable that runs from the surface to the 240 Level.

The psychrometers are monitored using five A3497 Cooling Current Interfaces. The A3497s are located in the same box as the CR7X and supply the excitation voltages to the psychrometers. The CR7X records the output from the psychrometers.

The thermocouples are monitored directly by the CR7X.

The data from the thermocouples and psychrometers is stored on the CR7X's internal memory and is backed up onto the URL network database daily. The CR7X is hooked to a fibre optic switch located on the 240 Level to accomplish

this. The switch is connected to the URL network via 280 m long fibre optic cable that runs from the 240 Level to the surface. Campbell Scientific LoggerNet Software is used to collect the data and transfer it to the URL network database.

#### *5.8.2.5 Time Domain Reflectometry Probes*

The TDRs installed in the shaft seal have cables that are only long enough to reach the 240 Level. Therefore a Campbell Scientific TDR100 time domain reflectometer is located on the 240 Level to monitor them. The TDR100's power and communications is supplied by a dedicated 4 wire cable that runs from the GSEB Lab to the 240 Level. The TDR100 sends the excitation signals to the TDR probes and records the reflected waveforms. The data from the TDR100 is then transferred to the surface by a RS232/RS485 data converter, located in the TDR caisson on the 240 Level, to another RS232/RS485 data converter that is connected to a computer on in the GSEB Lab. The surface computer is running custom interpretation software called TDR AECL that was created for the ESP by Guigues Environment (France). The TDR AECL software automatically interprets the collected waveforms and determines the pulse travel time along the probe robs. This data is then stored on the computer and backed up to the URL network database.

### 5.8.3 Dataloggers Installed on the 240 Level

As previously stated, there are two dataloggers located on the 240 Level of the URL; the TDR100 and CR7X.

The CR7X, which monitors the thermocouples and psychrometers, is a "sacrificial" datalogger that will lose functionality once it is submerged by passive flooding of the 240 Level. The estimated time for passive flooding to the back (roof) of the 240 Level is between 10 and 14 years (Dixon, Martino and Onagi 2009). To obtain the longest lifespan possible, the CR7X and fibre optic communications switch are mounted in boxes located on a shelf near the roof of the 240 Level, this shelf is 2.75 m above the 240 Level's floor (Figure 5.80). The boxes that house the CR7X and fibre optic switch are sealed shut, however they are only intended protect the equipment and are not waterproof. The psychrometer drip box is also located on the shelf on the 240 Level.

The TDR100 time domain reflectometer and RS232/RS485 data converter, used to monitor TDR probes, are encased in a high pressure watertight steel caisson designed and constructed by Guigues Environnment (France), see Figure 5.81. The caisson is designed to withstand 240 m of hydraulic head and will remain watertight even when the shaft is fully flooded. The connectors on the caisson for the TDR instrument cables and the power/communications cable are watertight, but were potted using Scotchcast 2130 polyurethane resin to provide extra waterproofing protection (Figure 5.82). The TDR caisson was mounted on a shelf hanging from an existing steel cantruss to increase the time before it is submerged. The shelf is located 1.9 m above the floor of the 240 Level, with the TDR caisson connectors located approximately 2.4 m above the floor (Figure 5.83). The waterproof steel caisson should protect the TDR100 and allow it to indefinitely monitor the shaft seal water uptake.

#### *5.8.3.1 Datalogger and Cable Tray Armouring*

The location where the CR7X datalogger and fibre optic switch are installed on the 240 Level is susceptible to damage from falling debris during decommissioning activities and falling rocks after the URL closure. Therefore, a steel deflection plate was installed above the datalogger shelf to protect the equipment from any falling objects (Figure 5.84). The deflection plate is constructed from welded 1/8” thick steel plates supported by an existing steel column and steel bars welded to rock bolts behind the plate. It is oriented at approximately 75° from horizontal and should be sufficiently strong to deflect any potential falling debris.

Also, a 1/4" steel plate is placed over the cable tray on the floor of the 240 Level to protect it from falling debris (Figure 5.84). This steel plate is supported by 8” x 8” wood timbers and should be sufficiently strong to deflect any potential falling debris.

### 5.8.4 Backup Power for ESP Dataloggers

The URL experiences many electrical blackouts and brownouts due to it remote location. Also, there is the threat of thunderstorms and blizzards that have the potential to cut off power to the URL for extended periods of time. Therefore, surge protection and backup power was needed for all of the data logging equipment installed in the ESP. This was accomplished by ensuring every piece of equipment was connected to an uninterruptable power supply (UPS) with

surge protection, see Figure 5.78. These UPSs are able to run all of the ESP computers and dataloggers for approximately 20 minutes, and can sustain the system during brief periods of power interruption. Additionally, all the UPSs are on an electrical circuit that is connected to the URL's backup generator. This generator is activated if power is lost more than a few seconds, and will power the ESP data acquisition system in the event of prolonged power loss.

## 5.9 Instrument Failures

As of March 31, 2010 there have been two instrument failures; a fibre optic deformation sensor and a vibrating wire total pressure cell.

The vertically oriented fibre optic deformation sensor installed near the centre of the upper concrete component (FOSC07) stopped responding from December 1, 2009 to December 10, 2009. This period of no response can be seen on the data plot for this instrument in Figure 6.16. Once FOSC07 began responding again the deformations it measured were much less compared to those measured by the other four (4) deformation sensors in the upper concrete component. This is an indication that the instrument is no longer functioning reliably, and therefore its readings should be disregarded. FOSC07 was installed in a location that left it susceptible to damage during the upper concrete pour, and this is likely when the damage occurred.

One of the VWTPCs installed at the concrete-rock interface of the upper concrete component (VWTPC04) lost the functionality of its internal thermistor on

November 26, 2009 immediately after the pouring of the upper concrete component. However, a temperature correction could still be applied to its raw readings using the temperature recorded by VWTPC05 which is located 90° away from VWTPC04 so no data was lost, see Appendix B for instrument locations. On March 9, 2010 VWTPC04 began giving intermittent readings and seemed to be losing the functionality of its vibrating wire pressure transducer. Although its intermittent pressure readings still agree with those recorded by VWTPC05, the data gathered from VWTPC04 should be interpreted with caution.

Both of the failed instruments are located in the upper concrete component, and their failure may be due to the stresses applied to them during pouring of the concrete. It is likely that the cables of these instruments may have been pulled on or twisted during the concrete pouring, and falling concrete or debris may have directly impacted and damaged the instruments.

It should be noted that care was taken during the upper concrete pour to avoid damaging the instruments, and the explanation that they were damaged during the pour is speculative.

Table 5.1: Instruments installed in the main shaft seal

| Instrument (Symbol) | Parameter | Quantity | Temperature |
|---|---|---|---|
| **Lower Concrete Segment** | | | |
| Vibrating Wire Piezometer (VWPZ) | Hydraulic Pressure | 3 | Yes |
| Thermocouple (Ct) | Temperature | 5 | N/A |
| Fibre Optic Deformation Sensor (FOSC) | Strain | 5 | No |
| **Bentonite-Sand Segment** | | | |
| Vibrating Wire Piezometer (VWPZ) | Pore-water Pressure | 3 | Yes |
| Fibre Optic Piezometer (FOPZ) | Pore-water Pressure | 5 | No |
| Vibrating Wire Total Pressure Cell (VWTPC) | Total Pressure | 3 | Yes |
| Fibre Optic Total Pressure Cell (FOTC) | Total Pressure | 5 | No |
| Thermocouple Psychrometer (Psy) | Water Content | 14 | Yes |
| Time Domain Reflectometry Probe (TDR) | Water Content | 4 | No |
| **Adjacent Rock** | | | |
| Packer with Vibrating Wire Piezometer (VWPZR) | Hydraulic Pressure | 3 | Yes* |
| **Upper Concrete Segment** | | | |
| Vibrating Wire Piezometer (VWPZ) | Hydraulic Pressure | 4 | Yes |
| Vibrating Wire Total Pressure Cell (VWTPC) | Total Pressure | 2 | Yes |
| Thermocouple (Ct) | Temperature | 5 | N/A |
| Fibre Optic Deformation Sensor (FOSC) | Strain | 5 | No |
| Fibre Optic Displacement Transducer (FODT) | Vertical Displacement | 2 | No |
| **Total** | | 68 | |

*The body of the instrument is in the bentonite-sand and does not measure rock temperature

Table 5.2: Suction potential of KCl solutions (AECL)

| | Suction (kPa) at Temperature | |
|---|---|---|
| **Molality (*m*)** | **10°C** | **25°C** |
| 0.1 | 437.6 | 460.7 |
| 0.2 | 856.2 | 901.6 |
| 0.3 | 1274.9 | 1342.5 |
| 0.5 | 2112.3 | 2224.2 |
| 0.75 | 3159.1 | 3326.4 |
| 1 | 4205.8 | 4428.6 |
| 1.1 | 4624.5 | 4869.5 |
| 1.2 | 5043.2 | 5310.3 |

Table 5.3: List of shaft cabling for the ESP

| Cable Type | Quantity |
|---|---|
| **Surface to Shaft Seal** | |
| VWPZ Instrument Cable | 13 |
| VWTPC Instrument Cable | 5 |
| FOPZ Instrument Cable | 5 |
| FOTPC Instrument Cable | 5 |
| FODT Instrument Cable | 2 |
| FO Strain Instrument Cable | 10 |
| **240 Level to Shaft Seal** | |
| Thermocouple Instrument Cable | 10 |
| Psychrometer Instrument Cable | 14 |
| TDR Instrument Cable | 4 |
| **Surface to 240 Level** | |
| TECK90 Power Cable | 1 |
| TDR Power/Comm Cable | 1 |
| FO Comm Cable | 1 |
| **Total** | 71 |

Table 5.4: Major data acquisition components

| Data Acquisition Component | Instruments Monitored |
|---|---|
| **Data Logging** | |
| Campbell Scientific CR10X | VWPZ, VWTPC |
| Campbell Scientific CR7X | Psy, Ct |
| PC w/ SOFOSDB Software | FOSC |
| PC w/ FISO Commander Software | FOTPC, FOPZ, FODT |
| PC w/ TDR-AECL Software | TDR |
| **Sensor Interface and Signal Conditioning** | |
| Campbell Scientific AVW4 Vibrating Wire Interface | VWPZ, VWTPC |
| Campbell Scientific A3497 Cooling Current Interface | Psy |
| Smartec SOFO V Reading Unit | FOSC |
| FISO DMI | FOTPC, FOPZ, FODT |
| Campbell Scientific TDR100 Time Domain Reflectometer | TDR |

Figure 5.1: Thermocouple with stainless steel housing and Synflex cable armouring (AECL stock photograph)




Figure 5.2: Schematic of a thermocouple

Figure 5.2 created by Blake Holowick

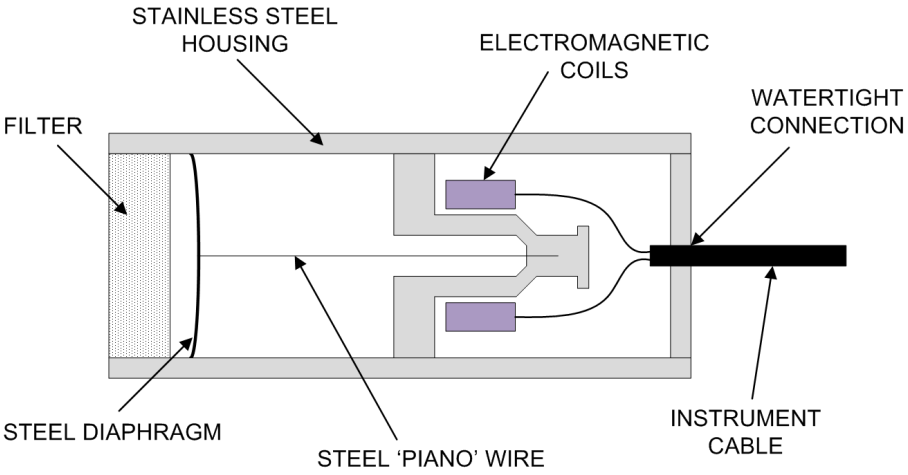


Figure 5.3: Diagram of a vibrating wire piezometer

Figure 5.3 created by Blake Holowick

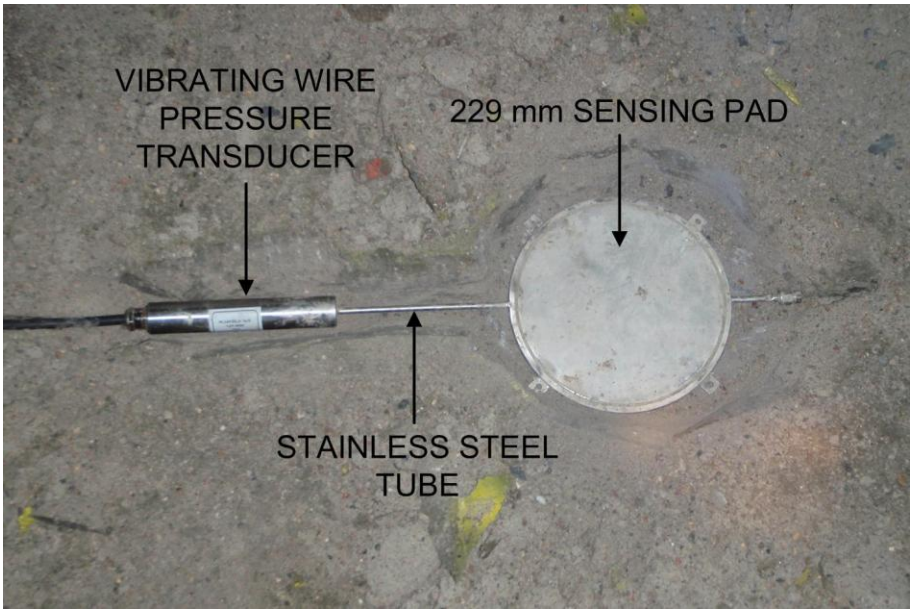


Figure 5.4: Vibrating wire total pressure cell (AECL stock photograph)

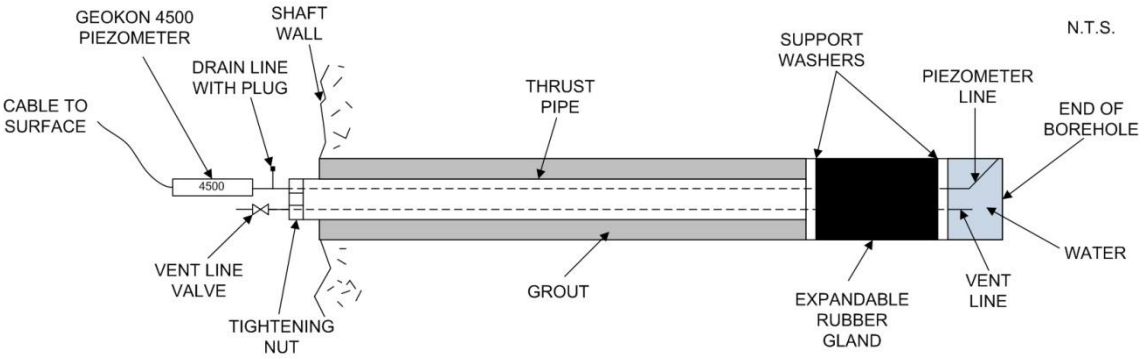


Figure 5.5: Diagram of a horizontal borehole pack installation (AECL)



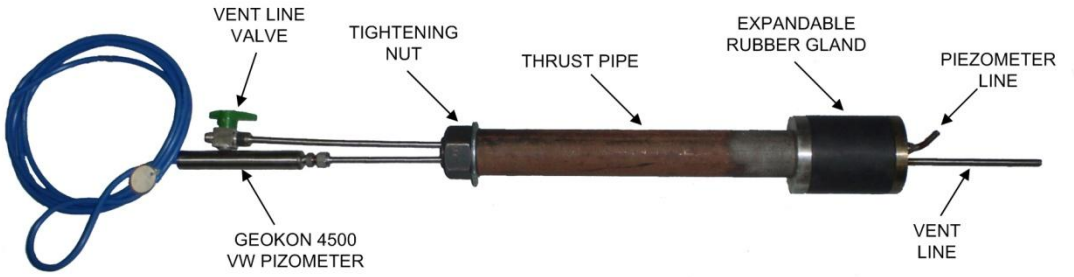


Figure 5.6: Photo of a mechanical packer with piezometer attached (AECL)

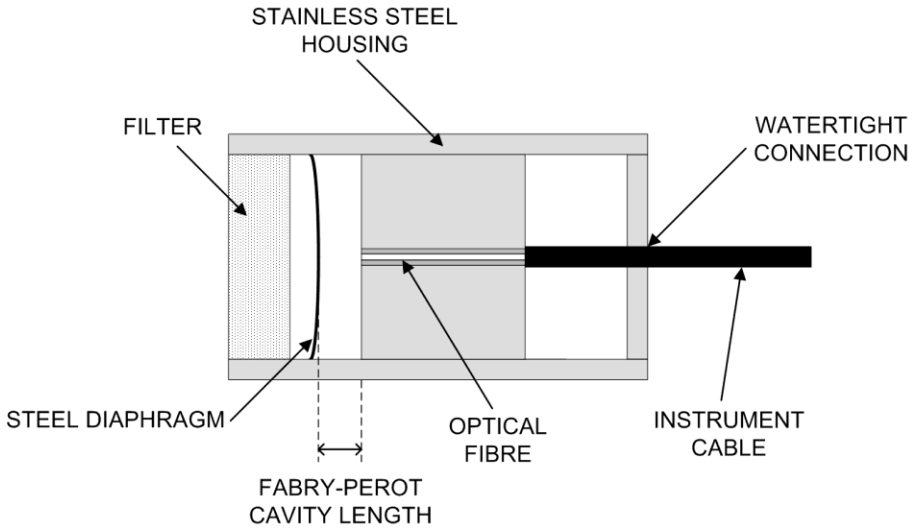


Figure 5.7: Diagram of a fibre-optic piezometer

Figure 5.7 created by Blake Holowick

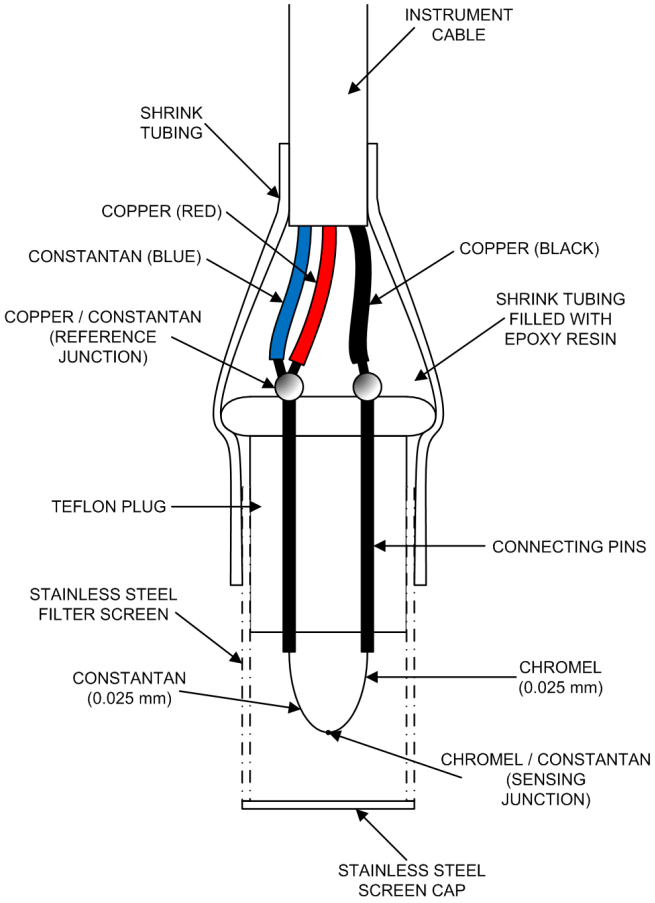


Figure 5.8: Schematic of a Wescor PST-55 thermocouple psychrometer

Figure 5.8 created by Blake Holowick

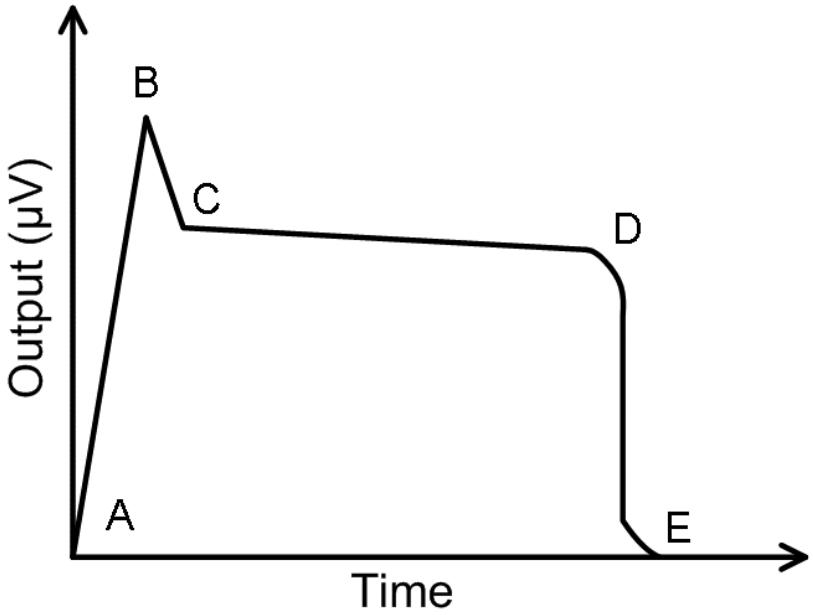


Figure 5.9: Typical output recorded during a psychrometer measurement (AECL)



Figure 5.10: TDR probe with 50 m cable (AECL stock photograph)

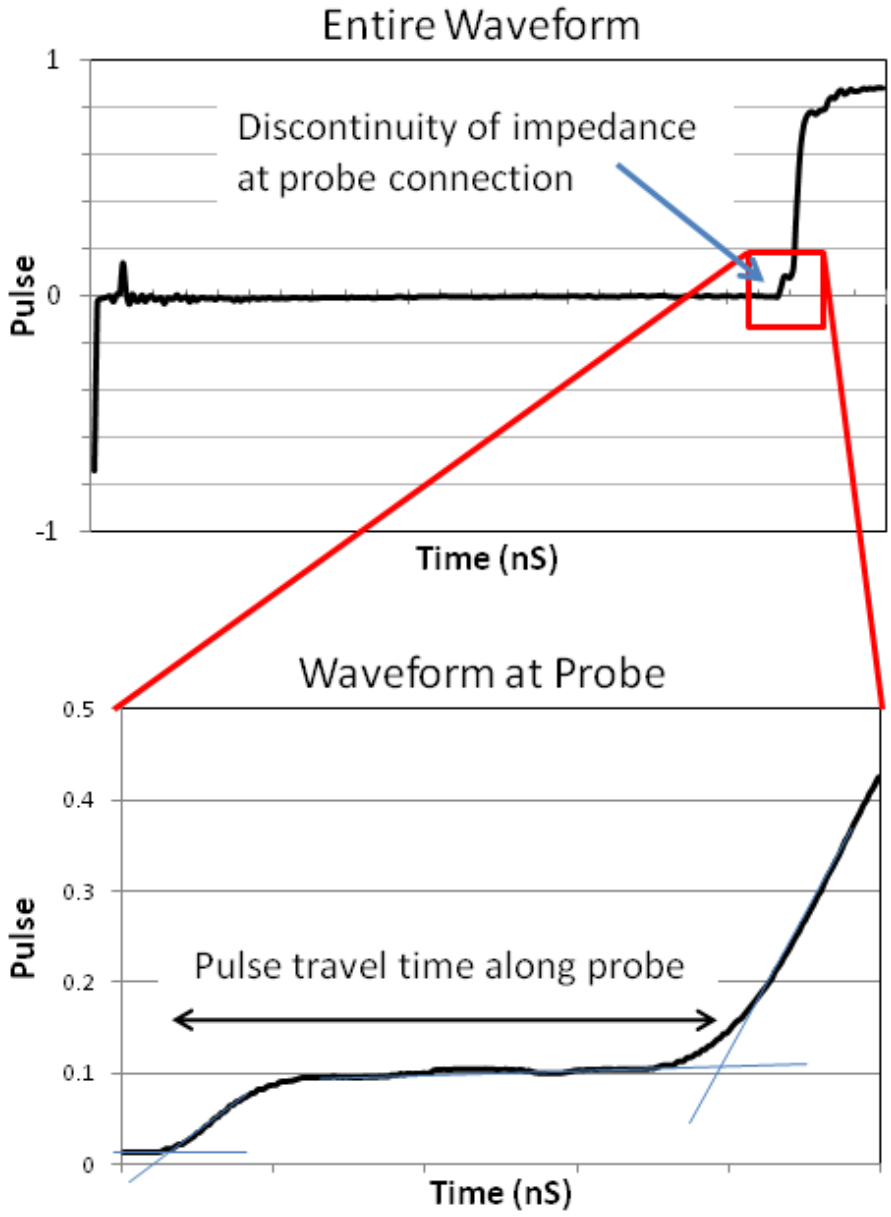


Figure 5.11: Example output and interpretation of a TDR reading (AECL)


Figure 5.12: Roctest fibre optic displacement transducer model FOD-F (AECL stock photograph)



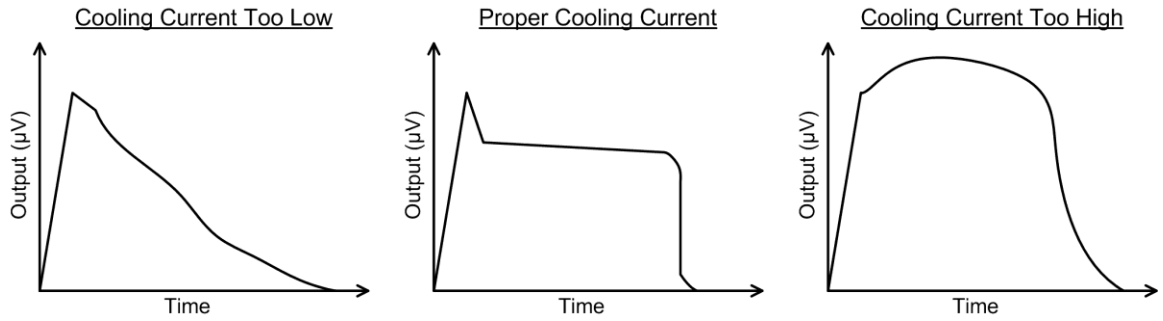


Figure 5.13: Typical psychrometer outputs with varying cooling currents

Figure 5.13 created by Blake Holowick

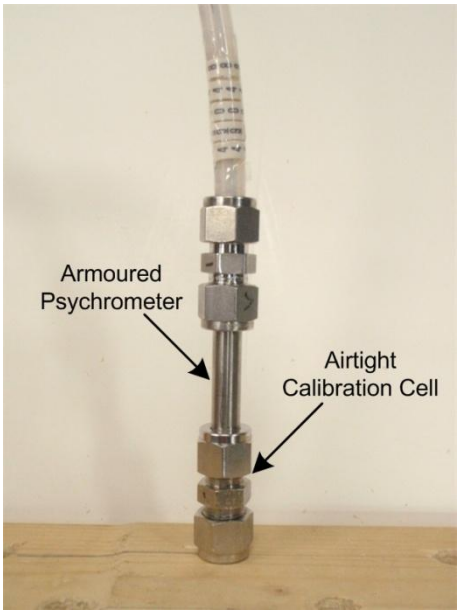


Figure 5.14: Suspending psychrometer above KCl solution in a calibration cell (AECL stock photograph)



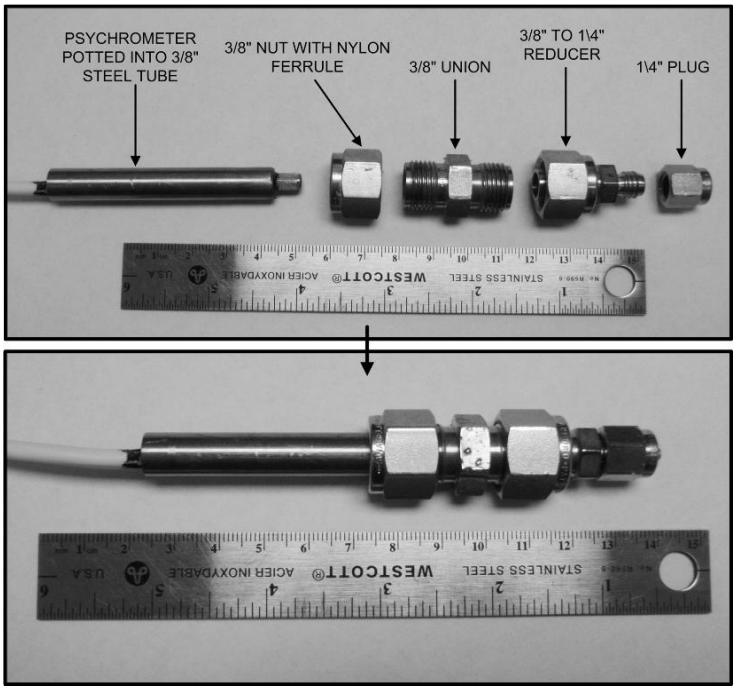


Figure 5.15: Psychrometer calibration cell components (AECL)

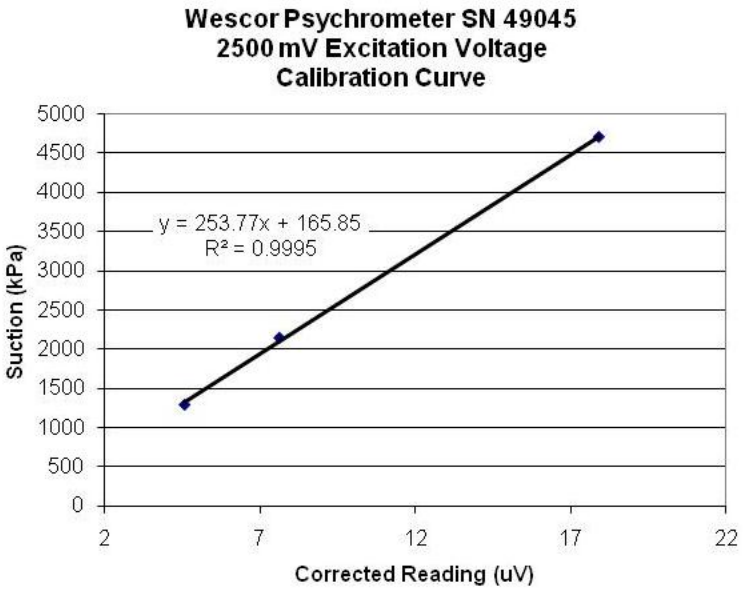


Figure 5.16: Example of a psychrometer calibration curve (AECL)



Figure 5.17: CR7X datalogger and psychrometers in environmental chamber (AECL stock photograph)

Figure 5.18: TDR probe inserted into a bentonite-sand cylinder for calibration (AECL stock photograph)



Figure 5.19: TDR calibration cylinder mould on the hydraulic press (AECL stock photograph)

Figure 5.20: TDR calibration water content sample (AECL stock photograph)



Figure 5.21: TDR probes inserted into precompacted bentonite-sand bricks (AECL stock photograph)

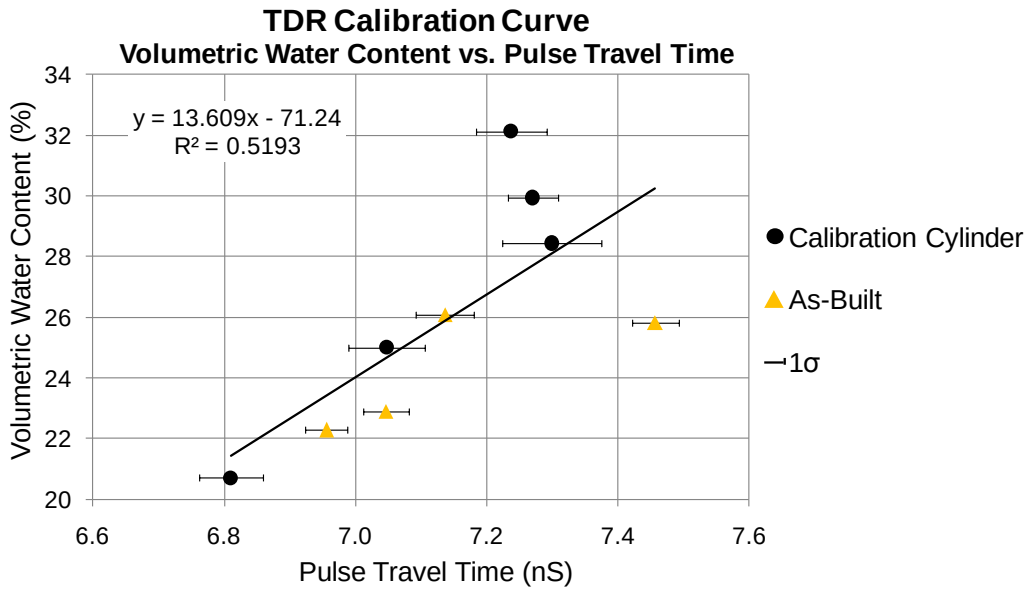


Figure 5.22: TDR calibration curve (AECL)



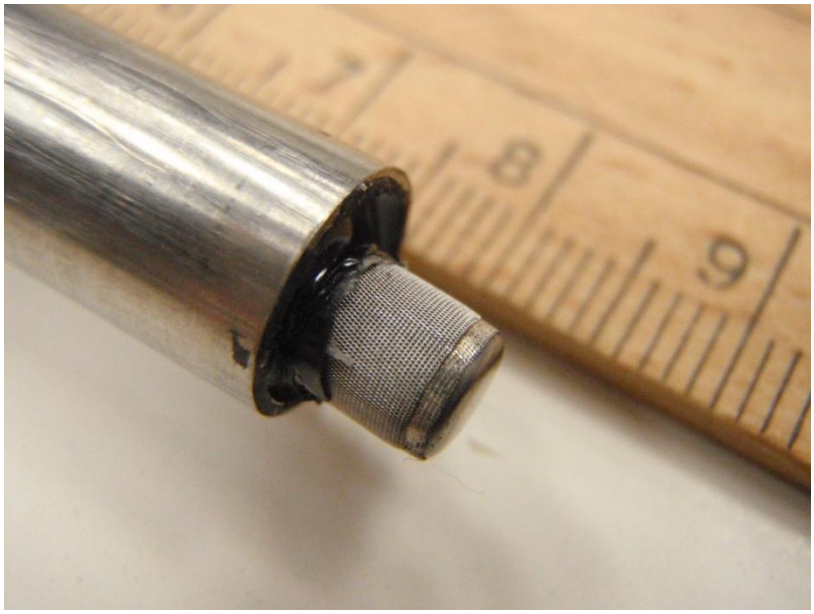

Figure 5.23: Psychrometer tip waterproofing and armouring (AECL stock photograph)

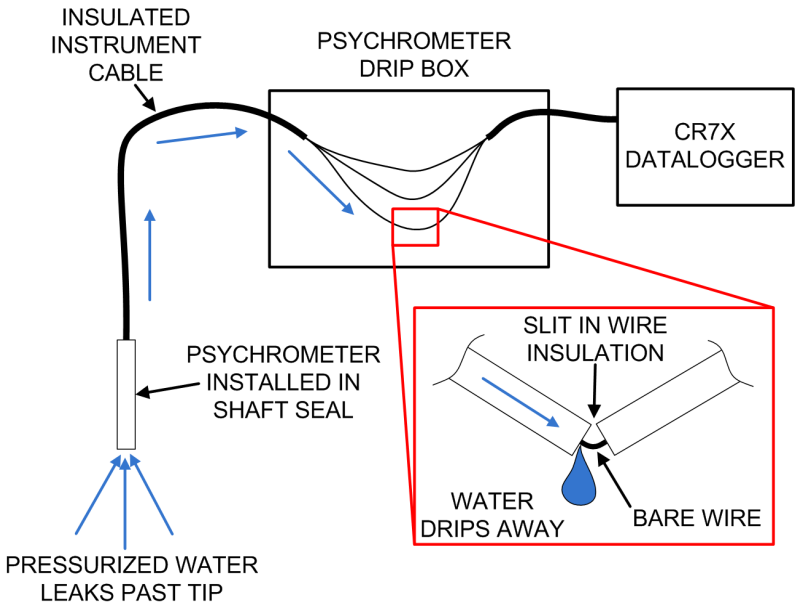


Figure 5.24: Psychrometer leakage protection by slitting wire insulation (AECL)



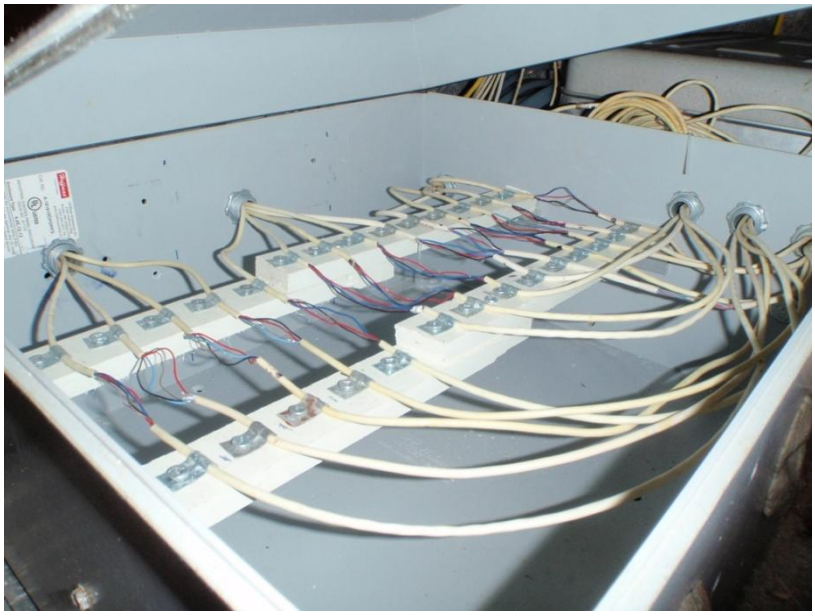

Figure 5.25: Photograph of the interior of the psychrometer drip box (AECL stock photograph)

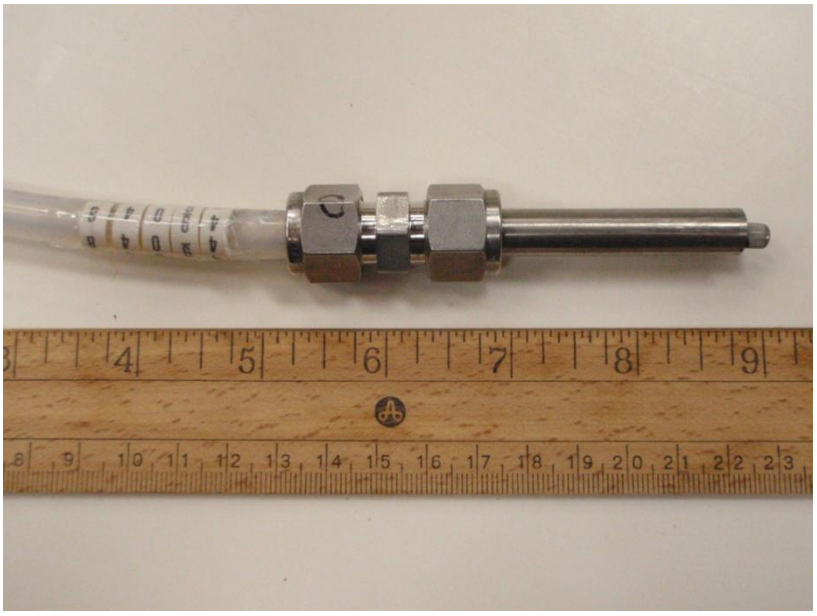

Figure 5.26: Psychrometer with stainless steel armouring tube and Synflex cable tubing (AECL stock photograph)



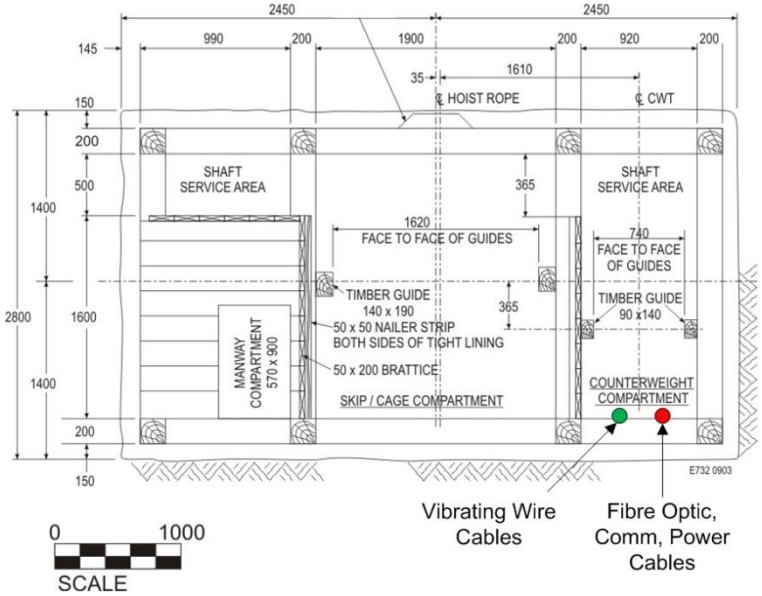


Figure 5.27: Locations of cable bundles in the main shaft (Dixon, Martino and Onagi 2009)

Figure 5.28: Cable bundles on cable stands ready to be lowered down shaft (AECL stock photograph)


Figure 5.29: Shiv wheel (top) and cable guide (bottom) used to lower shaft cabling (stitched photograph) (AECL stock photographs)

Figure 5.30: Plywood protection and support for total pressure cells (AECL stock photograph)




Figure 5.31: Manually reeling out cables during lowering (AECL stock photograph)

Figure 5.32: Attaching cables to the messenger wire (AECL stock photograph)



Figure 5.33: Anchoring messenger wire to shaft timbers (AECL stock photograph)


Figure 5.34: Plywood cable protection at the top of the shaft seal (AECL stock photograph)



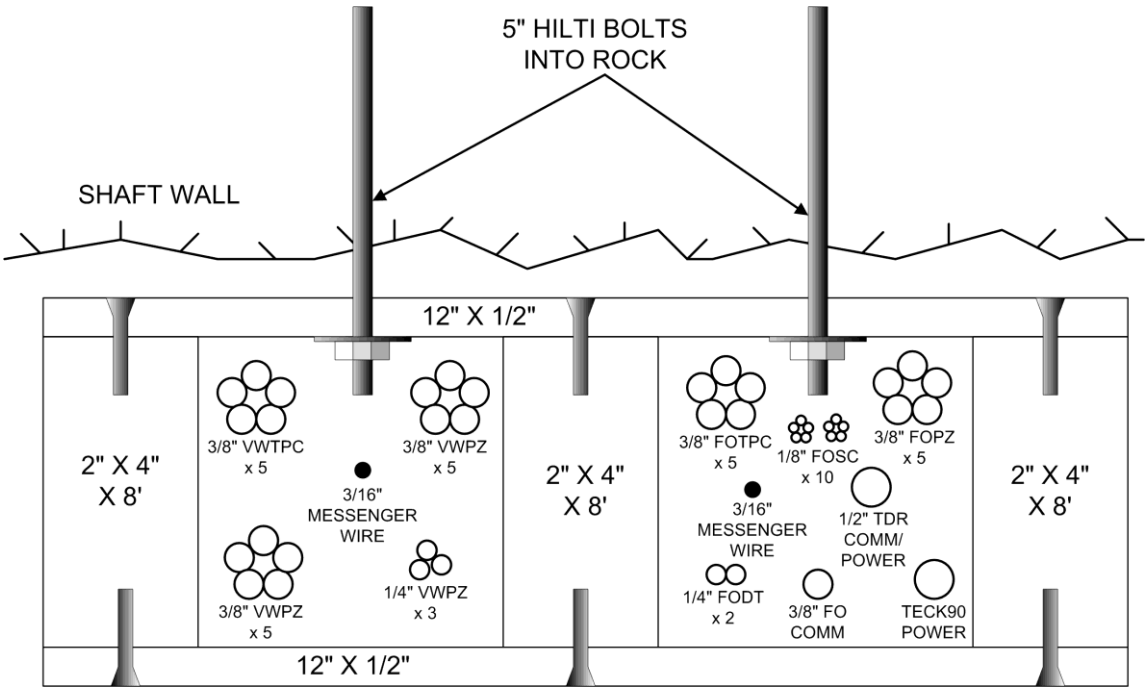


Figure 5.35: Diagram of shaft cabling protection box (AECL)

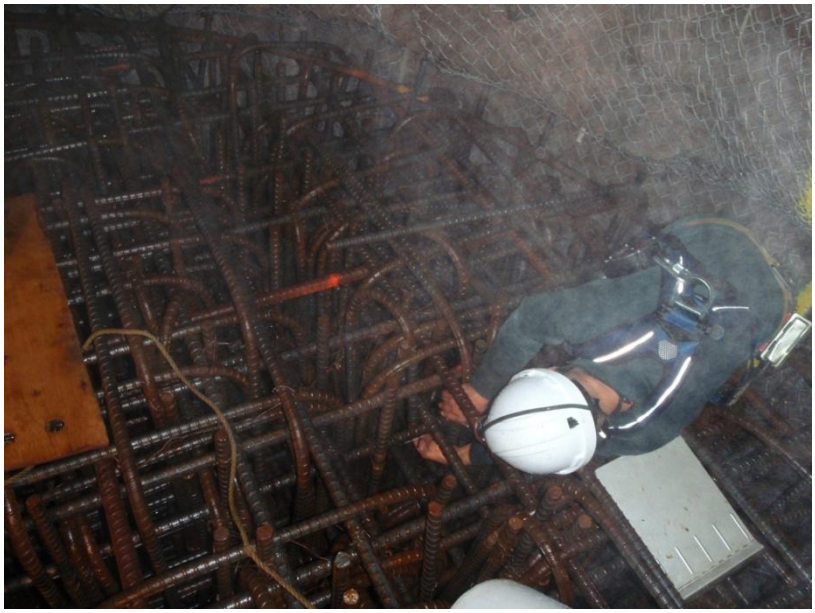

Figure 5.36: Difficulty when installing instruments in the lower concrete rebar (AECL stock photograph)



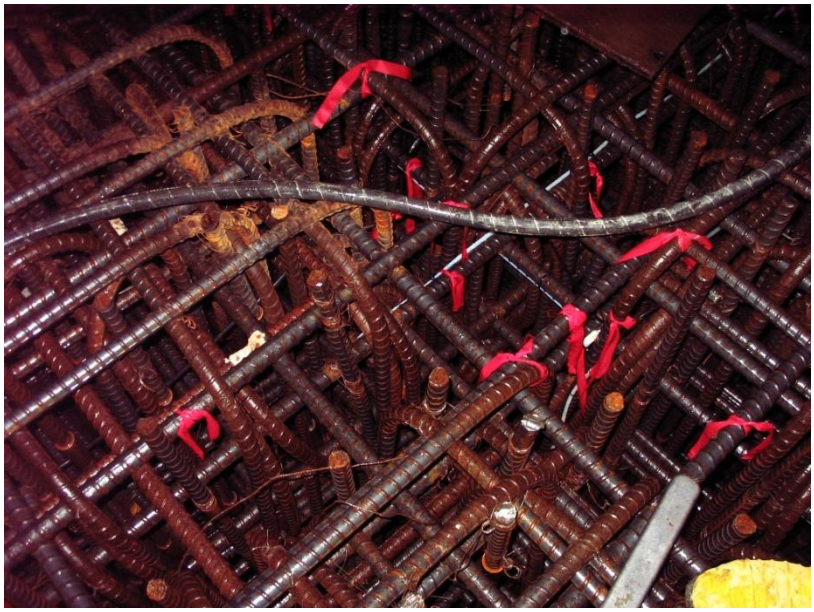

Figure 5.37: Flagging tape marks instrument locations for the lower concrete pour (AECL stock photograph)

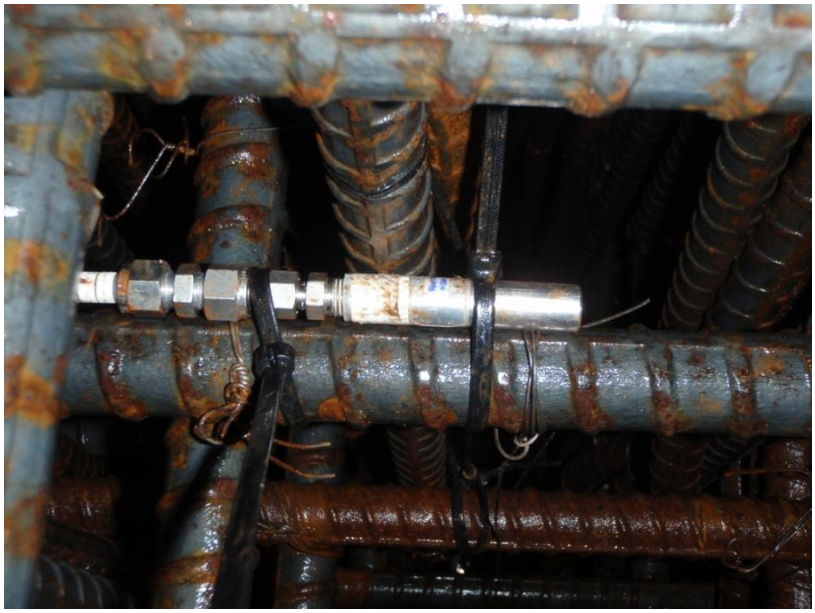

Figure 5.38: Thermocouple (Ct05) installed on the lower concrete component rebar (AECL stock photograph)



Figure 5.39: Two horizontal deformation sensors installed on the bottom concrete component rebar (AECL stock photograph)

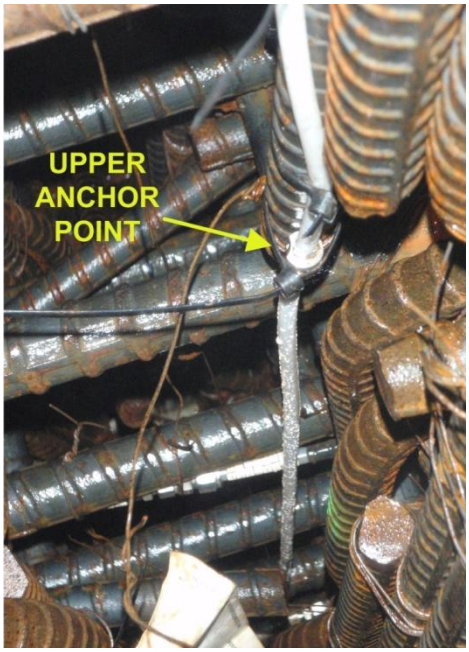


Figure 5.40: Vertical deformation sensor anchor point on lower concrete component rebar (AECL stock photograph)



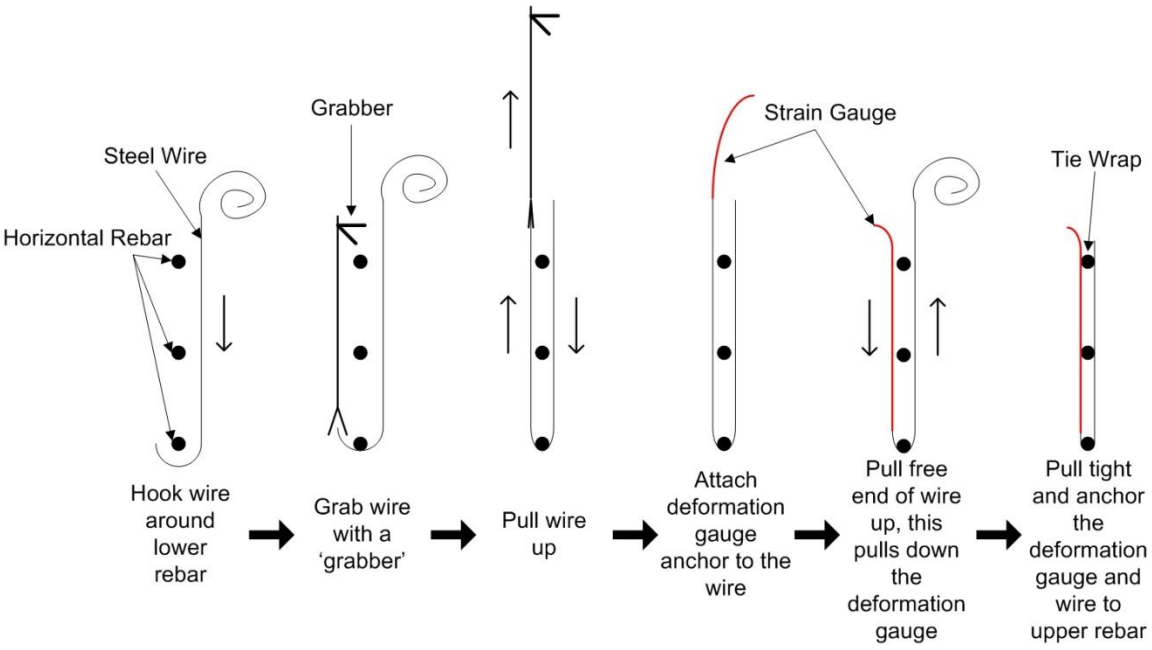


Figure 5.41: Installation method for vertical deformation sensors in the lower concrete component (AECL)

Figure 5.42: Vibrating wire piezometer filter tip wrapped with a geotextile sock (AECL stock photograph)



Figure 5.43: Installation of a vibrating wire piezometer on rebar at the lower concrete-rock interface (AECL stock photograph)

Figure 5.44: Installation of a vibrating wire piezometer on an I-bolt at the lower concrete-rock interface (AECL stock photograph)



Figure 5.45: Instrument cable separation in the bentonite-sand component (AECL stock photograph)

Figure 5.46: Smearing filter of a piezometer with saturated bentonite-sand material before installation (AECL stock photograph)



Figure 5.47: Installing a piezometer in the bentonite sand component (AECL stock photograph)

Figure 5.48: Installation of a total pressure cell at the lower clay-concrete interface (AECL stock photographs)

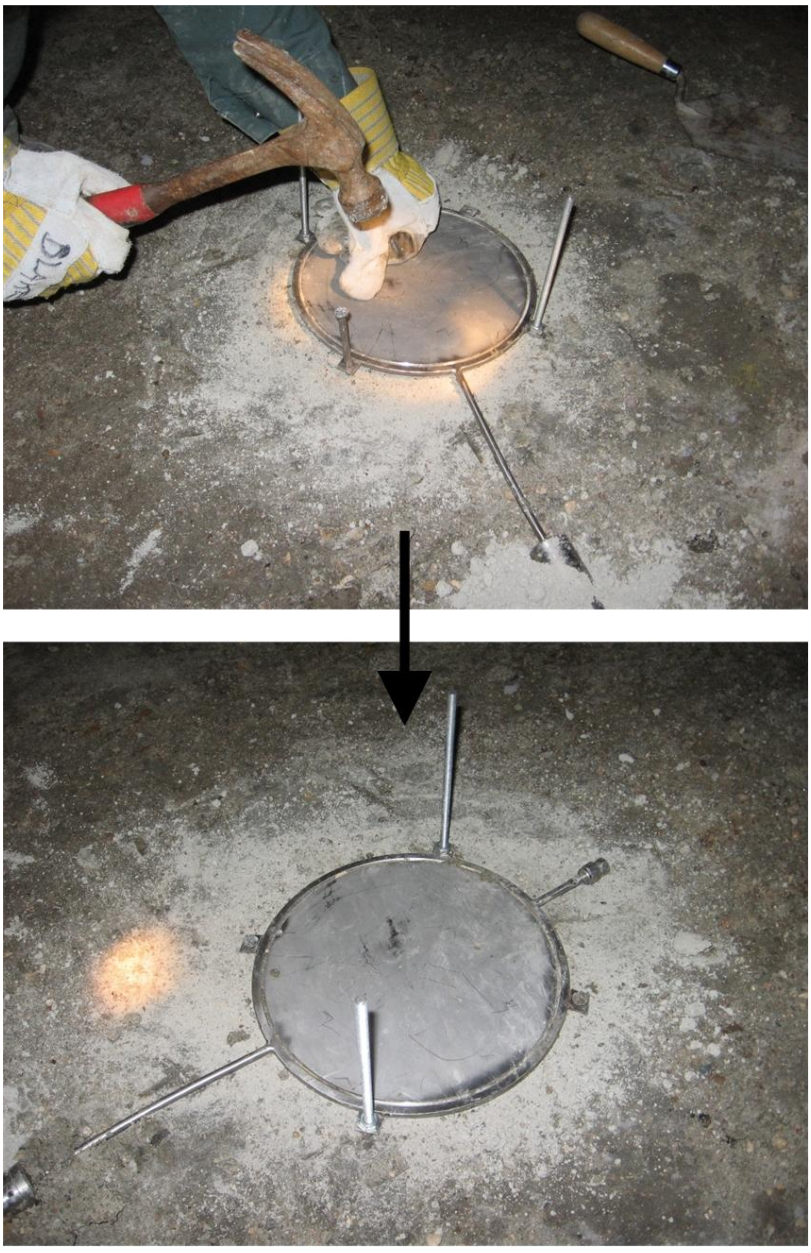

Figure 5.49: Installation of a total pressure cell at the upper clay-concrete interface (AECL stock photographs)

Figure 5.50: Two total pressure cells installed at the upper clay-concrete interface (AECL stock photograph)

Figure 5.51: Installation of a horizontal total pressure cell at the clay-rock interface (AECL stock photographs)

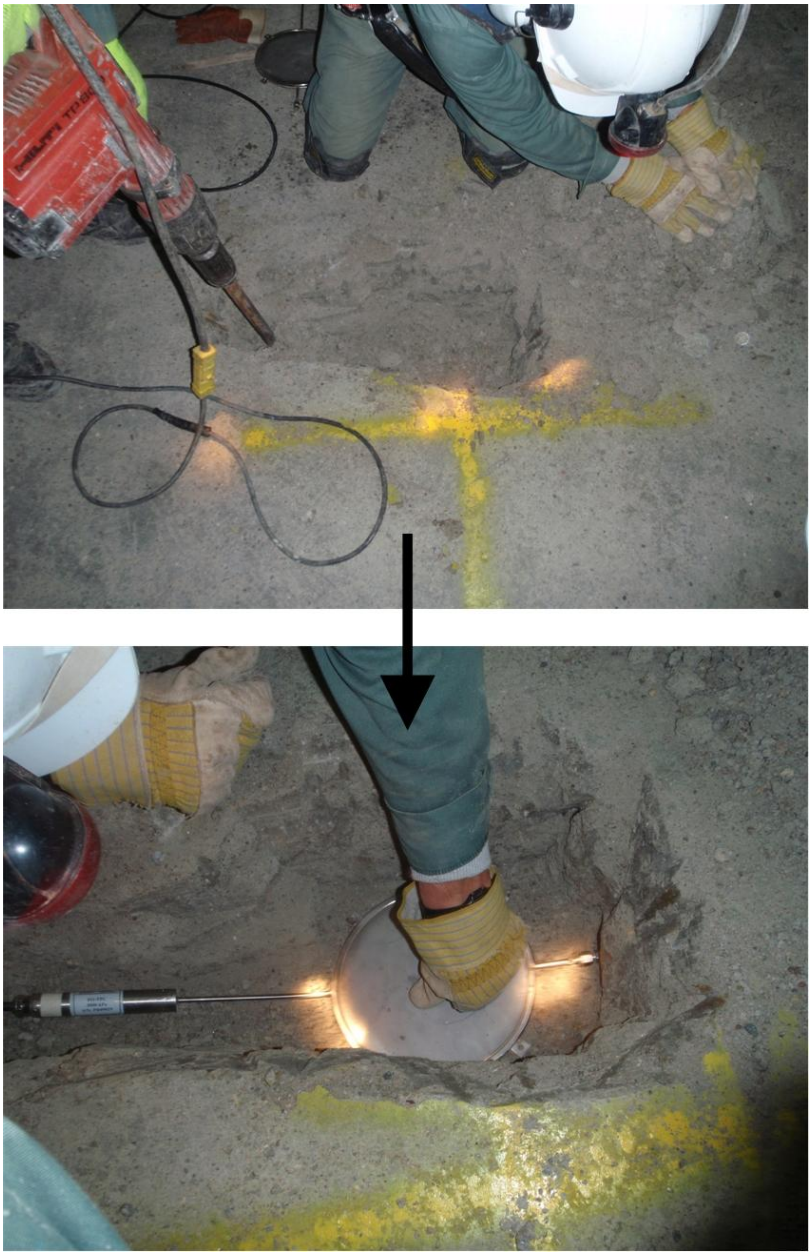

Figure 5.52: Installation of a total pressure cell at the interior of the bentonite-sand component (AECL stock photographs)

Figure 5.53: Backfilling and compaction after installing a total pressure cell in the bentonite-sand component (AECL stock photograph)

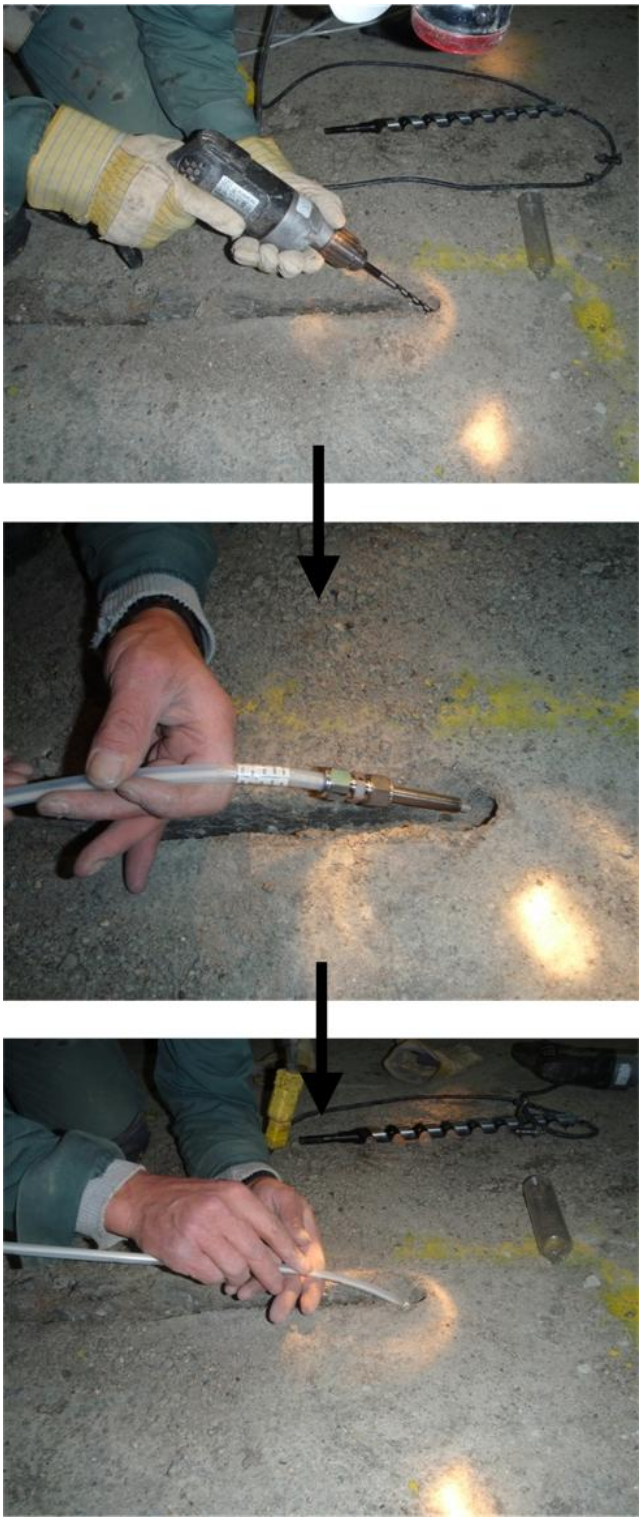

Figure 5.54: Installation of a thermocouple psychrometer (AECL stock photographs)

Figure 5.55: Drilling a precompacted bentonite-sand brick for TDR probe installation (AECL stock photograph)



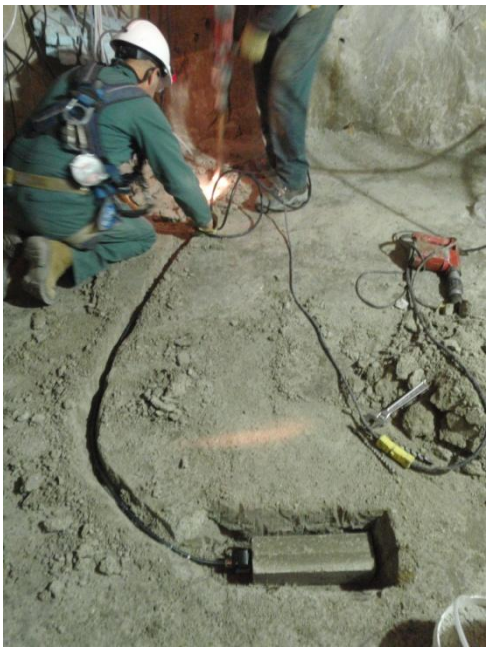

Figure 5.56: Installation of a time domain reflectometry probe (AECL stock photograph)

Figure 5.57: Time domain reflectometry probe installation prior to backfilling (AECL stock photograph)



Figure 5.58: Drilling horizontal boreholes for mechanical packers in adjacent rock (AECL stock photograph)

Figure 5.59: Inserting a mechanical packer into a horizontal borehole (AECL stock photograph)



Figure 5.60: Final installation of a mechanical packer with vibrating wire piezometer attached (AECL stock photograph)

Figure 5.61: Installing instruments on support cables in the upper concrete component (AECL stock photograph)

Figure 5.62: Instrument support cable anchors in the upper concrete component, I-bolt (Left) and turnbuckle (right) (AECL stock photographs)



Figure 5.63: Installing a vertical instrument support cable in the upper concrete component (AECL stock photograph)

Figure 5.64: Installation of a thermocouple in the upper concrete component (AECL stock photograph)

Figure 5.65: Installation of deformation sensors in the upper concrete component, looking south (AECL stock photograph)

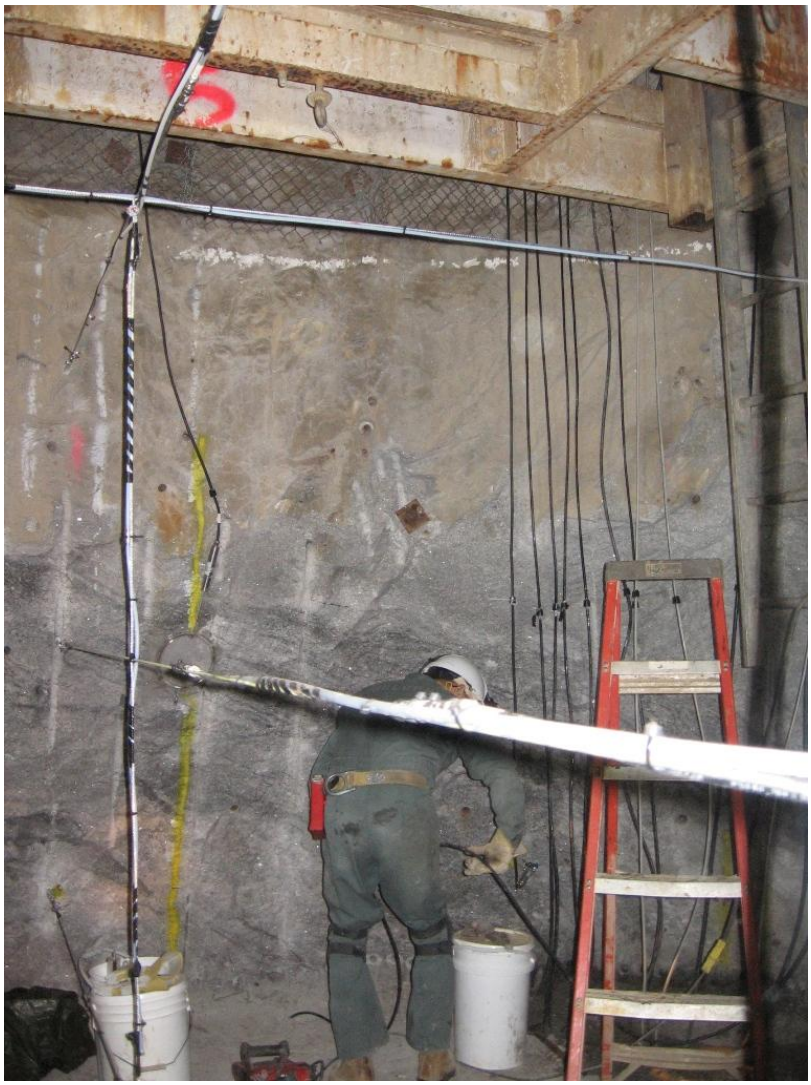

Figure 5.66: Installation of deformation sensors in the upper concrete component, looking north (AECL stock photograph)

Figure 5.67: Installation of a vibrating wire piezometer at the upper concrete-rock interface (AECL stock photograph)



Figure 5.68: Installation of a vibrating wire piezometer on the top surface of the upper concrete component (AECL stock photograph)

Figure 5.69: Hydraulic cement placed behind the sensing pad of a total pressure cell at the upper concrete-rock interface (AECL stock photograph)



Figure 5.70: Installation of a vibrating wire total pressure cell at the upper concrete-rock interface (AECL stock photograph)

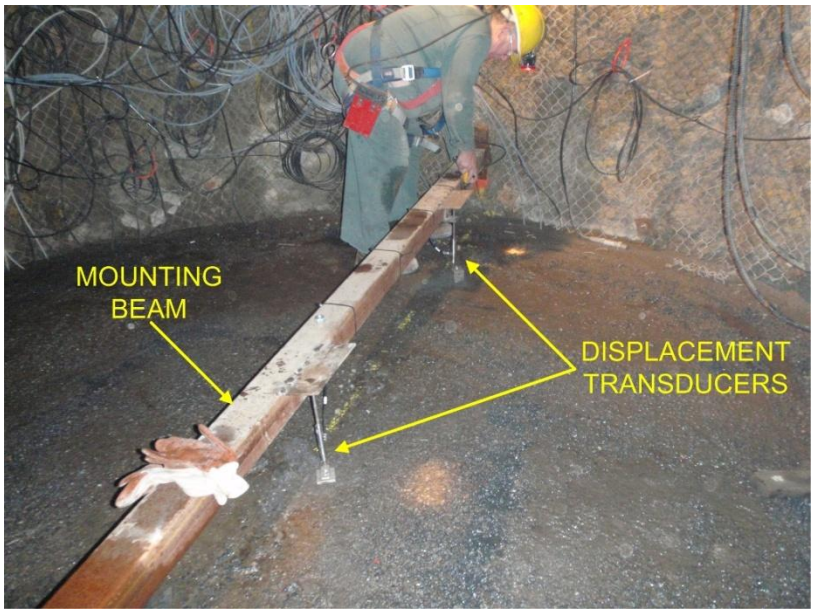


Figure 5.71: Fibre optic displacement transducers above the upper concrete component (AECL stock photograph)



Figure 5.72: Fibre optic displacement transducer mounting beam anchor (AECL stock photograph)

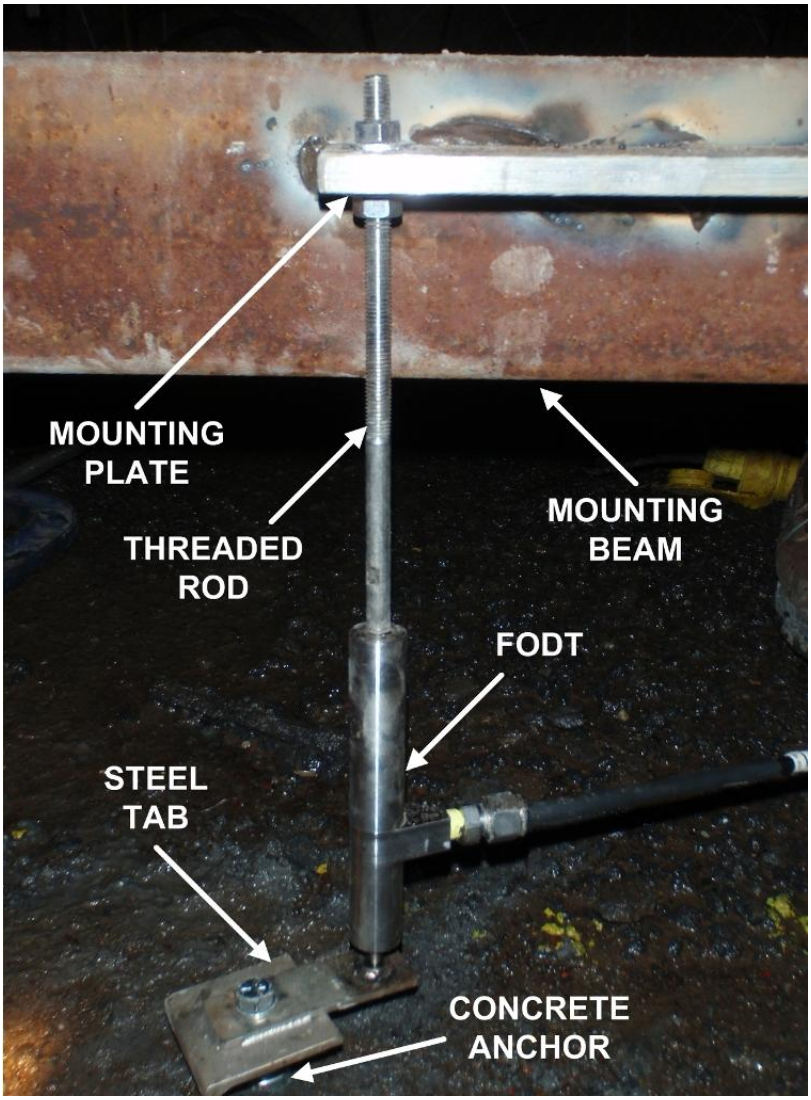


Figure 5.73: Components of a fibre optic displacement transducer installation (AECL stock photograph)

Figure 5.74: Wooden box covering the fibre optic displacement transducer mounting beam (AECL stock photograph)



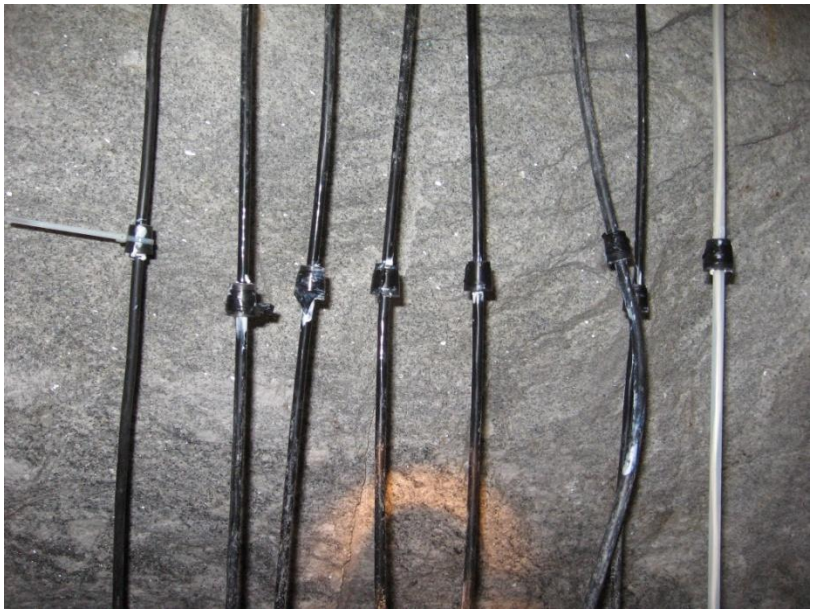

Figure 5.75: Instrument cable water stops in the upper concrete component (AECL stock photograph)

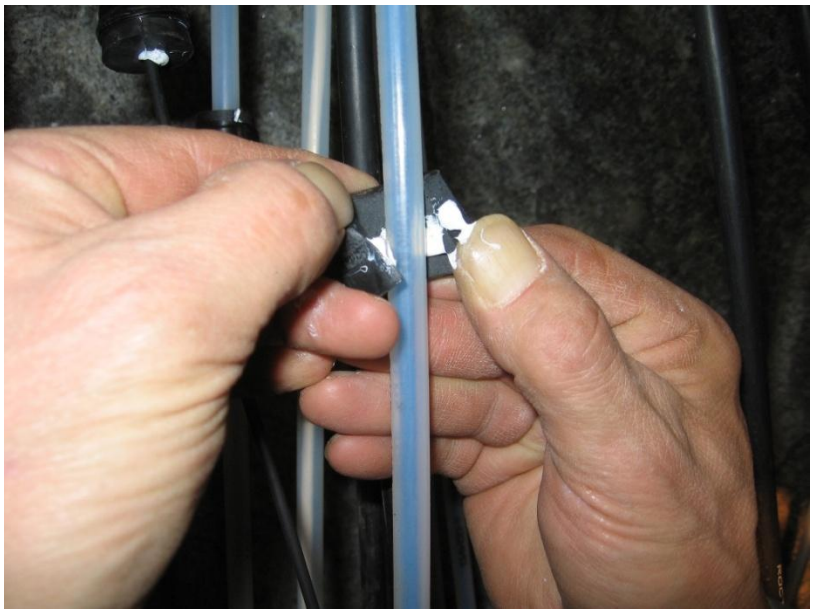

Figure 5.76: Installing an instrument cable water stop in the upper concrete component (AECL stock photograph)

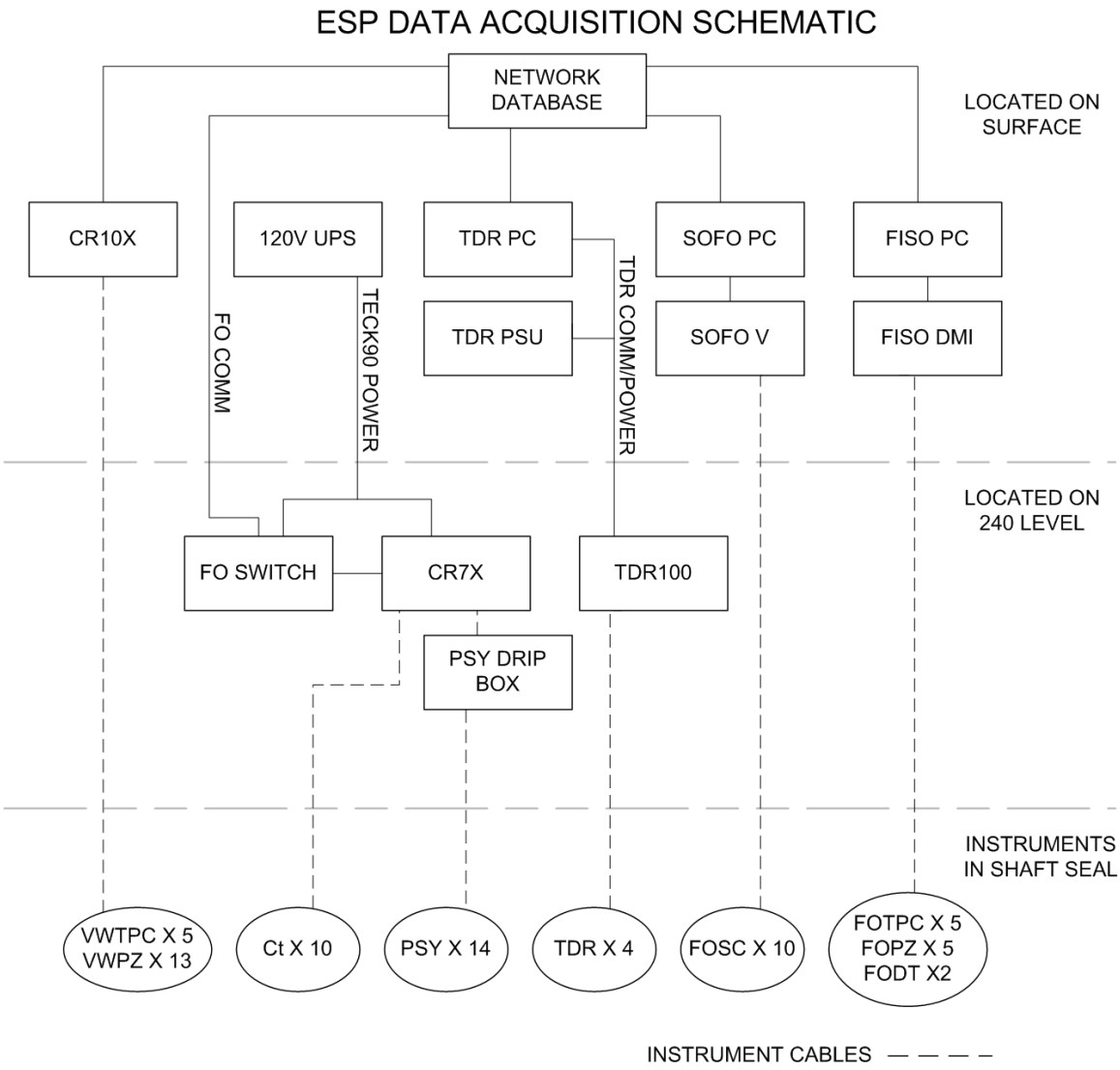


Figure 5.77: Simplified schematic of the ESP data acquisition system (AECL)

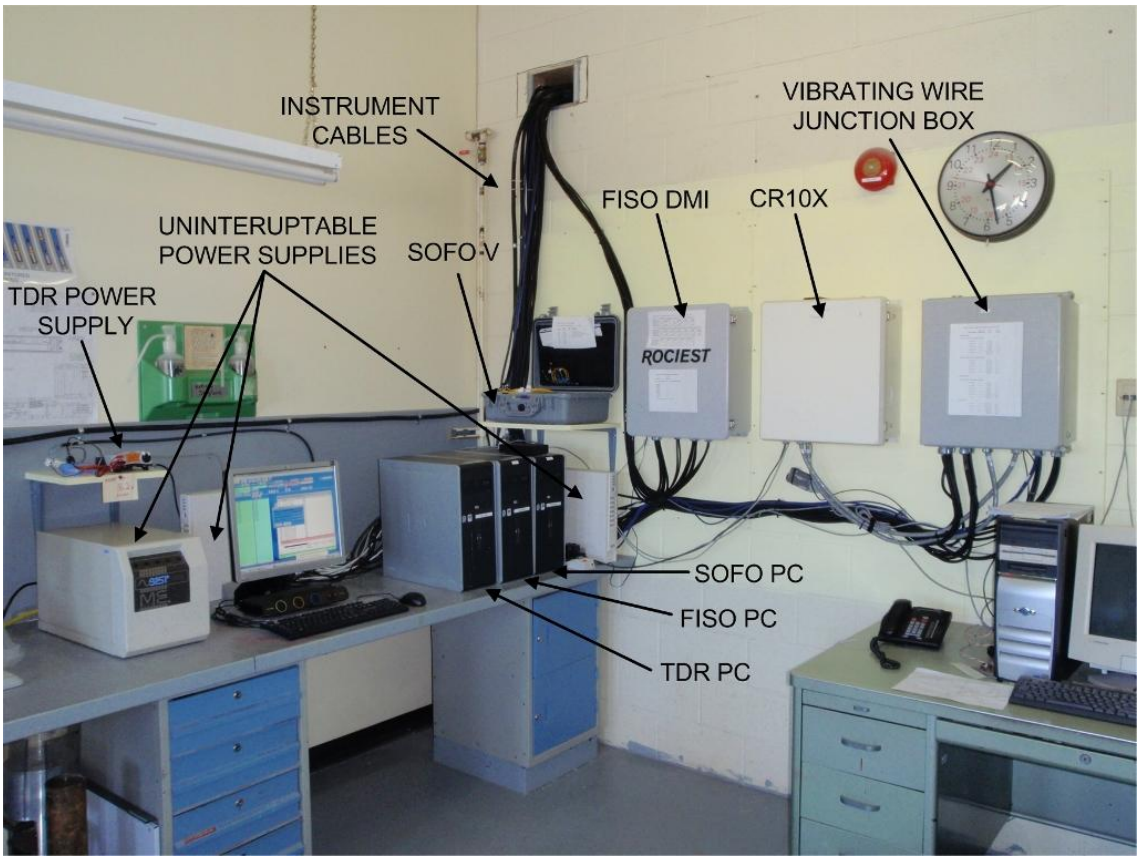


Figure 5.78: Surface dataloggers, signal conditioners and computers located in the GSEB Lab (AECL stock photograph)

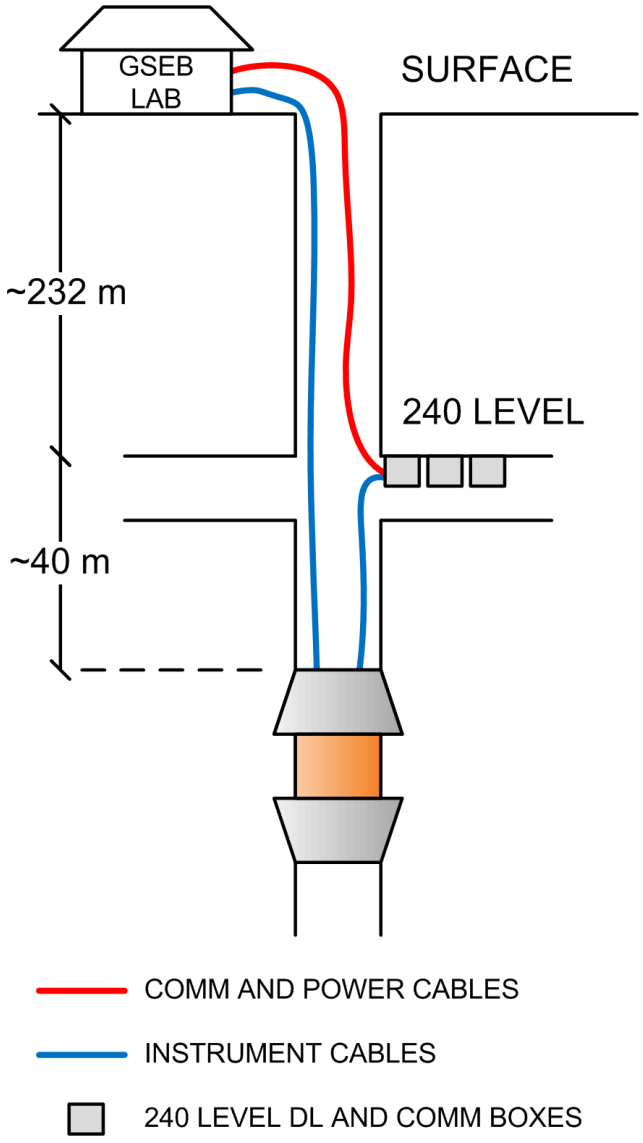


Figure 5.79: Simplified schematic showing routing of instrument cables depending on cable length limitations

Figure 5.79 created by Blake Holowick

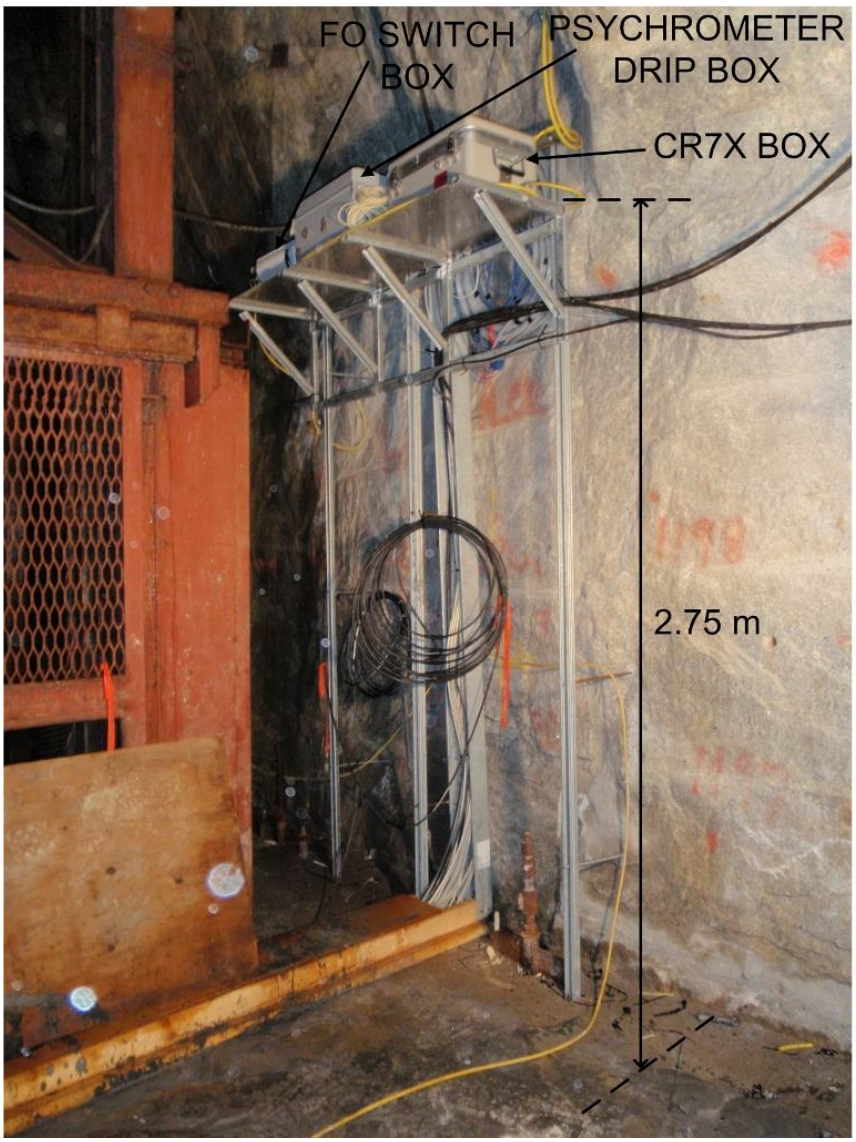


Figure 5.80: CR7X datalogger and fibre optic switch installed on a shelf at the 240 Level (AECL stock photograph)

Figure 5.81: High pressure watertight TDR datalogger caisson (AECL stock photograph)



Figure 5.82: Potting the TDR caisson connectors (AECL stock photograph)


Figure 5.83: Watertight TDR datalogger caisson installed on a shelf at the 240 Level (AECL stock photograph)

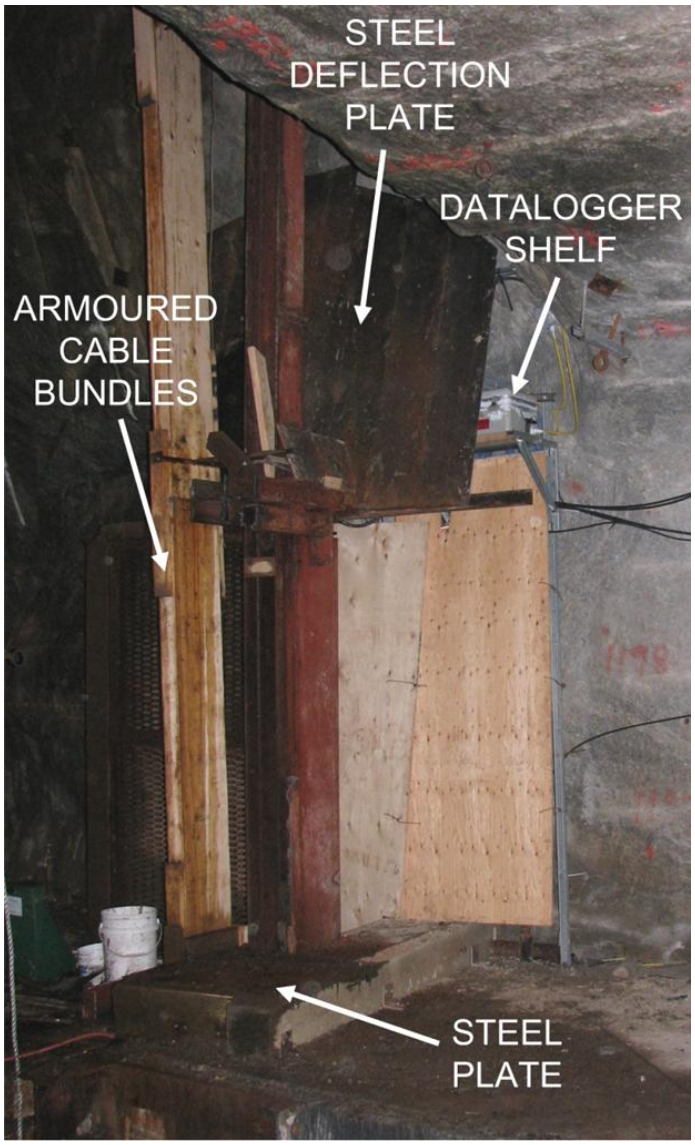


Figure 5.84: Deflection plates covering datalogger shelf and cable tray on the 240 Level (AECL stock photograph)

# 6 INTERPRETATION OF INITIAL MONITORING DATA

This section of the report briefly describes the initial monitoring data collected up to March 31, 2010. The only phase of monitoring that has been completed is the hydration temperature rise and shrinkage of both the upper and lower concrete components. For all of other instruments only initial trends and instrument performance will be commented on, since the evolution of the bentonite-sand component has only just begun.

When reading the legends on each data plot (Figures 6.1 to 6.20), the position of each instrument is typically indicated as follows:

Elevation / Position (Instrument Name)

Where “Elevation” is the distance above the base of the component it is installed in, and “Position” is the direction and distance from the shaft centreline. Note that, when indicating position, “north” is actually offset from true north by 23° in order to align it with the URL shaft orientation.

For example, psychrometer Psy05 is located 1.0 m above the base of the bentonite-sand component, and 1.25 m east (shaft east) from the shaft centreline. Therefore in the data plot legends it is indicated as:

1m Elev / 1.25m E of CL (Psy05)

## 6.1 Monitoring of the Lower Concrete Component

### 6.1.1 Temperature in the Lower Concrete Component

Temperature is monitored in the lower concrete component by five (5) thermocouples and three (3) thermistors associated with vibrating wire piezometers; temperature data from the first four months of concrete curing is plotted in Figure 6.1. The instruments recorded an as-placed concrete temperature of approximately 23.5°C, and showed a peak temperature of 39.5°C at the centre of the concrete mass. This leads to a concrete hydration temperature rise of approximately 16°C. This rise is comparable to the 20°C increase measured in the TSX concrete bulkhead (Chandler, et al. 2002). The reason for the smaller temperature rise in the shaft seal as compared to the TSX may be attributed to the presence of the large volume of reinforcing steel in the lower concrete component. This material will provide a means for more effective heat transfer away from the curing concrete mass than would be present in a structure that does not contain steel.

### 6.1.2 Strain in the Lower Concrete Component

Strain in the lower concrete component is monitored by five (5) fibre optic deformation sensors, two (2) of which are oriented vertically and three (3) horizontally; data from these instruments are plotted in Figure 6.2.

The sensors show an initial expansion of up to -50 με, followed by shrinkage that appears to be levelling off at approximately 250 με. Most of the instruments recorded remarkably similar strain, indicating that the shrinkage of the concrete is isotropic. The sensor located closest to the base of the concrete (FOSC01) is indicating a smaller shrinkage strain. This may be due to the base of the lower concrete component bonding to the concrete formwork, thereby supplying resistance to shrinkage.

These strain measurements provide insight into why the concrete-rock interface is not watertight. The total horizontal shrinkage of the concrete component is approximately 1.25 mm, assuming a shaft diameter of 5 m and a uniformly distributed shrinkage strain of 250 με. This leads to an estimated gap thickness of 0.625 mm around the perimeter of the lower concrete component, assuming no localized bonding of the concrete to the rock. This size of gap is large enough to allow easy passage of water along the concrete-rock interface.

### 6.1.3 Hydraulic Pressure at the Lower Concrete-Rock Interface

The hydraulic pressure along the concrete-rock interface of the lower concrete component is monitored by three (3) vibrating wire piezometers. Figure 6.3 shows data collected from these instruments3.

Two of the piezometers (VWPZ01 and VWPZ02) indicate groundwater recharge and infiltration along the concrete-rock interface, while the third piezometer (VWPZ03) is not showing any hydraulic pressure response. It is likely that either

the filter tip of VWPZ03 is completely encased in concrete or no local open pathway for water movement is present in this location, and hence it is not showing a pressure response. This reasoning is supported by the significantly higher suction measured by VWPZ03 during the initial curing and shrinkage of the concrete; see mid-September 2009 data on Figure 6.3.

The two piezometers giving hydraulic pressure readings indicate that the groundwater in the shaft reached the bottom of the shaft seal near the end of November 2009. The piezometers show a continuous increase in hydraulic pressure that seems to be accelerating near the beginning of March 2010. It should be noted that pumping of water from the top of the shaft seal was stopped on March 12, 2010, which marked the beginning of passive flooding of the URL.

## 6.2 Monitoring of the Bentonite-Sand Component

### 6.2.1 Water Content and Soil Suction in the Bentonite-Sand

Water content in the bentonite-sand component is being measured directly by four (4) TDR probes and indirectly, in terms of suction, by fourteen (14) psychrometers. Figures 6.4 to 6.11 show the readings from the TDR probes and psychrometers.

#### *6.2.1.1 Water Content Measured by TDR Probes*

The volumetric water content readings measured by the TDR probes (Figure 6.4) show a significant amount of scatter. This scatter, along with the uncertainty of the calibration equation, makes it nearly impossible to detect any minor changes in water content. However, the overall trend in the measurements can still be interpreted. Three of the TDR probes are reading water contents that are close to the initial expected values. The initial gravimetric water content of the bentonite-sand component was approximately 12%, which equates to a volumetric water content of roughly 22%. The readings from TDR4 show a volumetric water content approximately 7-8% higher than it should be. This variability is possibly due to the method for creating the calibration equation (Section 5.4.3), and the assumption when applying the equation that all of the TDR probes behave exactly the same

The TDR probes are installed near the centre of the bentonite-sand mass, where the material has not likely experienced any major changes in water content. This seems to agree with the relative stability of the TDR readings. As the bentonite-sand continues to saturate the TDR probes should show an increasing response and eventual stabilization once saturation is reached.

#### *6.2.1.2 Soil Suction Measured by Thermocouple Psychrometers*

Data for the total soil suction collected by all fourteen psychrometers are shown in Figures 6.5 to 6.11. Some of the psychrometers are already indicating

saturation (~500 kPa suction) while others are showing very dry conditions (high suction). The perimeter of the lower half of the bentonite-sand component appears to be saturating rapidly, as shown in Figures 6.5 to 6.7, while the top half of the bentonite-sand component is showing a slower rate of water uptake as seen in Figures 6.8 to 6.11. This pattern of soil suction agrees with the points of water inflow observed during the shaft seal construction, with most inflow entering at-or-below FZ2 in the south-west quadrant of the shaft.

### 6.2.3 Pore-Water Pressure in the Bentonite-Sand Component

The eight (8) piezometers located in the bentonite-sand component have not yet shown any significant increase in pore-water pressure (Figure 6.12); the maximum recorded increase is roughly 5 kPa. The saturation of the bentonite-sand material is still in its early stages, and it is likely that the pore-water has not yet reached the location of the piezometers. As the bentonite-sand continues to hydrate and swell the piezometers will eventually show a pore-water pressure response.

### 6.2.4 Total Pressure in the Bentonite-Sand Component

There are a total of eight (8) TPCs in the bentonite-sand component. Five (5) TPCs measure total vertical pressures inside the bentonite-sand and at the clay-concrete interfaces, and three (3) measure total horizontal pressures at the clay-rock interface.

#### *6.2.4.1 Total Vertical Pressure in the Bentonite-Sand Component*

The recorded total vertical pressures inside the bentonite-sand component and at the upper and lower clay-concrete interfaces are shown in Figure 6.13.

VWTPC01, located at the lower clay-concrete interface, clearly shows an increase in pressure during the installation of the bentonite-sand material from October 6, 2009 to November 10, 2010. The total pressure reached approximately 65 kPa before the upper concrete component was poured. The in situ compacted bentonite-sand had an average bulk unit weight of 19.9 kN/m$^3$, which leads to an overburden pressure of 119.4 kPa for the 6-m-thick bentonite-sand component. It is assumed that a portion of the load due to the self weight of the bentonite-sand was transferred to the rock by side-wall friction, or that bridging may have taken place over the TPC.

All of the TPCs showed an increase in pressure immediately following the pouring of the upper concrete on November 26, 2009. Interestingly the pressure measured by the two total pressure cells at the upper clay-concrete interface dropped to zero roughly two (2) months after the concrete pour. This reduction in applied pressure can be explained by shrinkage of the upper concrete component. However, as the bentonite-sand hydrates and swells these TPCs should start to respond again.

At the beginning of February 2010 the pressure measured at the lower clay-concrete interface started to increase gradually. This may be due to the initial

swelling of the clay in the lower half of the bentonite-sand component. It is too early to make any conclusive analysis.

#### *6.2.4.2 Total Horizontal Pressure at the Clay-Rock Interface*

The total horizontal pressure at the clay-rock interface along the north edge of the bentonite-sand component is monitored by three (3) horizontally oriented FOTPCs. Figure 6.14 shows the data collected from these instruments.

The readings from the FOTPCs show a considerable amount of noise during the installation of the bentonite-sand component. This may be due to the vibratory compaction techniques used to compact the material. However, after the upper concrete component was poured the readings stabilized considerably.

All three of the FOTPCs are giving similar values for total horizontal pressure, starting at roughly 40 kPa after the upper concrete pour and steadily rising to approximately 120 kPa as of March 31, 2010. The gradual increase in pressure may be due to “relaxing” of the bentonite-sand, as some locked-in stresses and initial suction are dissipated, and possibly some small swelling pressure beginning to develop at the clay-rock interface.

The similar readings from the three (3) FOTPCs are an indication that the instruments are functioning properly.

## 6.3 Monitoring of the Upper Concrete Component

### 6.3.1 Temperature in the Upper Concrete Component

Temperature is monitored in the upper concrete component by five (5) thermocouples and nine (9) thermistors or thermocouples associated with other instruments. Figure 6.15 shows the temperature data from the first four months of curing. The instruments recorded an as-placed concrete temperature of approximately 17°C and a maximum temperature during hydration of 35.6°C at the centre of the concrete mass. This equates to a maximum hydration temperature rise of 18.6°C, which is comparable to curing temperature rise measured in the lower concrete component and the Tunnel Sealing Experiment concrete bulkhead (Chandler, et al. 2002). It is also slightly higher than was observed in the lower concrete component of the shaft seal, likely due to the lack of heat-conducting reinforcing steel in the upper concrete component.

As of the end of March 2010 the entire upper concrete component seems to be approaching an ambient temperature of roughly 12°C.

### 6.3.2 Strain in the Upper Concrete Component

Strain in the upper concrete component is monitored by five (5) fibre optic deformation sensors, two (2) of which are oriented vertically and three (3) horizontally; data from these instruments are plotted in Figure 6.16. Note that one of the vertically oriented sensors (FOSC07) stopped functioning for 10 days,

and is giving data that are inconsistent with the other sensors. The erroneous sensor has been deemed non-functional (see Section 5.8), and therefore data supplied by FOSC07 should be ignored.

The remaining sensors indicate an initial expansion after pouring of up to -50 με, which is consistent with data for the lower concrete component. After the initial expansion the concrete begins to shrink, and is levelling off at about 350 με of compression. Similarly to the upper concrete component, the concrete shrinkage seems to be isotropic with similar strain recorded along all three axes.

The shrinkage of the upper concrete component is roughly 100 με more than the bottom concrete component. The higher shrinkage in the upper concrete component can be explained by lack of reinforcing steel in the concrete. The lower concrete component was heavily reinforced to support the weight of the shaft seal and overlying water after shaft flooding.

### 6.3.3 Hydraulic Pressure at the Upper Concrete-Rock Interface and Above the Shaft Seal

The hydraulic pressure at the upper concrete-rock interface is measured by three (3) vibrating wire piezometers. There is also a vibrating wire piezometer located on the top surface of the shaft seal that measured the head of water in the shaft. Figure 6.17 shows the data from these instruments.

It is clear that the upper concrete-rock interface is permeable, since the data measured by the three piezometers installed at the interface mirror the hydraulic head above the shaft seal, with the different readings corresponding to the elevation of each piezometer. The undulating readings are a result of successive water collection and pumping water from the top of the shaft seal. This is an indication that that water on top of the shaft seal is likely moving along this interface and supplying water to the bentonite-sand component. However, the high permeability of this interface will not adversely affect the sealing performance of the shaft seal as the bentonite-sand material is the main sealing element.

As the shaft floods, data from VWPZ10, located on top of the shaft seal, will be used to estimate the time required to flood the 240 Level. This piezometer provides an accurate measurement of the height of water above the shaft seal and can be used to calculate the rate of groundwater inflow, since the volume of the shaft excavation is known.

### 6.3.4 Total Pressure at the Upper Concrete-Rock Interface

The total pressure at the upper concrete-rock interface is monitored by two (2) VWTPCs. However, as indicated in Section 5.9, VWTPC04 is only giving intermittent pressure readings and its internal thermistor has failed. Therefore data from VWTPC04 should be interpreted with caution. Figure 6.18 shows the data from these VWTPCs.

On comparing the data from Figures 6.17 and 6.18 the readings from the VWTPCs are very similar to the hydraulic pressures along the concrete-rock interface. This indicates that no significant swelling pressures have developed yet, and the upper concrete component is not yet actively restraining the swelling bentonite-sand. It is expected that, with time, the reaction force along this interface will increase as the bentonite swells.

### 6.3.5 Vertical Displacement of the Upper Concrete Component

The vertical displacement of the upper concrete component is measured by two (2) fibre optic displacement transducers mounted on a steel beam directly above the top surface of the shaft seal. The tips of the plungers of the FODTs are anchored to the top of the upper concrete component. Figure 6.19 shows the displacement data from these instruments.

The FODTs show some movement immediately after they were installed in mid-December 2009. At this time the wooden box covering the FODT mounting beam was being constructed, and it is likely that some external loading was being applied to the beam, causing it to flex. However, the readings stabilized after construction of the protection box was completed.

FODT02 shows zero vertical displacement, while FODT01 is showing a periodic up-and-down pattern of roughly 0.15 mm displacement in Figure 20. The displacement exhibited by FODT02 is likely the result of a noisy signal from the instrument, since FODT01 is not showing a similar pattern. As of March 30,

2010, the readings from the FODTs can be interpreted as showing no vertical displacement of the upper concrete component.

## 6.4 Monitoring of Rock Immediately Adjacent to the Shaft Seal

### 6.4.1 Pore-Water Pressure in Adjacent Rock

The pore-water pressure in the rock adjacent to the shaft seal is measured at three horizontal distances into the rock (0.5 m, 1.0 m and 1.85 m) at a height of 4.5 m above the base of the bentonite-sand component. The rock pore-water pressure is monitored by three horizontal borehole packers equipped with vibrating wire piezometers. Figure 6.20 shows the data collected from these instruments.

Two of the piezometers, VWPZR01 and VWPZR02, show an initial spike up to roughly 60 kPa that dissipates over approximately the first month of monitoring. This initial spike is due to the installation method used for the packers and piezometers. Water was injected into the packer vent line using a syringe until it began leaking from the piezometer line drain plug, at which point the vent line valve and drain plug were closed while still applying pressure to the syringe. This was done to ensure the packers were completely full of water. The injection pressure from the syringe is what caused the initial pressure spike. Note that VWPZR03 did not show an initial pressure spike, since the syringe was removed before the vent line was closed.

As of March 31, 2010 the deepest packer, at 1.85 m horizontal distance into the rock, is showing a gradual increase in pore-water pressure that is likely the result of groundwater recharge in the vicinity of the shaft seal. The two shallower packers show dissipation of pressures induced by installation but have yet to show any significant pressure increase. This may be due to their interconnectivity to the EDZ which allows excess pressure to dissipate.

## 6.5 Summary of Initial Monitoring

As of March 31, 2010 the instruments installed in the shaft seal have shown that:

- Strain related to curing of the concrete components is complete.
- Water ingress into the bentonite-sand component is beginning to take place, however no significant swelling pressures have yet developed.
- The concrete-rock interface associated with both of the concrete components is not watertight and is likely a major pathway for saturating water to enter the bentonite-sand.
- The groundwater table adjacent to the shaft seal has started to recharge.

The initial behaviour of the shaft seal is progressing as expected, and will continue to evolve with time as the bentonite-sand saturates.

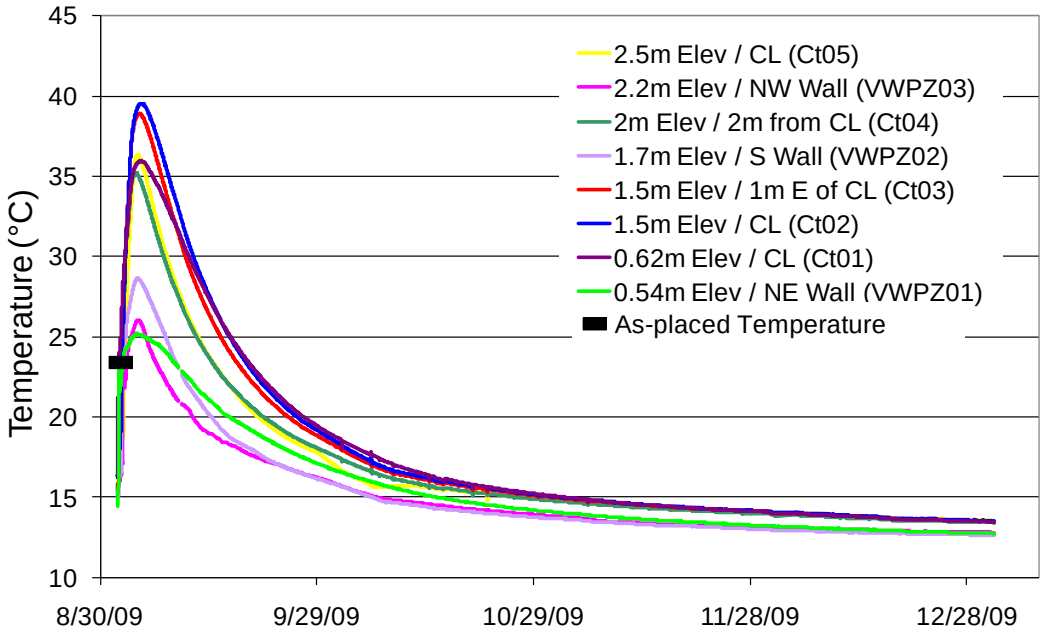


Figure 6.1: Temperature rise in the lower concrete component (AECL)



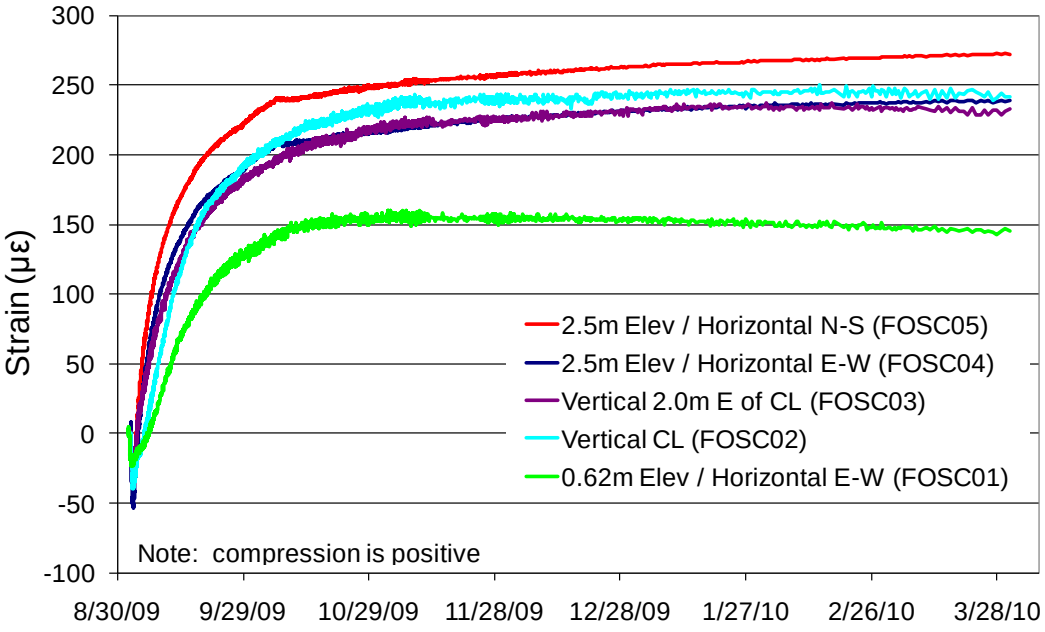


Figure 6.2: Strain in the lower concrete component (AECL)

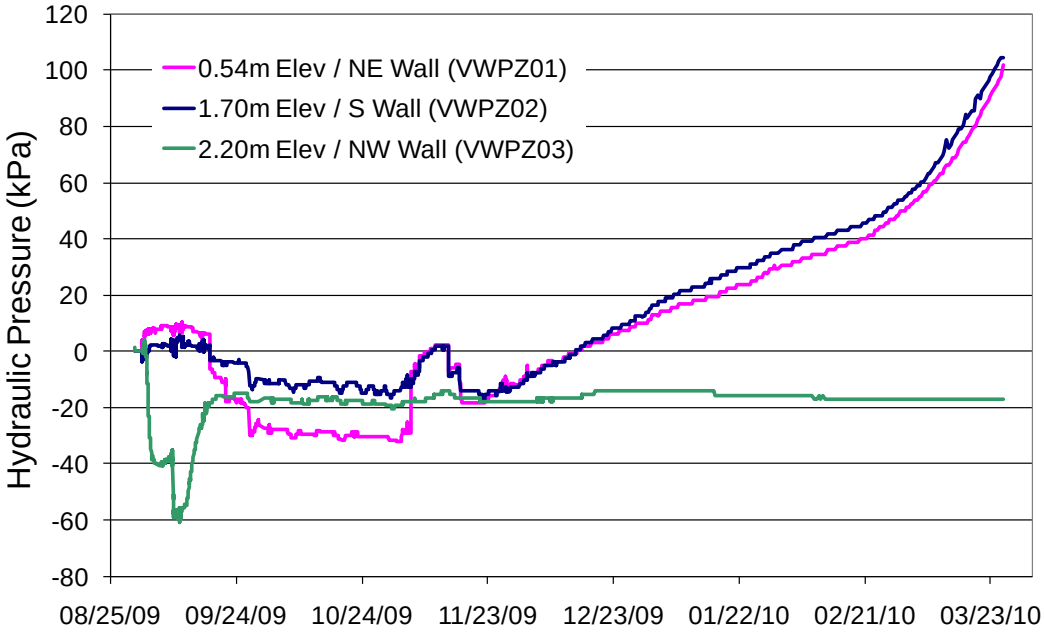


Figure 6.3: Hydraulic pressure at the lower concrete-rock interface (AECL)



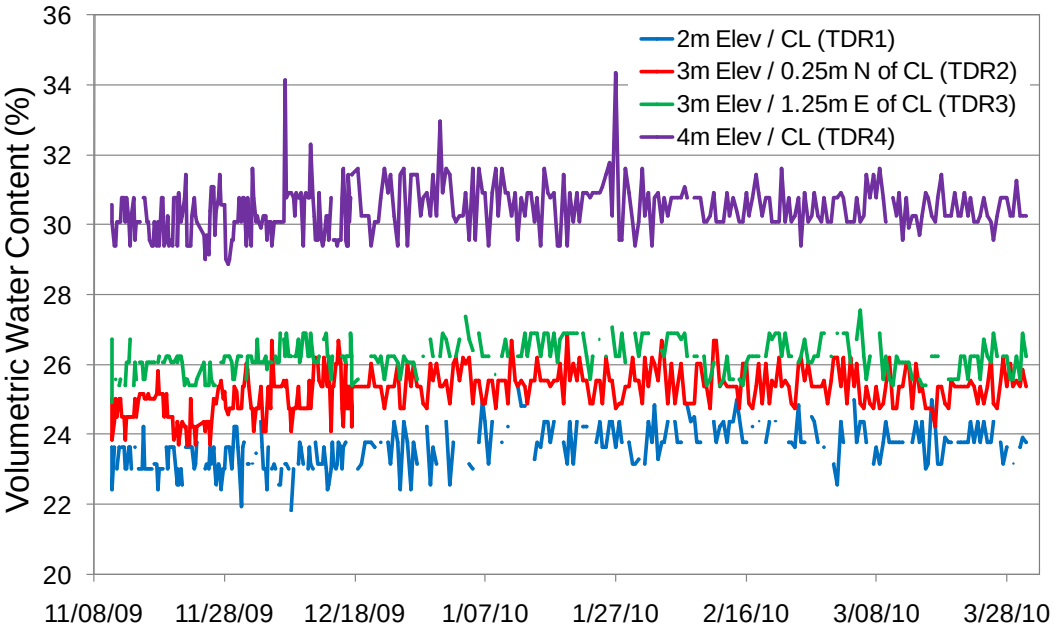


Figure 6.4: Volumetric water content measured by TDR probes (AECL)

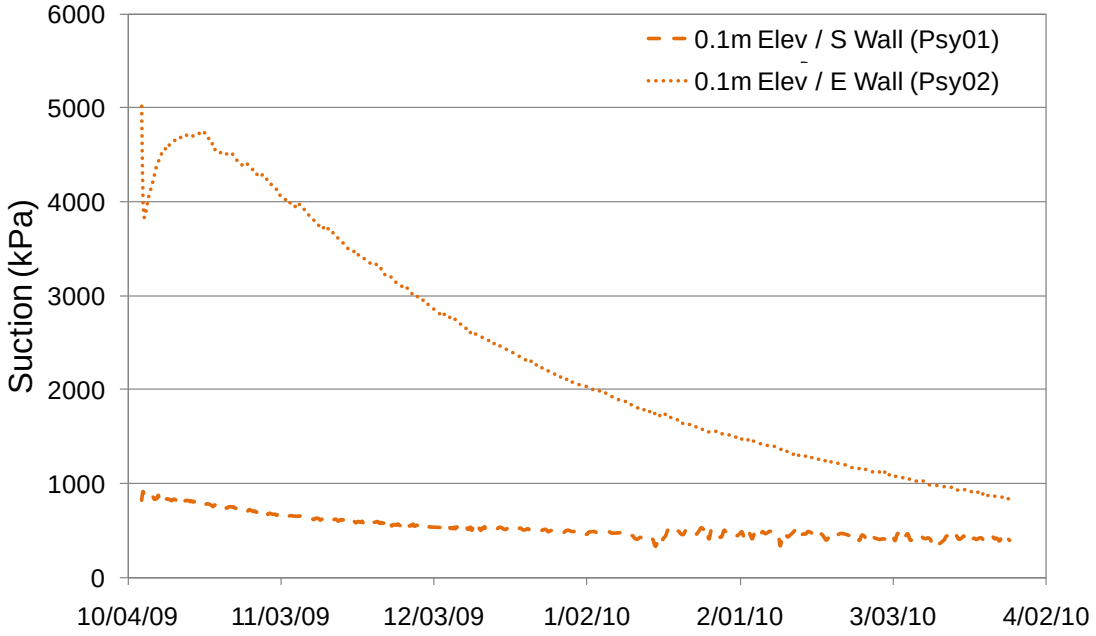


Figure 6.5: Suction at 0.1 m height in the bentonite-sand component (AECL)



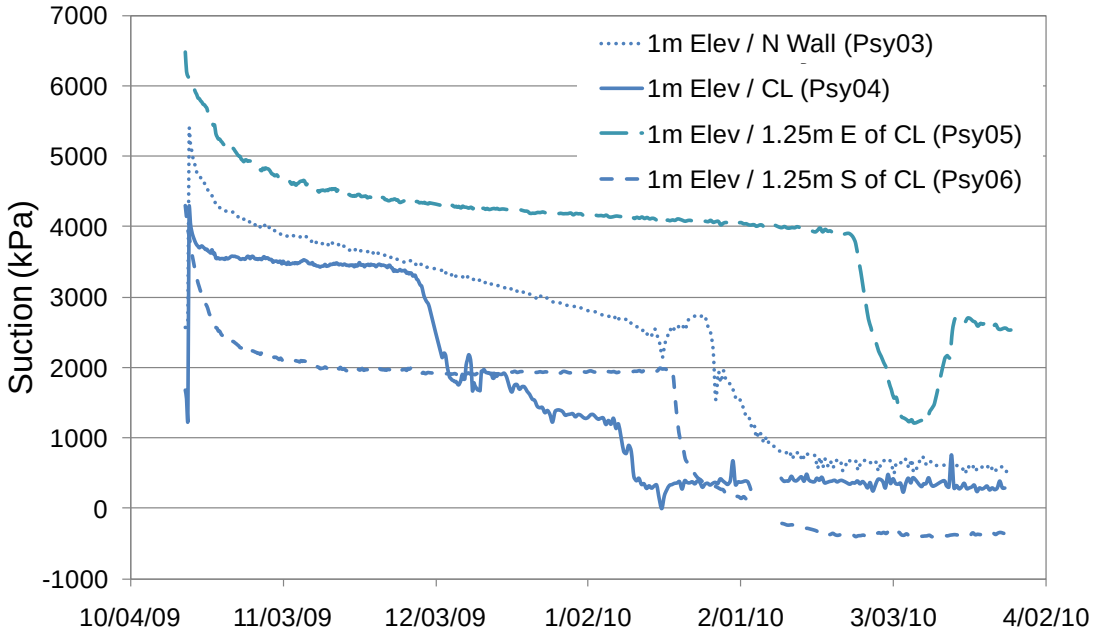


Figure 6.6: Suction at 1 m height in the bentonite-sand component (AECL)

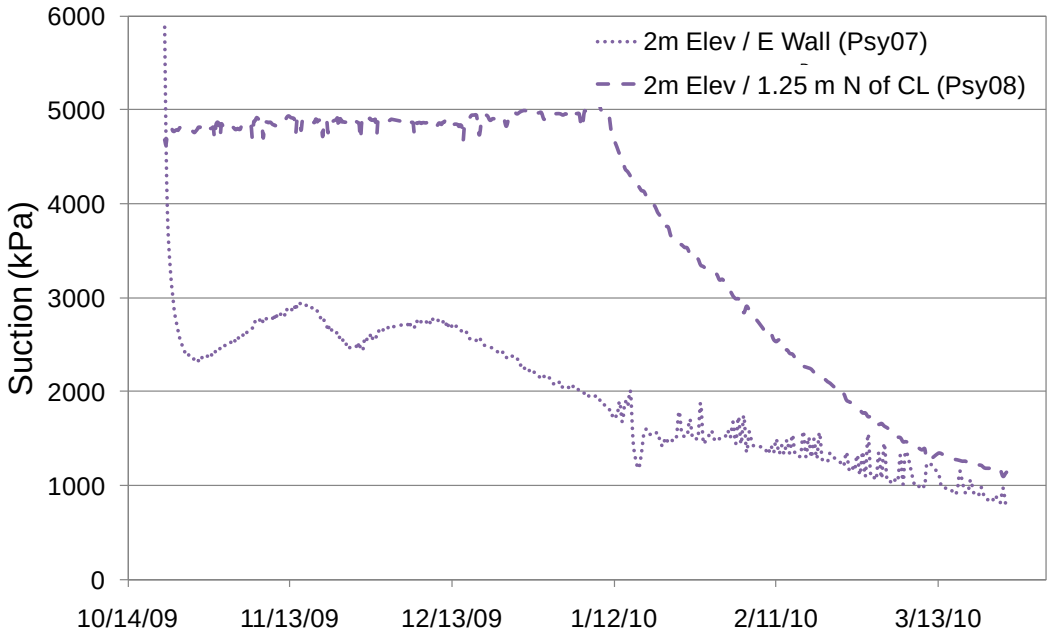


Figure 6.7: Suction at 2 m height in the bentonite-sand component (AECL)



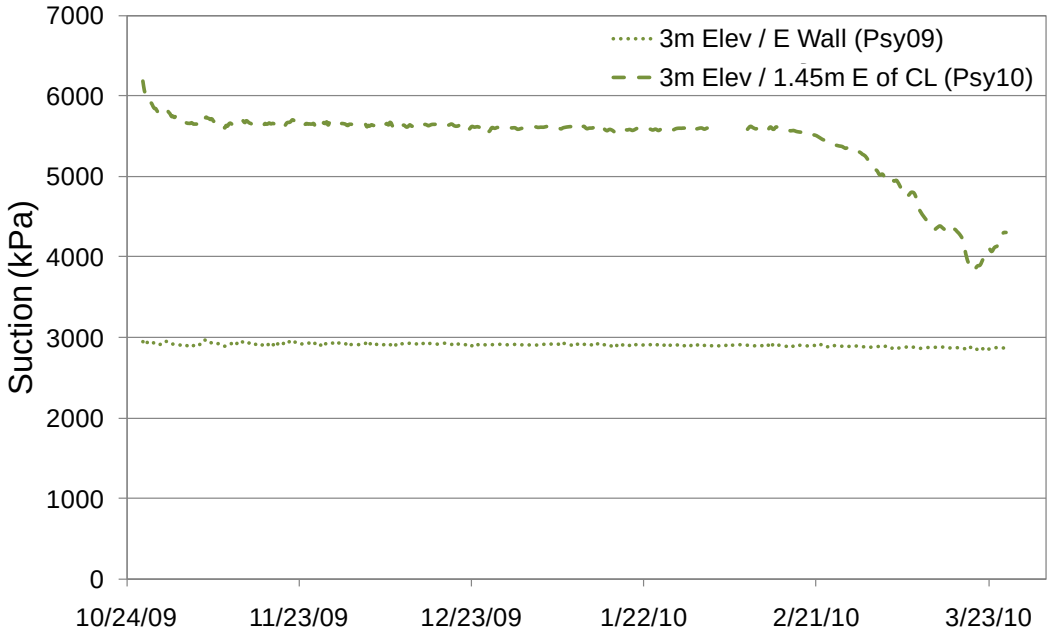


Figure 6.8: Suction at 3 m height in the bentonite-sand component (AECL)

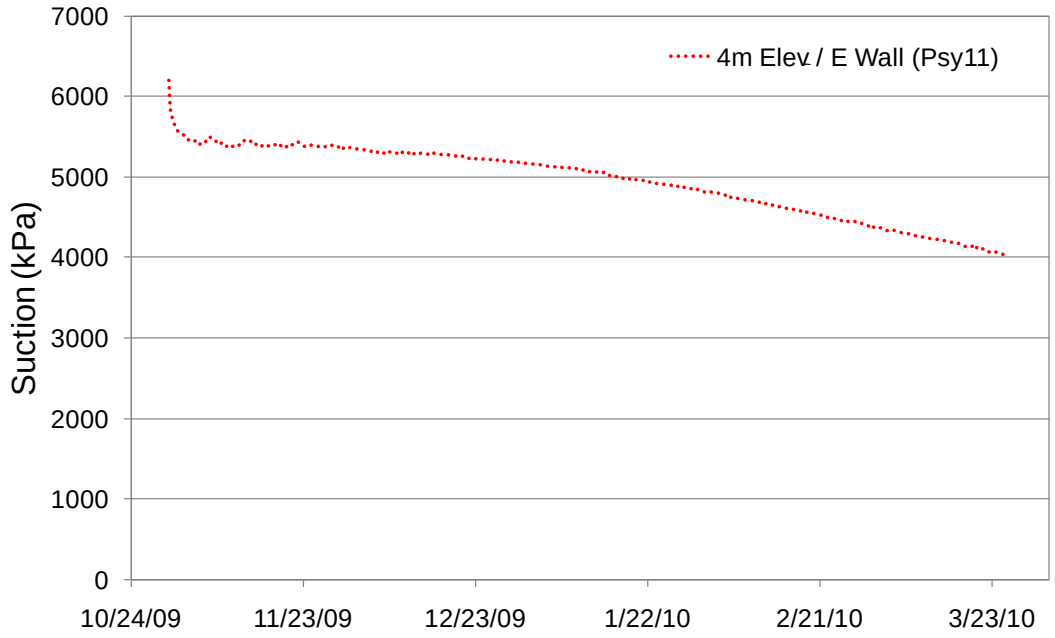


Figure 6.9: Suction at 4 m height in the bentonite-sand component (AECL)



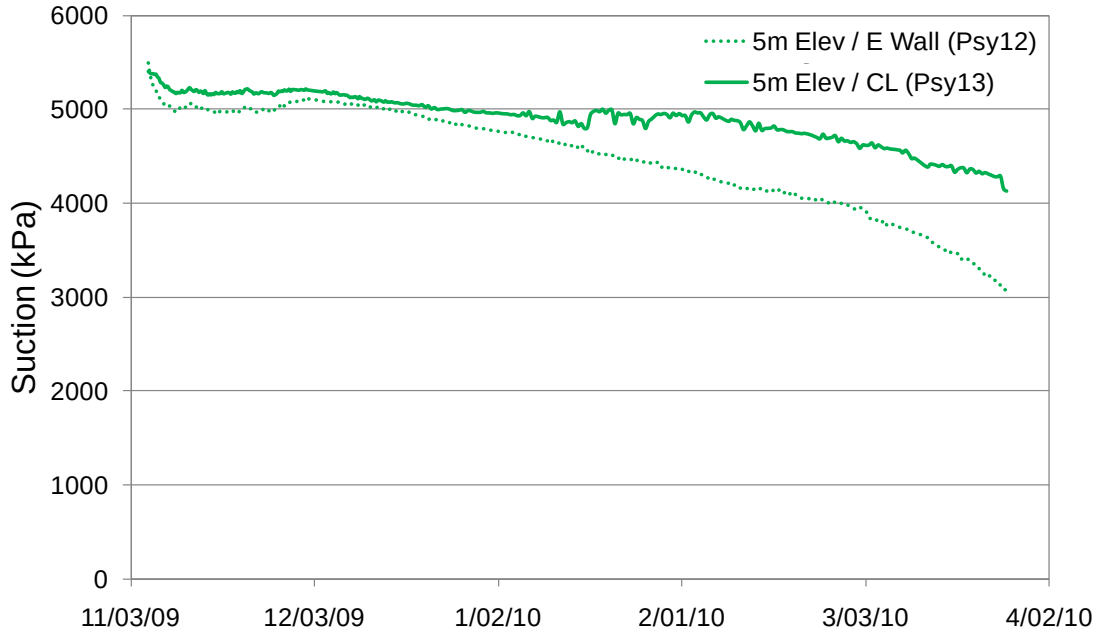


Figure 6.10: Suction at 5 m height in the bentonite-sand component (AECL)

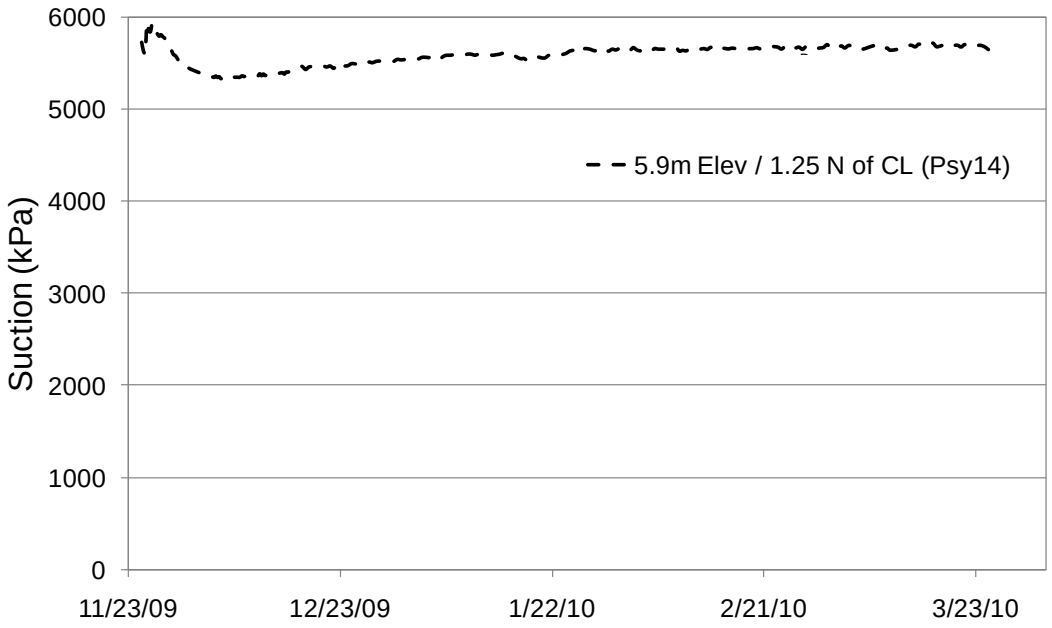


Figure 6.11: Suction at 5.9 m height in the bentonite-sand component (AECL)



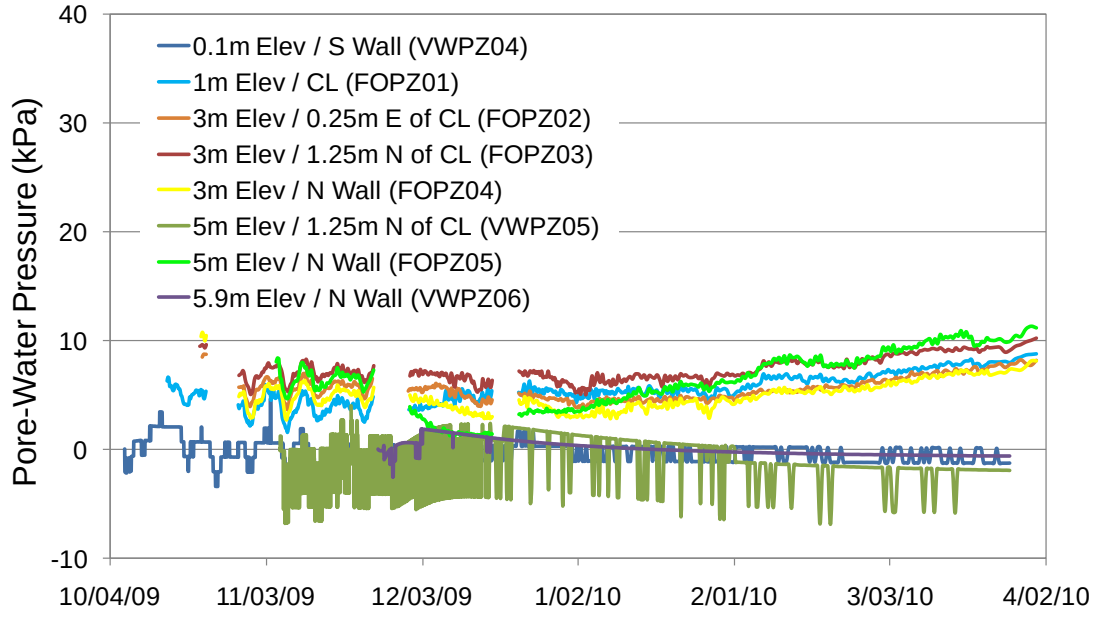


Figure 6.12: Pore-water pressure in the bentonite-sand component (AECL)

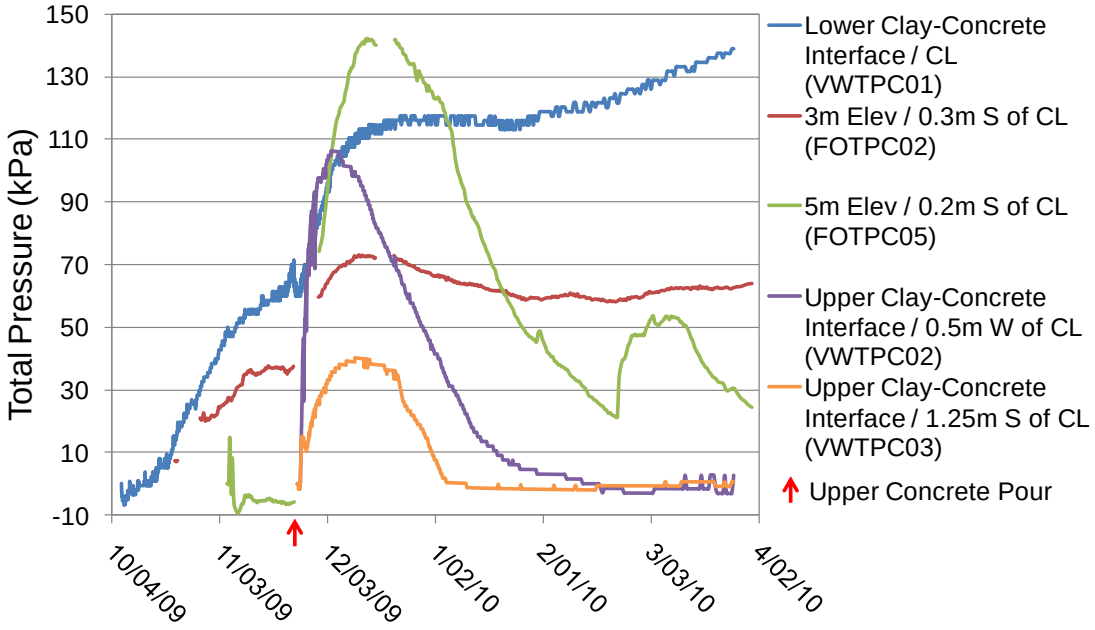


Figure 6.13: Total vertical pressure in the bentonite-sand component and at the clay-concrete interfaces (AECL)



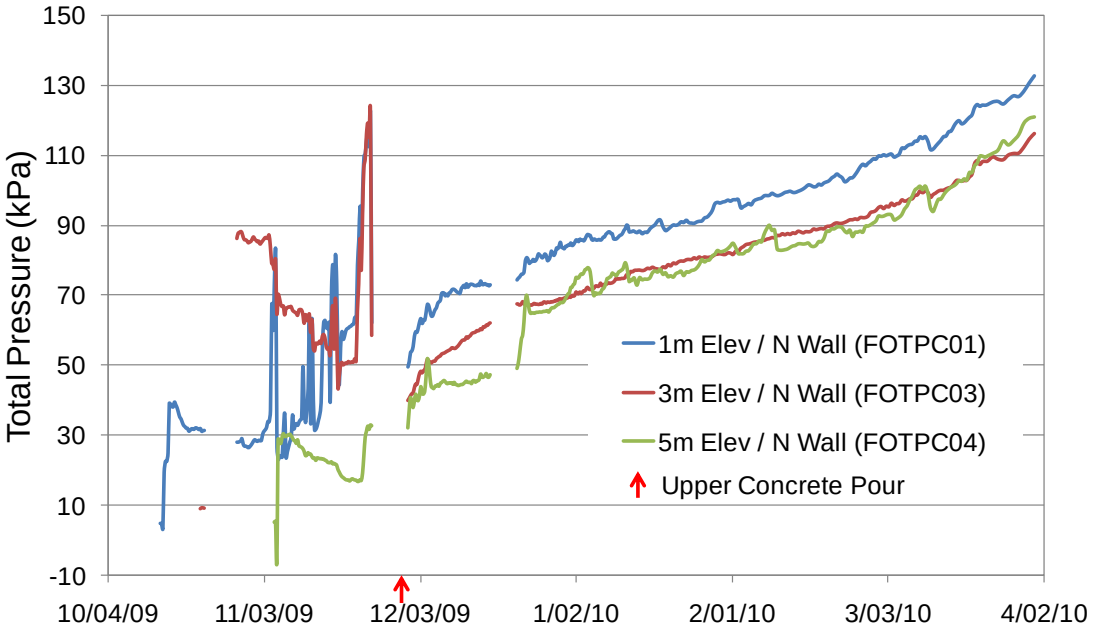


Figure 6.14: Total horizontal pressure at the clay-rock interface (AECL)

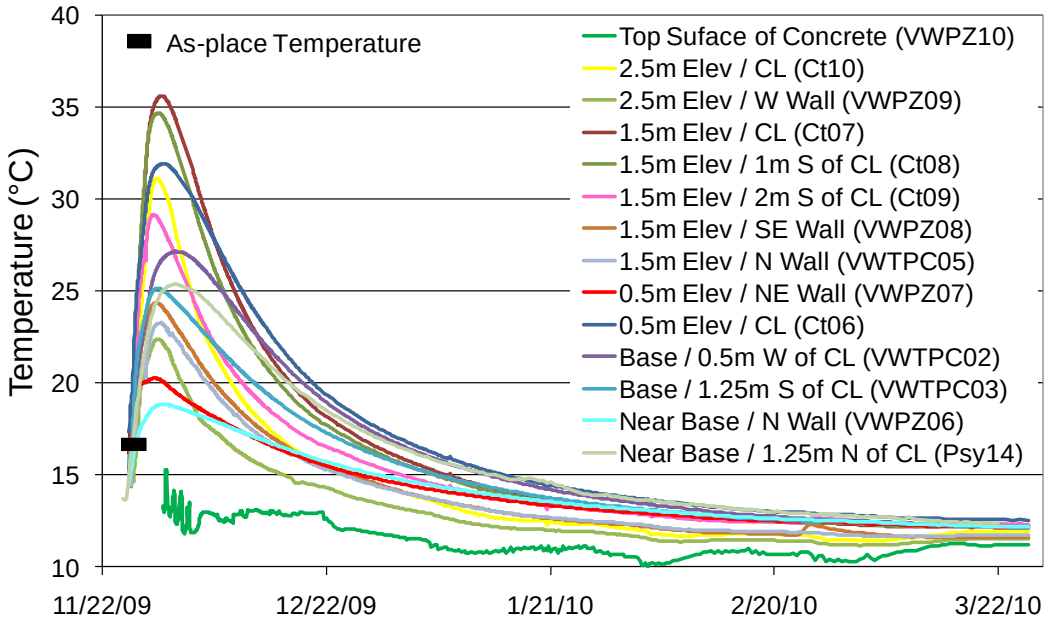


Figure 6.15: Temperature in the upper concrete component (AECL)



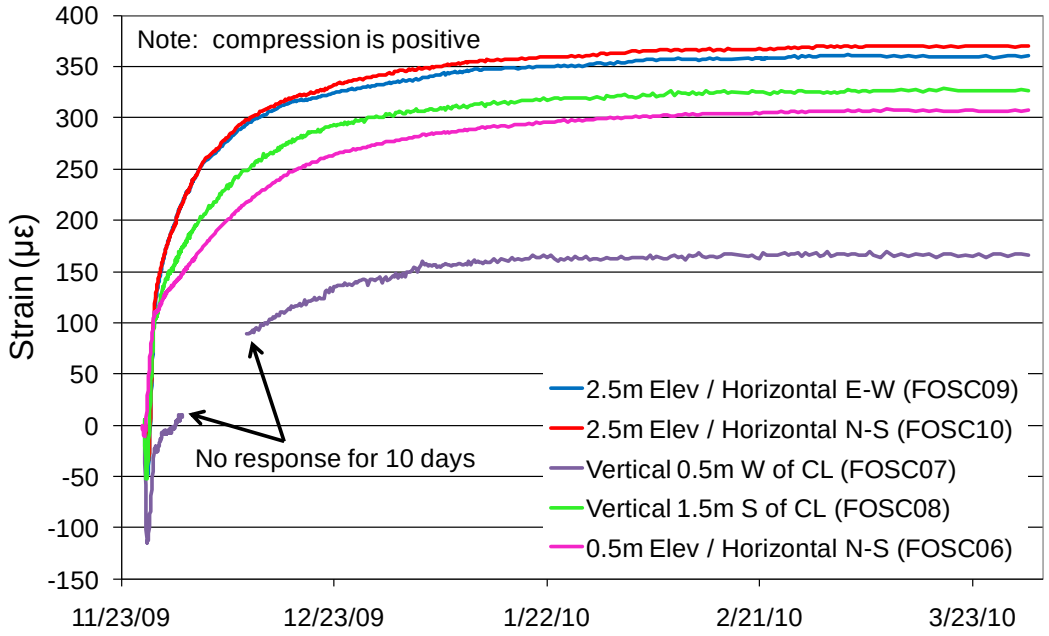


Figure 6.16: Strain in the upper concrete component (AECL)

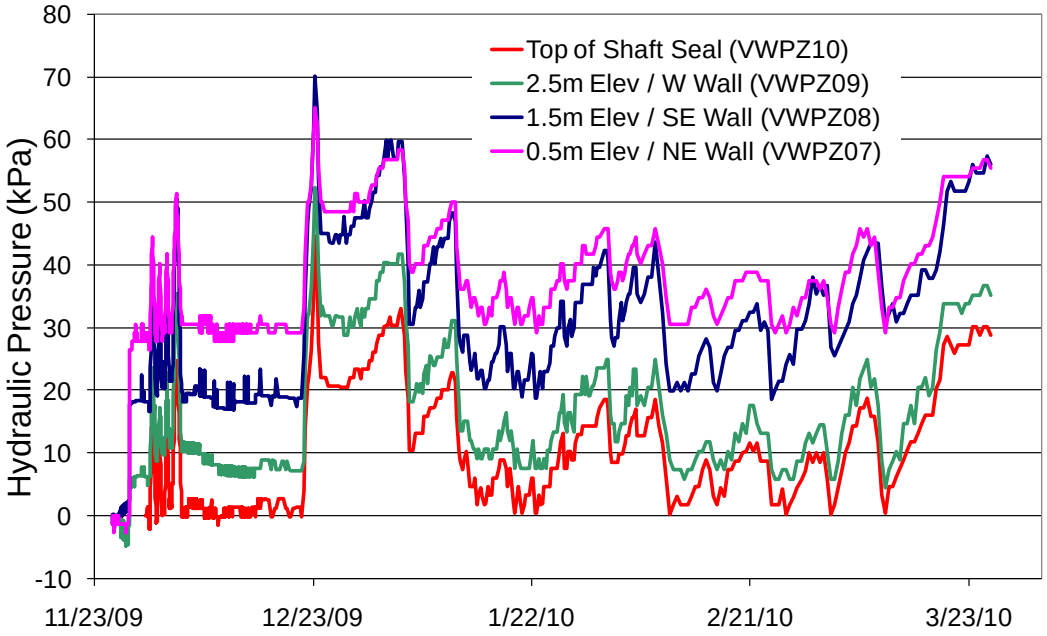


Figure 6.17: Hydraulic pressure at the upper concrete-rock interface (AECL)



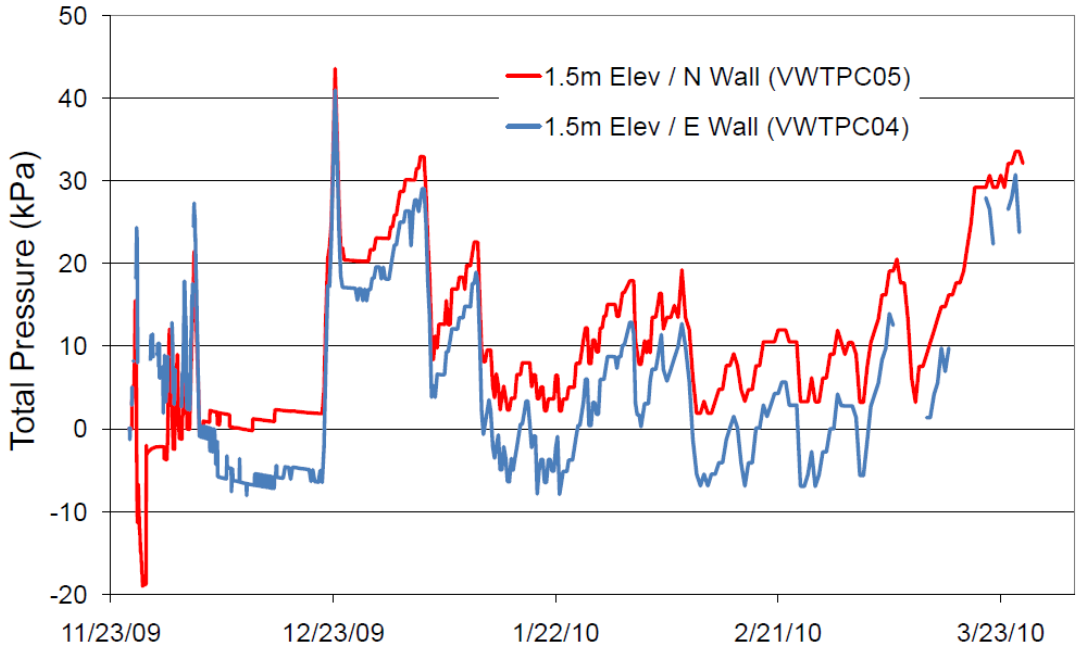


Figure 6.18: Total pressure at the upper concrete-rock interface (AECL)

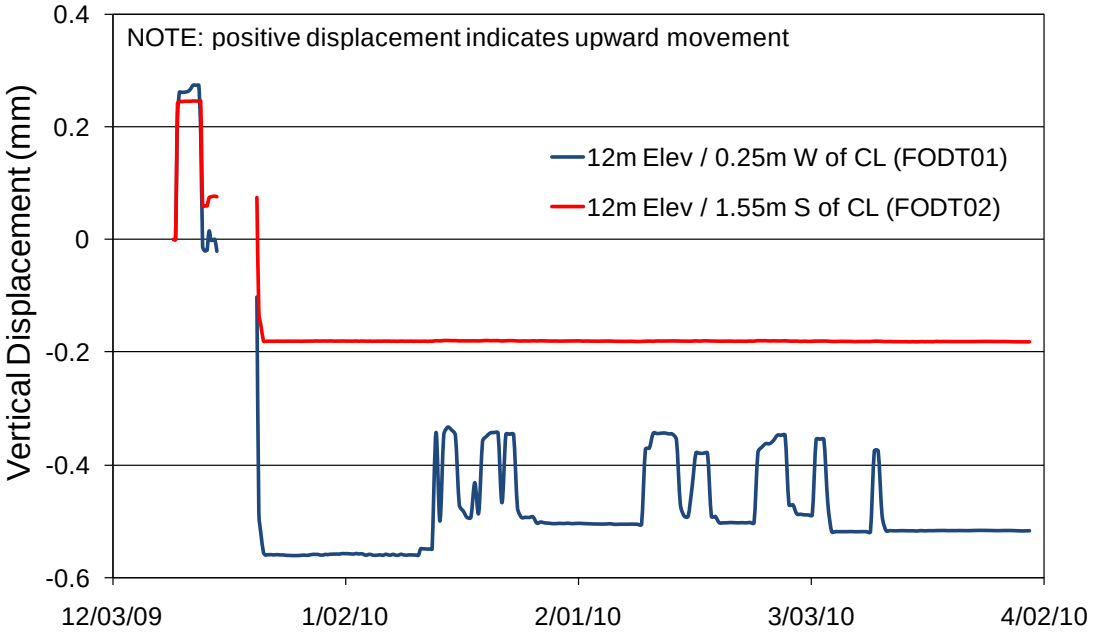


Figure 6.19: Vertical displacement of the upper concrete component (AECL)



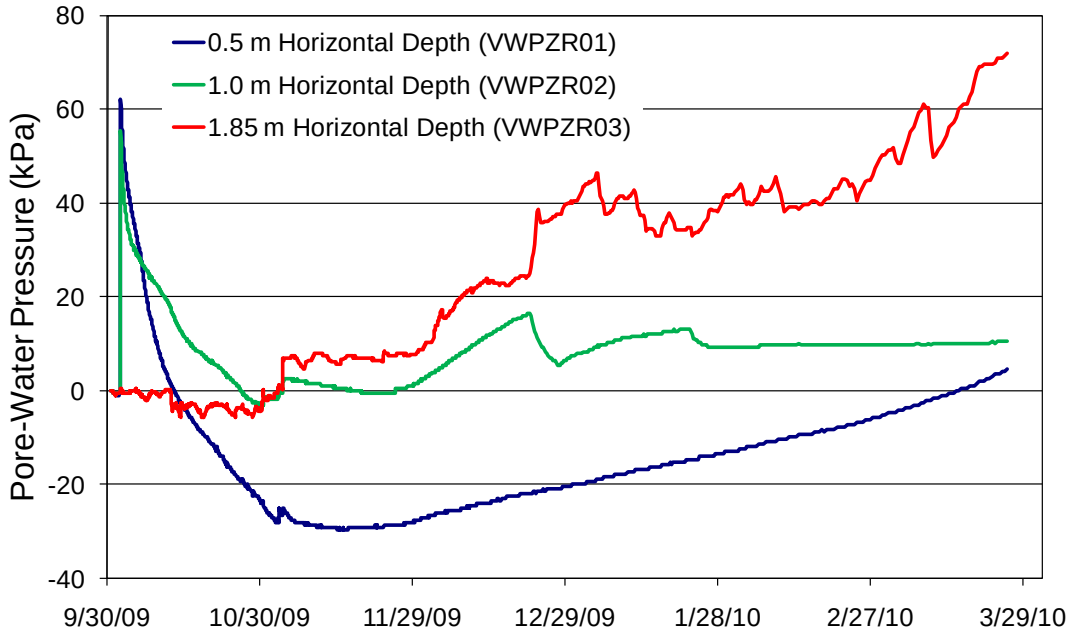


Figure 6.20: Pore-water pressure in the rock adjacent to the bentonite-sand component (AECL)

# 7 CONCLUSIONS AND DISCUSSION

The main shaft seal at AECL's URL has successfully been installed at a depth of 275 m at the intersection of the main shaft and a hydraulically active facture zone. The seal will assist in returning the URL site to its pre-development state by limiting the potential mixing of deeper saline groundwater with shallower less-saline groundwater.

Instrumentation for observing the hydro-mechanical evolution of the shaft seal has been successfully installed and is being monitored from the surface using a variety of datalogging techniques. It has been shown that a shaft seal installed at depth can be effectively monitored using mostly conventional instrumentation technologies. The instrumentation is monitoring a key set of hydro-mechanical parameters that, combined with the strategic placement of the instruments, should allow the future performance of the seal to be evaluated.

The four (4) objectives of this thesis, which were outlined in Section 1.3, are discussed below.

*Objective 1: Comment on the materials and construction methods used to build the main shaft seal.*

The construction materials and methods used to build the main shaft seal have been described. This information provides an explanation of how shaft seals can

be installed using common construction materials and simple installation techniques.

*Objective 2: Document the monitoring technologies and techniques used for the ESP.*

The instrument and datalogging technologies used in the ESP have been described in detail. Also, the installation method for each instrument type has been documented. This information will be useful for potential monitoring of a future DGR, future sealing experiments and other comparable applications.

*Objective 3: Comment on the performance and reliability of the various instrumentation technologies used.*

As of March 31, 2010 the performance and reliability of the installed instruments has exceeded expectations. Of the sixty eight (68) instruments installed, only two (2) have shown partial failure, and were likely damaged during the shaft seal construction. The remaining instruments are all functioning properly and are providing valuable information regarding the initial hydro-mechanical behaviour of the shaft seal. The long term functionality of the instruments will be assessed in the future.

The various data logging technologies have also proved to be very reliable, with only minor data loss during the first seven (7) months of monitoring. The dataloggers installed underground, on the 240 Level, are still functional and any

issues encountered with them have been fixed remotely from the surface. This bodes well for their future performance and long term functionality.

*Objective 4: Interpret initial data collected from the ESP.*

The initial data collected up to March 30, 2010 has been analyzed and discussed. The curing of both concrete components was successfully monitored, and monitoring of the initial saturation of the bentonite-sand component is underway. The data thus far is following the expected trends and can be easily interpreted and explained.

In the future, the seal performance and monitoring data will be discussed and analyzed as the data collection process continues over the coming years.

## REFERENCES


AECL. *Environmental impact statement on the concept for disposal of Canada's nuclear fuel waste.* Atomic Energy of Canada Limited Report, AECL-10711, AECL, 1994.

Berkeley Lab. *Berkeley Lab Earth Sciences Division web site.* 2000 йил 25-August. http://esd.lbl.gov/NW/tips/tipaft6r2m0.pdf (accessed 2009 йил 16-December).

Campbell Scientific Inc. “Instruction Manual S3497X Psychrometer Software and A3497 TC Psychrometer Cooling Current Interface.” Campbell Scientific Inc., 1992.

—. “Instruction manual: TDR100.” Campbell Scientific Inc., 2008.

Chandler, N A, et al. *The five year report on the tunnel sealing experiment: an international project of AECL, JNC, ANDRA and WIPP.* Atomic Energy of Canada Limited Report, AECL-12127, AECL, 2002.

Dahlstrom, L-O. *Experiences from the design and construction of plug II in the prototype repository.* SKB R-Series Report, R-09-49, SKB, 2009.

Dahlstrom, L-O. *Test plan for the prototype repository.* Äspö Hard Rock Laboratory Progress Report, HRL-98-24, SKB, 1998.

Dixon, D A, J B Martino, and D P Onagi. *Enhanced Sealing Project (ESP): Design, Construction and Instrumentation Plan.* Nuclear Waste Management Organization Report, APM-REP-01601-0001, NWMO, 2009.

Dixon, D A, M N Gray, and A W Thomas. “A study of the compaction properties of potential clay-sand buffer mixtures for use in nuclear fuel waste disposal.” *Engineering Geology* 21 (1985): 247-255.

Dixon, D, L Borgesson, D Gunnarsson, and J Hansen. *Plugs for use in tunnels of a deep geologic repository in crystalline rock: concepts and international experiences.* Soon to be published SKB report, SKB, 2010.

Dixon, D, P Thompson, N Chandler, and E Kozak. *Instrumentation summary report for the isothermal and buffer/container experiments.* Ontario Power Generation Report, 06819-REP-01200-10035-R00, OPG, 2000.

Edlefsen, N E, and B C Anderson. “Thermodynamics of soil moisture.” *Hilgardia* 15, no. 1 (1943): 31-298.

Ekblad, J, and U Isacsson. “Time-domain reflectometry measurements and soil-water characteristic curves of coarse granular materials used in road pavements.” *Canadian Geotechnical Journal* 44 (2007): 858-872.

Everitt, R, J McMurray, A Brown, and C Davison. “Geology of the Lac du Bonnet batholith, inside and out: AECL's Underground Research Laboratory, Southeastern Manitoba - field trip guidebook B5.” *Geological Association of Canada/Mineralogical Association of Canada Annual Meeting.* Winnipeg, Manitoba, 1996.

Fredlund, D G, and H Rahardjo. *Soil mechanics for unsaturated soils.* John Wiley & Sons, Inc., 1993.

Garamszeghy, M. *Nuclear fuel waste projections in Canada - 2008 Update.* Nuclear Waste Management Organization Report, NWMO TR-2008-18, NWMO, 2008.

Garcia-Sineriz, J L, and I Barcena. “Reliability of THM instrumentation for underground research laboritories.” *Advances in Understanding Engineered Clay Barriers: Proceedings of the International Symposium on Large Scale Field Tests in Granite.* Sitges, Spain, 2003.

Geokon Inc. “Instruction manual: Model 4500 vibrating wire piezometer.” Geokon Inc., 1993.

Graham, J, N A Chandler, D A Dixon, P J Roach, and A Wan. *The buffer/container experiment: results, synthesis, issues.* Atomic Energy of Canada Limited Report, AECL-11746, COG-97-46-I, AECL, 1997.

Gray, M. *OECD/NEA International stripa project overview volume III.* Stockholm: SKB, 1993.

Gunnarsson, D, L Borgesson, H Hokmark, L Johannesson, and T Sanden. *Report on the installation of the backfill and plug test.* SKB International Progress Report, IPR-01-17, SKB, 2001.

Huertas, F, et al. *Full-scale engineered barriers experiment for a geep geologic repository for high-level radioactive waste in crystalline host rock (FEBEX project).* Final Report, EUR 19147 EN, European Commission, Nuclear Science and Technology, 2000.

Johannesson, L E, D Gunnarsson, T Sanden, and L, Karlzen, R Borgesson. *Prototype Repository: installation of buffer, canisters, backfill, plug and instruments in section II.* SKB International Progress Report, IPR-04-13, SKB, 2004.

Johannesson, L E, L Borgesson, R Goudarzi, T Sanden, D Gunnarsson, and C Svemar. “Prototype repository: A full scale experiment at Äspö HRL.” *Physics and Chemistry of the Earth* 32 (2007): 58-76.

Johnston, Frank, interview by Blake Holowick. *AECL Instrumentation Technician* (2009 йил 17-June).

Kjartanson, B H, and J B Martino. “Composite seal experiment in AECL's underground research laboratory.” *Proceedings of the 57th Annual Canadian Geotechnical Society Conference.* Quebec City, Canada, 2004.

Martino, J B. *The tunnel sealing experiment 10 year summary report.* Atomic Energy of Canada Limited, URL-121550-REPT-001, AECL, 2008.

Martino, J B, D A Dixon, and P M Thompson. *Instruments and systems for monitoring the engineering performance of repository seals.* Ontario Power Generation Report, 06819-REP-01200-10072-R00, OPG, 2001.

Martino, J B, D A Dixon, S G Keith, N A Chandler, and B H Kjartanson. “Sealing studies at the URL.” *Proceedings of the 56th Annual Canadian Geotechnical Society Conference.* Winnipeg, Canada, 2003.

McGee, T D. *Principles and methods of temperature measurement.* John Wiley & Sons, Inc., 1988.

Pusch, R, and L Borgesson. “Examples of the performance of tunnel plugs with and without recesses - theory and practice.” *Proceedings of the International Symposium on Large Scale Field Tests in Granite.* Sitges, Spain, 2003.

Pusch, R, L Borgesson, and G Ramqvist. *Final report of the borehole, shaft and tunnel sealing test - Volume III: tunnel plugging.* Stripa Project Technical Report, 87-03, SKB, 1987c.

Pusch, R, L Borgesson, and G Ramqvist. *Final report of the borehole, shaft, and tunnel sealing test - Volume II: shaft plugging.* Stripa Project Technical Report, 87-02, SKB, 1987b.

Pusch, R, L Borgesson, and G Ramqvist. *Final report on the borehole, shaft and tunnel sealing test - Volume I: borehole plugging.* Stripa Project Technical Report, 87-01, SKB, 1987a.

Rao, Y J, D A Jackson, R Jones, and C Shannon. “Development of prototype fibre-optic-based fizeau pressure sensors with temperature compensation and signal recovery by coherence reading.” *Journal of Lightwave Technology* 12, no. 9 (1994): 1685-1695.

Read, R S. “20 years of excavation response studies at AECL’s underground research laboratory.” *International Journal of Rock Mechanics & Mining Sciences* 41 (2004): 1252-1275.

Richards, B G. “Measurement of the free energy of soil moisture by the psychrometric technique using thermistors.” *Moisture equilibria and moisture changes in soils beneath covered areas, a symposium in print.* Australia: Butterworths, 1965. 39-46.

Roctest Ltd. “Instruction manual: Sensoptic fibre-optic displacement transducer model FOD.” Roctest Ltd., 2000.

—. “Instruction manual: Fibre-optic pressure transducer FOP series.” Roctest Ltd., 2000a.

—. “Instruction manual: Fibre-optic total pressure cell models FO-TPC and FO-EPC.” Roctest Ltd., 2000b.

—. “Instruction manual: Vibrating wire piezometer model PW.” Roctest Ltd., 2005a.

—. “Instruction manual: Vibrating wire pressure cells model TPC & EPC.” Roctect Ltd., 2005b.

SCK-CEN. “Our Research: SCK-CEN.” *SCK-CEN The Belgium Nuclear Research Centre.* 2005. http://www.sckcen.be/en/Our-Research/Scientific-Reports/Scientific-Report-2005 (accessed 2010 йил 20-March).

Siemens, Gregory Allen. *Influence of boundary conditions on the hydraulic-mechanical behaviour of unsaturated swelling soil.* PhD Thesis, Winnipeg: University of Manitoba, 2006.

Sitz, P, G Koch, and M Gruner. “Results from the large scale in situ drift sealing experiment in the salt mine Sondershausen.” In *Clays in Natural and Engineered Barriers for Radioactive Waste Confinement: Experiments in Underground Laboritories*, 28-35. Chatenay-Malabry, France: ANDRA Science and Technology Series, 2003.

SKB. *Äspö Hard Rock Laboratory Annual Report 2004.* SKB Technical Report, TR-05-10, SKB, 2005.

SKB. *Äspö Hard Rock Laboratory Annual Report 2008.* SKB Technical Report, TR-09-10, SKB, 2009.

Villar, M V, J L Garcia-Sineriz, I Barcena, and A Lloret. “State of the bentonite barrier after five years operation of an in situ test simulating a high level radioactive waste repository.” *Engineering Geology* 80 (2005): 175-198.

Wan, Alan W L. *The use of thermocoulpe psychrometers to measure in situ suctions and water contents in compacted clays.* PhD Thesis, Winnipeg, Manitoba: University of Manitoba, 1996.

Wescor Environmental Products Division. “PST-55(-SF) and PCT-55(-SF) Soil Hygrometer/Psychrometer Instructions For Use With Wescor Water Potential Systems.”

# APPENDIX A: TABLES OF INSTRUMENT LOCATIONS

**VIBRATING WIRE PIEZOEMTERS**

| Name | Serial Number | X (m) | Y (m) | Z (m) | Angle ( ° ) | Distance from Wall (m) | Component | Notes | Date Installed |
|---|---|---|---|---|---|---|---|---|---|
| VWPZ01 | 100C09047 | 1.6 | 2.1 | 0.54 | 37.3 | 0 | Lower Concrete | Attached to reinforcement | Aug. 17, 2009 |
| VWPZ02 | 100C09046 | 0.65 | -2.75 | 1.70 | 166.7 | 0 | Lower Concrete | Attached to I-bolt | Aug. 20, 2009 |
| VWPZ03 | 100C09048 | -2.7 | 1.7 | 2.20 | 302.2 | 0 | Lower Concrete | Attached to reinforcement | Aug. 26, 2009 |
| VWPZ04 | 100C09044 | 0.86 | -2.07 | 3.10 | -- | 0.25 | Bentonite-Sand | Near clay-rock interface | Oct. 6, 2009 |
| VWPZ05 | 100C09049 | 0.00 | 1.25 | 8.00 | -- | -- | Bentonite-Sand | Approximately halfway between shaft centre and wall | Nov. 5, 2009 |
| VWPZ06 | 100C09051 | 0.00 | 2.70 | 8.90 | -- | 0.10 | Bentonite-Sand | Considerable rock breakout in this area | Nov. 24, 2009 |
| VWPZ07 | 100C09052 | -- | -- | 9.50 | 30° | 0 | Upper Concrete | At rock-concrete interface | Nov. 19, 2009 |
| VWPZ08 | 100C09050 | -- | -- | 10.50 | 150° | 0 | Upper Concrete | At rock-concrete interface | Nov. 19, 2009 |
| VWPZ09 | 100C09053 | -- | -- | 11.50 | 270° | 0 | Upper Concrete | At rock-concrete interface | Nov. 19, 2009 |
| VWPZ10 | 100C09045 | -0.7 | -2.3 | 12.00 | -- | -- | Upper Concrete | Measures head of water above plug | Nov. 30, 2009 |
| VWPZR01 | 25194 | -- | 0.55 | 7.53 | -- | -- | Adjacent Rock | Installed on 0.5 m mechanical packer | Sept. 30, 2009 |
| VWPZR02 | 25199 | -- | 0.00 | 7.49 | -- | -- | Adjacent Rock | Installed on 1.0 m mechanical packer | Sept. 30, 2009 |
| VWPZR03 | 25195 | -- | -0.48 | 7.50 | -- | -- | Adjacent Rock | Installed on 1.85 m mechanical packer | Sept. 30, 2009 |

**VIBRATING WIRE TOTAL PRESSURE CELLS**

| Name | Serial Number | X (m) | Y (m) | Z (m) | Angle ( ° ) | Distance from Wall (m) | Component | Notes | Date Installed |
|---|---|---|---|---|---|---|---|---|---|
| VWTPC01 | 078E09136 | 0.00 | 0.00 | 3.00 | -- | -- | Bentonite-Sand | Vertical pressure at lower concrete-clay interface | Oct. 6, 2009 |
| VWTPC02 | 078E09137 | -0.50 | 0.00 | 9.00 | -- | -- | Bentonite-Sand | Vertical pressure at upper concrete-clay interface | Nov. 24, 2009 |
| VWTPC03 | 078E09138 | 0.00 | -1.25 | 9.00 | -- | -- | Bentonite-Sand | Vertical pressure at upper concrete-clay interface | Nov. 24, 2009 |
| VWTPC04 | 078E09134 | -- | -- | 10.50 | 90° | 0 | Upper Concrete | Horizontal pressure at upper concrete-rock interface | Nov. 19, 2009 |
| VWTPC05 | 078E09135 | -- | -- | 10.50 | 0° | 0 | Upper Concrete | Horizontal pressure at upper concrete-rock interface | Nov. 19, 2009 |

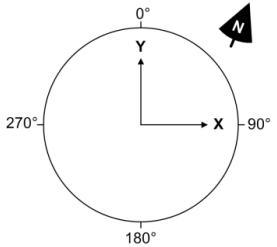


NOTE: The centre of the plug is at X=0, Y=0

Z - Distance above base the lower concrete component

The "Distance from Wall" is only indicated for instruments installed at, or close to, the shaft wall

The "Angle" is measured from 0° and was only recorded for some instruments

**FIBRE OPTIC PIEZOMETERS**

| Name | Serial Number | X (m) | Y (m) | Z (m) | Distance from Wall (m) | Component | Notes | Date Installed |
|---|---|---|---|---|---|---|---|---|
| FOPZ01 | PR09020 | 0.00 | 0.05 | 4.00 | -- | Bentonite-Sand | Near centre of shaft | Oct. 15, 2009 |
| FOPZ02 | PR09023 | 0.25 | 0.00 | 6.00 | -- | Bentonite-Sand | Near centre of shaft | Oct. 26, 2009 |
| FOPZ03 | PR09021 | 0.00 | 1.25 | 6.00 | -- | Bentonite-Sand | Approximately halfway between shaft centre and wall | Oct. 26, 2009 |
| FOPZ04 | PR09022 | 0.00 | *2.125 | 6.00 | 0.30 | Bentonite-Sand | Near clay-rock interface | Oct. 26, 2009 |
| FOPZ05 | PR09024 | -0.30 | 2.35 | 8.00 | 0.10 | Bentonite-Sand | Near clay-rock interface | Nov. 5, 2009 |

*4.85 m shaft diameter assumed

**FIBRE OPTIC TOTAL PRESSURE CELLS**

| Name | Serial Number | X (m) | Y (m) | Z (m) | Distance from Wall (m) | Component | Notes | Date Installed |
|---|---|---|---|---|---|---|---|---|
| FOTPC01 | PR09025 | 0.00 | 2.50 | 4.00 | 0 | Bentonite-Sand | Horizontal pressure at clay-rock interface | Oct. 14, 2009 |
| FOTPC02 | PR09027 | 0.00 | -0.30 | 6.00 | -- | Bentonite-Sand | Vertical pressure inside bentonite-sand | Oct. 26, 2009 |
| FOTPC03 | PR09026 | 0.00 | *2.425 | 6.00 | 0 | Bentonite-Sand | Horizontal pressure at clay-rock interface | Oct. 26, 2009 |
| FOTPC04 | PR09028 | 0.00 | 2.45 | 8.00 | 0 | Bentonite-Sand | Horizontal pressure at clay-rock interface | Nov. 5, 2009 |
| FOTPC05 | PR09029 | 0.05 | -0.20 | 8.00 | -- | Bentonite-Sand | Vertical pressure inside bentonite-sand | Nov. 5, 2009 |

*4.85 m shaft diameter assumed

**FIBRE OPTIC DISPLACEMENT TRANSDUCERS**

| Name | Serial Number | X (m) | Y (m) | Z (m) | Distance from Wall (m) | Component | Notes | Date Installed |
|---|---|---|---|---|---|---|---|---|
| FODT01 | DR0903 | -0.25 | -0.05 | 12.00 | -- | Upper Concrete | Mounted above the shaft seal on a steel beam | Dec. 9, 2009 |
| FODT02 | DR0902 | -0.25 | -1.55 | 12.00 | -- | Upper Concrete | Mounted above the shaft seal on a steel beam | Dec. 9, 2009 |

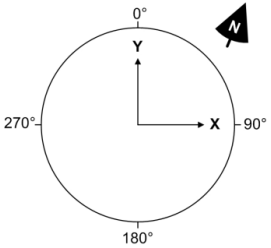


NOTE: The centre of the plug is at X=0, Y=0

Z - Distance above base the lower concrete component

The "Distance from Wall" is only indicated for instruments installed at, or close to, the shaft wall

**THERMOCOUPLES**

| Name | Serial Number | X (m) | Y (m) | Z (m) | Distance from Wall (m) | Component | Notes | Date Installed |
|---|---|---|---|---|---|---|---|---|
| Ct01 | 13309031 | 0 | -0.1 | 0.62 | -- | Lower Concrete | Installed on steel reinforcement | Aug. 17, 2009 |
| Ct02 | 13309034 | 0 | -0.1 | 1.50 | -- | Lower Concrete | Installed on steel reinforcement | Aug. 20, 2009 |
| Ct03 | 13309033 | 1 | -0.1 | 1.50 | -- | Lower Concrete | Installed on steel reinforcement | Aug. 20, 2009 |
| Ct04 | 13309032 | 2 | -0.1 | 1.50 | -- | Lower Concrete | Installed on steel reinforcement | Aug. 20, 2009 |
| Ct05 | 13309035 | 0.1 | -0.15 | 2.50 | -- | Lower Concrete | Installed on steel reinforcement | Aug. 26, 2009 |
| Ct06 | 13309036 | -0.5 | 0.0 | 9.50 | -- | Upper Concrete | Installed on steel support cable | Nov. 20, 2009 |
| Ct07 | 13309037 | -0.5 | 0.0 | 10.50 | -- | Upper Concrete | Installed on steel support cable | Nov. 20, 2009 |
| Ct08 | 13309038 | -0.5 | -1.0 | 10.50 | -- | Upper Concrete | Installed on steel support cable | Nov. 20, 2009 |
| Ct09 | 13309039 | -0.5 | -2.0 | 10.50 | -- | Upper Concrete | Installed on steel support cable | Nov. 20, 2009 |
| Ct10 | 13309040 | -0.5 | 0.0 | 11.50 | -- | Upper Concrete | Installed on steel support cable | Nov. 20, 2009 |

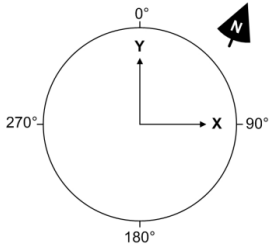


NOTE: The centre of the plug is at X=0, Y=0

Z - Distance above base the lower concrete component

The "Distance from Wall" is only indicated for instruments installed at, or close to, the shaft wall

**THERMOCOUPLE PSYCHROMETERS**

| Name | Serial Number | X (m) | Y (m) | Z (m) | Distance from Wall (m) | Component | Notes | Date Installed |
|---|---|---|---|---|---|---|---|---|
| Psy01 | 49056 | 2.40 | 0.00 | 3.10 | 0.10 | Bentonite-Sand | Near clay-rock-concrete interface | Oct. 6, 2009 |
| Psy02 | 49047 | 0.88 | -2.30 | 3.10 | 0.10 | Bentonite-Sand | Near clay-rock-concrete interface | Oct. 6, 2009 |
| Psy03 | 49050 | -0.35 | 2.40 | 4.00 | 0.10 | Bentonite-Sand | Near clay-rock interface | Oct. 15, 2009 |
| Psy04 | 49053 | 0.00 | -0.05 | 4.00 | -- | Bentonite-Sand | Near centre of shaft | Oct. 15, 2009 |
| Psy05 | 49048 | 1.25 | 0.00 | 4.00 | -- | Bentonite-Sand | Approximately halfway between shaft centre and wall | Oct. 14, 2009 |
| Psy06 | 49058 | 0.00 | -1.25 | 4.00 | -- | Bentonite-Sand | Approximately halfway between shaft centre and wall | Oct. 14, 2009 |
| Psy07 | 49059 | 2.20 | 0.00 | 5.00 | 0.10 | Bentonite-Sand | Near clay-rock interface | Oct. 20, 2009 |
| Psy08 | 49045 | 0.00 | 1.25 | 5.00 | -- | Bentonite-Sand | Approximately halfway between shaft centre and wall | Oct. 20, 2009 |
| Psy09 | 49051 | *2.225 | 0.00 | 6.00 | 0.20 | Bentonite-Sand | Near clay-rock interface | Oct. 26, 2009 |
| Psy10 | 49057 | 1.45 | 0.00 | 6.00 | -- | Bentonite-Sand | Approximately halfway between shaft centre and wall | Oct. 26, 2009 |
| Psy11 | 49046 | 2.17 | 0.00 | 7.00 | 0.20 | Bentonite-Sand | Near clay-rock interface | Oct. 30, 2009 |
| Psy12 | 49054 | 2.25 | 0.00 | 8.00 | 0.10 | Bentonite-Sand | Near clay-rock interface | Nov. 5, 2009 |
| Psy13 | 49049 | 0.00 | 0.10 | 8.00 | -- | Bentonite-Sand | Near centre of shaft | Nov. 5, 2009 |
| Psy14 | 49052 | 0.00 | 1.25 | 8.90 | -- | Bentonite-Sand | Approximately halfway between shaft centre and wall | Nov. 24, 2009 |

*4.85 m shaft diameter assumed

**TIME DOMAIN REFLECTOMETRY PROBES**

| Name | Serial Number | X (m) | Y (m) | Z (m) | Distance from Wall (m) | Component | Notes | Date Installed |
|---|---|---|---|---|---|---|---|---|
| TDR1 | TDR1 | 0.00 | 0.00 | 5.00 | -- | Bentonite-Sand | Oriented at a 45° angle | Oct. 20, 2009 |
| TDR2 | TDR2 | 0.00 | 0.25 | 6.00 | -- | Bentonite-Sand | Oriented at a 45° angle | Oct. 26, 2009 |
| TDR3 | TDR3 | 1.25 | 0.00 | 6.00 | -- | Bentonite-Sand | Oriented along 0°-180° axis | Oct. 26, 2009 |
| TDR4 | TDR4 | 0.00 | 0.00 | 7.00 | -- | Bentonite-Sand | Oriented at a 45° angle | Oct. 30, 2009 |

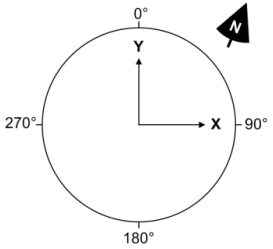


NOTE: The centre of the plug is at X=0, Y=0

Z - Distance above base the lower concrete component

The "Distance from Wall" is only indicated for instruments installed at, or close to, the shaft wall

**FIBRE OPTIC DEFORMATION SENSORS (STRAIN GAUGES)**

| Name | Serial Number | X1 (m) | Y1 (m) | Z1 (m) | X2 (m) | Y2 (m) | Z2 (m) | Active Length (m) | Orientation | Component | Date Installed |
|---|---|---|---|---|---|---|---|---|---|---|---|
| FOSC01 | 7593 | -0.6 | 0.1 | 0.62 | 0.4 | 0.1 | 0.62 | 1.0 | Horizontal | Lower Concrete | Aug. 17, 2009 |
| FOSC02 | 7596 | 0.15 | -0.15 | 2.0 | 0.15 | -0.15 | 1.0 | 1.0 | Vertical | Lower Concrete | Aug. 26, 2009 |
| FOSC03 | 7594 | 2.0 | -0.15 | 1.9 | 2.0 | -0.15 | 0.9 | 1.0 | Vertical | Lower Concrete | Aug. 26, 2009 |
| FOSC04 | 7598 | -1.4 | 0.15 | 2.5 | 1.6 | 0.15 | 2.5 | 3.0 | Horizontal | Lower Concrete | Aug. 26, 2009 |
| FOSC05 | 7597 | 0.15 | 1.45 | 2.5 | 0.15 | -1.55 | 2.5 | 3.0 | Horizontal | Lower Concrete | Aug. 26, 2009 |
| FOSC06 | 7599 | -0.5 | 1.5 | 9.5 | -0.5 | -1.5 | 9.5 | 3.0 | Horizontal | Upper Concrete | Nov. 20, 2009 |
| FOSC07 | 7592 | -0.5 | 0.5 | 9.75 | -0.5 | 0.5 | 10.75 | 1.0 | Vertical | Upper Concrete | Nov. 20, 2009 |
| FOSC08 | 7595 | -0.5 | -1.5 | 9.75 | -0.5 | -1.5 | 10.75 | 1.0 | Vertical | Upper Concrete | Nov. 20, 2009 |
| FOSC09 | 7601 | -1.5 | 0.5 | 11.5 | 1.5 | 0.5 | 11.5 | 3.0 | Horizontal | Upper Concrete | Nov. 20, 2009 |
| FOSC10 | 7600 | -0.5 | 1.5 | 11.5 | -0.5 | -1.5 | 11.5 | 3.0 | Horizontal | Upper Concrete | Nov. 20, 2009 |

Note: X1,Y1,Z1 and X2,Y2,Z2 are the locations of each anchor at the end of the sensors' active zones

Strain gauges installed in the Lower and Upper Concrete are attached to steel reinforcement and support cables, respectively

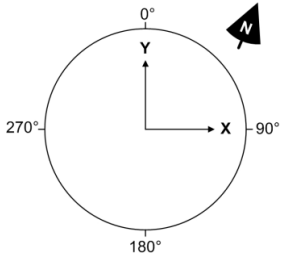


NOTE: The centre of the plug is at X=0, Y=0

Z - Distance above base the lower concrete component

# APPENDIX B: DRAWINGS OF INSTRUMENT LOCATIONS

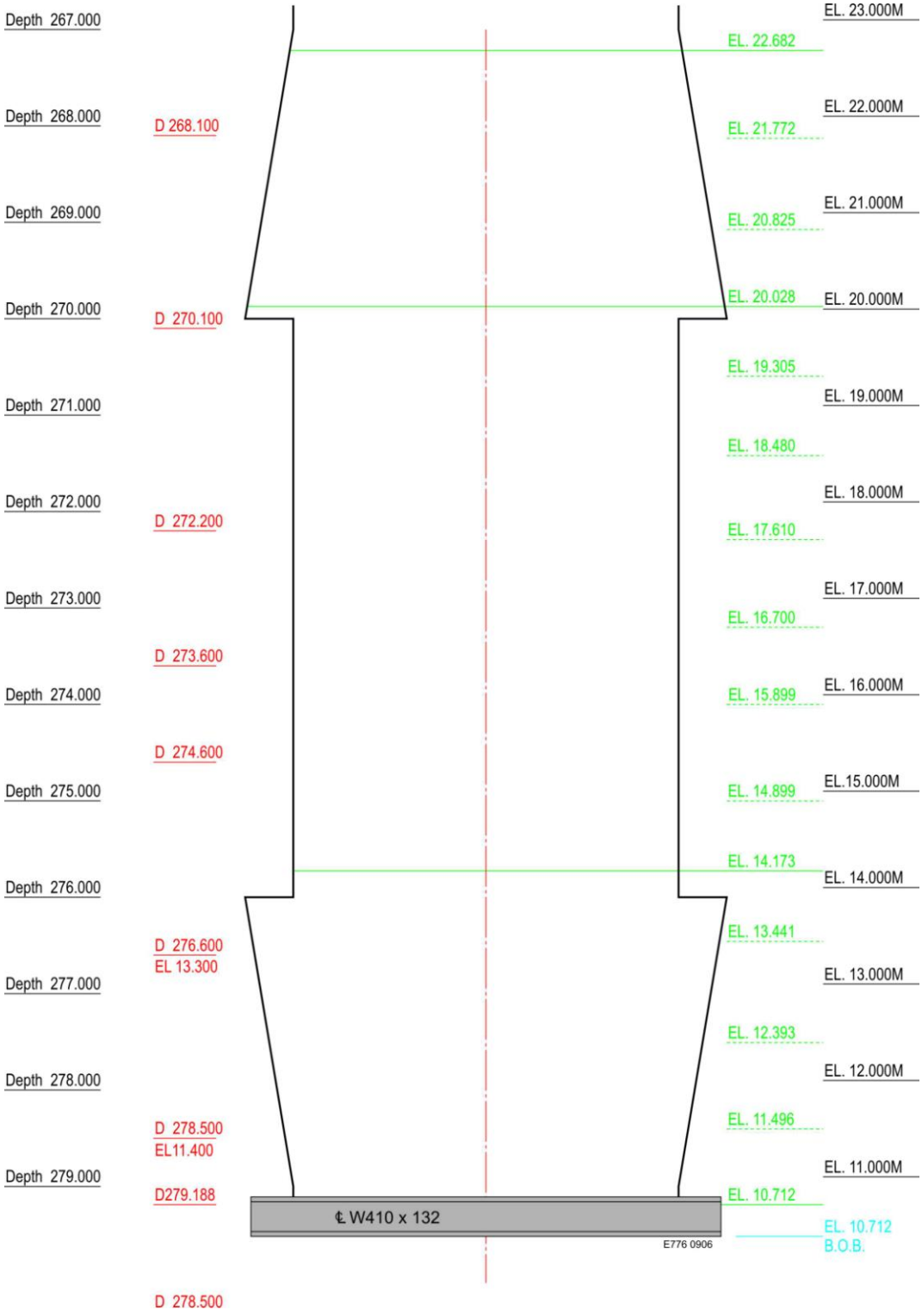


Reference elevations and depths for the main shaft seal